Optical label-controlled transparent metro-access network interface

Osadchiy, Alexey Vladimirovich

Publication date:
2010

Document Version
Publisher's PDF, also known as Version of record

Technical University of Denmark

Optical Signal Routing and Interfacing for Converged Metropolitan Access Networks

Alexey V. Osadchiy

DTU Fotonik
Department of Photonics Engineering

June 2010

Abstract

This thesis presents results obtained during the course of my PhD research on optical signal routing and interfacing between the metropolitan and access segments of optical networks. Due to both increasing capacity demands and variety of emerging services types, new technological challenges are arising for seamlessly interfacing metropolitan and access networks. Therefore, in this PhD project, I have analyzed those technological challenges and identified the key aspects to be addressed. I have also proposed and experimentally verified a number of solutions to metropolitan and access networks interfacing and signal routing.

Equipment and infrastructure simplification was recognized as the path towards more efficient metropolitan and access networks providing a spectrum of high-bandwidth services to large number of users. Several approaches have been proposed and developed in order to enable such simplification, including architectural solutions like fusion of metropolitan and access networks, service broadcasting and distribution of wireless signals over common fiber infrastructure; and physical layer solutions like introducing colorless operation for metropolitan network nodes and gain transient control.

Highlights of my research include my proposal and experimental proof of principle of an optical coherent detection based optical access network architecture providing support for a large number of users over a single distribution fiber; a spectral amplitude

encoded label detection technique for metropolitan and access signal routing and the incorporation of both wireless and wireline signal transmission for extended reach converged metropolitan access networks.

Resumé

Denne afhandling præsenterer resultater opnået igennem min PhD forskning om routing af optiske signaler og om forbindelse mellem metro og access segmenterne af optiske netværk. Som følge af dels øgede krav om kapacitet og dels forskelligartetheden af nye service typer er nye udfordringer opstået i forhold til signal routing samt gnidningsfri forbindelse mellem metro- og access-netværk Jeg har derfor i dette PhD projekt analyseret de teknologiske udfordringer og identificeret de vigtigste aspekter som må belyses. Ydermere har jeg foreslået og eksperimentelt verificeret et antal løsninger på metro- og access-netværk forbindelser samt signal routing

Simplificering af udstyr og infrastruktur er blevet identificeret som en vej hen mod mere effektive metro og access netværk, som vil være i stand til at tilbyde et bredt spektrum af høj-båndbredde ydelser til et stort antal brugere. Flere metoder er foreslået og udviklet for at opnå denne simplificering, fra arkitektoniske løsninger som fusion af metro og access netværk, Broadcast af ydelser, samt distribution af trådløse signaler over en fælles fiber infrastruktur til løsninger på det fysiske niveau som for eksempel introduktion af farvefri operation af metro netværk samt kontrol af forstærknings transienter.

Højdepunkter i min forskning inkluderer mit forslag og experimentel princip-demonstration af optisk kohærent detektion baseret access netværk, der understøtter et stort antal brugere gennem en enkelt distributionsfiber; spektral amplitude label

kodning og detektion for metro og access netværk samt inkorporering af både trådløs og kablet signal transmission til brug i konvergerede metro access netværk med forøget rækkevidde.

Acknowledgements

I would like to thank my supervisor, Professor Idelfonso Tafur Monroy, for allowing me the opportunity to pursue doctoral studies within the Metro Access and Short Range Systems group, and for giving valuable advice concerning paper writing and manuscript preparation; as well as providing expertise and feedback during my experimental work. I am also grateful to my co-supervisor, Professor Palle Jeppesen, for providing guidance and expertise at evaluating my results and providing me with helpful literature, especially that concerning optical coherent detection.

I am also thankful to my senior colleagues: to Jesper Bevensee Jensen for being a great aid at my experimental work and providing expertise of multi-level modulation formats; to Darko Zibar for helping me with the coherent detection setup and always giving weighted and concise critique of my work; Timothy Braidwood Gibbon for always being there to lend a hand when something doesn't work; and Xianbin Yu for helping me with UWB and some other experiments, and just being one of the coolest persons I met. I must also express my gratitude to other senior members of our cluster: Christophe Peucheret for all the practical aid he provided; Jorge Seoane, Beata Zsigri, and Anders Clausen for interesting conversations and good advice they gave me; Leif Katsuo Oxenløwe – for the interesting conversations we had and for being such a great supervisor for our other PhD students; and to Hans Christian Hansen Mulvad

for being a good person.

I would also thank my Polish colleague, Marcin Wieckowski, and his supervisor, Jarek Turkiewicz, for the interesting and new experience of remote co-supervision of Master and Bachelor students. I would also like to thank my Master supervisor Boris Chernov for all the knowledge he gave me.

I would like to thank my colleagues and friends: Kamau Prince for being a great friend, for all the help and for coming to the lab on week-ends to help finish that experiment; Neil Guerrero Gonzalez – for being a great friend and for helping with all the fancy DSP stuff which I would never be able to figure out myself; Yongshen Cao, Xu Zhang, Antonio Caballero Jambrina and Roberto Rodes Lopez – for being cool guys and helping me every time I ask; Ning Kang – for being a great friend and buying me cake; Janaina Laguardia Areal, Maisara Binti Othman, Yi An and Ji Hua – for always being the ones to smile and bring some sweets; Jing Xu – for the good jokes; Evarist Palushani – for being a great friend and making me laugh till it hurts (sic!). I would also like to thank Elaine Wong for making me look at some things in a new way.

I also would like to thank the people I met and befriended while performing my studies at DTU: Yuri Gorbanev, Anastasiya Permyakova, Ignas Lapienis, Anatoly Belenkin and others – спасибо вам, ребята!

I would like to thank my friends for the support they gave me over the three years of my studies: Dima, Lena, Sergey, Michael, David, Tuyara, Sardana, Galiya, Ayun, Airat and many, many others – I doubt I would be able to keep going without them. I

am also grateful to some people who taught me a valuable lesson: Alexander Panchenko, Lena Kirillina, Maria Starostina and some others.

Finally, I would like to thank my family: my parents, Vladimir and Irina, for all the support they gave me (not to mention my life); my sister Eugenia for being there to answer the most stupid questions; and my grandmother, Zlata, for familiarizing me with the world of science and for some good discussions we had over a cup of tea; I am also infinitely grateful to my late grandfathers, Vasiliy and Aleksey, and my late grandmother Evdokia for teaching me so much and making me want to learn more.

Contents

List of Figures

List of Abbreviations

256-QAM	256-position quadratic-amplitude modulation
3GPP LTE	3rd Generation Partnership Project long-term evolution
ASK	Amplitude shift keying
AWG	Arrayed waveguide grating
CATV	Cable television
CO	Central office
DQPSK	Differential quaternary phase-shift keying
DSP	Digital signal processing
FCC	Federal Communications Commission
FWM	Four-wave mixing
HD	High-definition
HDTV	High-definition television
HNLF	Highly-nonlinear fiber
IPTV	IP television
IR UWB	Impulse radio ultra-wideband
ITU	International Telecommunication Union
LO	Local oscillator
LRC	Local routing cabinet
LTE	Line termination equipment
MAN	Metropolitan network

NDSF	Non-zero dispersion-shifted fiber
OCDM	Optical code division multiplexing
O-E-O	Optical-to-electrical-to-optical
ONU	Optical network unit
OPS	Optical packet switching
OXC	Optical crossconnect
PDM	Polarization division multiplexing
PON	Passive optical network
QPSK	Quaternary phase-shift keying
RF	Radio frequency
RoF	Radio-over-fiber
RSOA	Reflective semiconductor optical amplifier
SAC	Spectral amplitude coding
SMF	Single-mode fiber
SNR	Signal-to-noise ratio
SOA	Semiconductor optical amplifier
TAT-1	The first Transatlantic Telephone cable
TDM	Time division multiplexing
UWB	Ultra-wideband
VoIP	Voice over IP
WAP	Wireless access point
WDM	Wavelength division multiplexed
WiMAX	Worldwide Interoperability for Microwave Access

Symbols

P	Optical power	W, dBm
ω	Angular frequency	Hz
φ	Phase offset	rad
λ	Wavelength	nm

Summary of Original Work

This work is based on the following original publications:

Paper A Jesper Bevensee Jensen, Alexey V. Osadchiy, Idelfonso Tafur Monroy, Palle Jeppesen, "Colorless DQPSK Receiver for Wavelength Routed Packet-Switched Networks," **IEEE Photonics Technology Letters**, 20, no. 22, pp 1839-1841 (2008)

Paper B Alexey V. Osadchiy, Jesper B. Jensen, Palle Jeppesen, Idelfonso Tafur Monroy, "Crossconnect architecture for colorless detection of DQPSK modulated payload signals in packet switched networks," **Optical Switching and Networking** (UNDER REVIEW) (2010)

Paper C Marcin Wieckowski, Alexey V. Osadchiy, Jarek P. Turkiewicz, Idelfonso Tafur Monroy, "Performance assessment of flexible time-wavelength routing for a self-aggregating transparent Metro-access interface," *35th European Conference on Optical Communication*, Paper P6.16 (2009)

Paper D Timothy Braidwood Gibbon, Alexey V. Osadchiy, Rasmus Kjær, Jesper Bevensee Jensen, Idelfonso Tafur Monroy, "Gain transient control for wavelength division multiplexed access networks using semiconductor optical amplifiers," **Optical Fiber Technology**, 15, no. 3, pp 279-282 (2009)

Paper E Alexey V. Osadchiy, Kamau Prince, Neil Guerrero Gonzalez, Antonio Caballero, Ferney Orlando Amaya, Jesper B. Jensen, Darko Zibar, Idelfonso Tafur Monroy, "Coherent Detection Passive Optical Access Network Enabling Converged Delivery of Broadcast and Dedicated Broadband Services," **Optical Fiber Technology** (ACCEPTED FOR PUBLICATION) (2010)

Paper F Alexey V. Osadchiy, Kamau Prince, Idelfonso Tafur Monroy, "Converged delivery of WiMAX and wireline services over an extended reach passive optical access network," **Optical Fibre Technology**, 16, no. 3, pp 182-186 (2010)

Paper G Kamau Prince, Jesper Bevensee Jensen, Antonio Caballero, Xianbin Yu, Timothy Braidwood Gibbon, Darko Zibar, Neil Guerrero, Alexey V. Osadchiy, Idelfonso Tafur Monroy, "Converged Wireline and Wireless Access Over a 78-km Deployed Fiber Long-Reach WDM PON," **IEEE Photonics Technology Letters**, 21, no. 17, pp 1274-1276 (2009)

Paper H Alexey V. Osadchiy, Idelfonso Tafur Monroy, "Coherent detection for spectral amplitude coded optical label switching systems," **Microwave and Optical Technology Letters** (ACCEPTED FOR PUBLICATION) (2010)

Paper I Yongsheng Cao, Alexey V. Osadchiy, Xiangjun Xin, Xiaoli Yin, Chongxiu Yu and Idelfonso Tafur Monroy, "Recognition of spectral amplitude codes by frequency swept coherent detection for flexible optical label switching," **Photonic Network Communications** (ACCEPTED FOR PUBLICATION) (2010)

Paper J Alexey V. Osadchiy, Neil Guerrero, Jesper Bevensee Jensen, Idelfonso Tafur Monroy, "Coherent spectral amplitude coded label detection for DQPSK payload signals in packet-switched metropolitan area networks," **Optical Fiber Technology** (ACCEPTED FOR PUBLICATION) (2010)

Paper K Alexey V. Osadchiy, Xianbin Yu, Xiaoli Yin, Idelfonso Tafur Monroy, "Spectral Encoded Optical Label Detection for Dynamic Routing of Impulse Radio Ultra-Wideband Signals in Metro-Access Networks," **Microwave and Wireless Components Letters** (UNDER REVIEW) (2010)

Other publications during this project:

1. Yongsheng Cao, Alexey V. Osadchiy, Xiangjun Xin, Xiaoli Yin, Chongxiu Yu, Xu Zhang, Idelfonso Tafur Monroy, "Performance analysis of IM, DPSK and DQPSK payload signals with frequency swept coherent detected spectral amplitude code labeling," **Optical Switching and Networking** (UNDER REVIEW) (2010)

2. Janaina Laguardia Areal, Hao Hu, Christophe Peucheret, Evarist Palushani, Ricardo S. Puttini, Anders T. Clausen, Michael S. Berger, Alexey V. Osadchiy, Leif K. Oxenløwe, "Analysis of a Time-lens based Optical Frame Synchronizer and Retimer for 10G Ethernet Aiming at a Tb/s Optical Router/Switch Design," *14th Conference on Optical Network Design and Modeling* (2010)

3. Alexey V. Osadchiy, Jesper Bevensee Jensen, Palle Jeppesen, Idelfonso Tafur Monroy, "Colorless receiver enabling crossconnect based metro-access interfacing nodes for optically labelled DQPSK payload signals," *IEEE 21st Annual Meeting of the Lasers and Electro-Optics Society*, pp. 612-613 (2008)

4. Kamau Prince, Alexey V. Osadchiy, Idelfonso Tafur Monroy, "WiMAX radio-on-fibre in 118-km long-reach PON with deployed fibre," *35th European Conference on Optical Communication*, Paper 2.4.1 (2009)

5. Kamau Prince, Alexey V. Osadchiy, Idelfonso Tafur Monroy, "Full-duplex transmission of 256-QAM

WiMAX signals over an 80-km long-reach PON," *IEEE 22nd Annual Meeting of the Lasers and Electro-Optics Society, IEEE LEOS Annual Meeting Conference Proceedings*, pp 547-548 (2009)

6. Idelfonso Tafur Monroy, Kamau Prince, Alexey V. Osadchiy, Neil Guerrero Gonzalez, Antonio Caballero, Darko Zibar, Timothy Gibbon, Xianbin Yu, Jesper Bevensee Jensen, "Converged wireline and wireless signal transport over optical fibre access links," *14th OptoElectronics and Communications Conference* (2009)

7. Timothy Braidwood Gibbon, Alexey V. Osadchiy, Rasmus Kjær, Jesper Bevensee Jensen, Idelfonso Tafur Monroy, "Gain transient suppression for WDM PON networks using semiconductor optical amplifier," **Electronics Letters**, 44, no. 12, pp 756-758 (2008)

8. Alexey V. Osadchiy, Xianbin Yu, Xiaoli Yin, Idelfonso Tafur Monroy, "Spectral Encoded Optical Label Detection For Dynamic Routing Of Impulse Radio Ultra-wideband Signals In Metro-access Networks," *Access Networks and In-house Communications*, Paper AWC5 (2010)

9. Alexey V. Osadchiy, Xianbin Yu, Xiaoli Yin, Idelfonso Tafur Monroy, "Spectral Encoded Optical Label Detection for Dynamic Routing of Impulse Radio Ultra-Wideband Signals in Metro-Access Networks," *36th European Conference on Optical Communication* (ACCEPTED FOR PUBLICATION) (2010)

1. Introduction

Communications have always played a significant role in human life – ability to deliver orders, reports and other information has proven invaluable over the course of human history, becoming vital for the success of any state, business or military endeavor. People of the modern world rely on communications technologies more than our ancestors used to: it is said that a late XX-century weekly newspaper contains more information from remote locations than an average XIX-century person would receive over their lifetime.

Nowadays, telecommunications have become more than just means of delivering verbal images and audiovisual broadcasting it used to be in the middle of XX century: with the recent advances in computer technology, new forms of information have appeared, and with the maturing of the computers and other data-centered devices the amount of computer users in the World has increased from mere hundreds of researchers (in sixties) to about one in six to one in seven people on Earth in 2006 [1]. This, in turn, has greatly increased the amounts of information produced and consumed by the users around the World.

Telecommunication networks now serve as a means to connect all those computer users – via the access networks – World Wide Web and the Internet, and the infrastructure supporting the latter comprises

now a significant portion of all the telecommunication systems. Due to gradual and steady maturing of the telecommunication technologies caused by – and supporting – the growth in bandwidth demand, the cost of efficient and high-bandwidth telecommunication systems has gone down. This reduction in price has made high-bandwidth access systems feasible [2].

Two major trends could be observed for the past decade: rapid growth of the amount of broadband access subscribers and steady growth of the bandwidth demands of an average subscriber. While the former trend can be easily attributed to the reduction in broadband access subscription price, and thus it becoming more affordable, the latter is mainly dictated by the appearance and spreading of bandwidth-demanding services. These two trends have caused the service providers to search for effective low-cost access solutions. While re-use of already installed telephone lines and cable television cables seemed to be a perfect solution just a few years ago, it is now obvious that in the near future those technologies will not be able to satisfy the bandwidth demands of an average user. On the other hand, optical fiber-based technology provides vast bandwidth capacity and is already mature enough to make it affordable for a broadband access service subscriber [3].

But it would be erroneous to assume that the only issues faced by the telecommunications community are assembled in the area of providing high-bandwidth access services. The issue of growing bandwidth demand is perceived on all levels of network hierarchy, but the circle of dominant issues differs from level to level. The need for high-bandwidth long-range transmission systems was significant even 20 years ago, especially in scenarios where installing multiple transmission links would be unreasonably complex, expensive or otherwise unacceptable. One of the examples of such a scenario is transoceanic telecommunications: the first Transatlantic Telephone

cable (TAT-1) carrying 36 telephone lines was installed in 1955 and cost about 120 Mil. GBP (about 2.68 Bn. USD in 2010 prices), while the fiber-based TAT-8 installed in 1988 was already carrying 40.000 telephone lines and cost 335 Mil. USD (608 Mil. USD in 2010 prices) [4]. More fiber-optic submarine links were installed over the 2 decades since TAT-8 was installed, and the technology has proven invaluable for supporting transcontinental connectivity at high bandwidth [5].

1.1. Network hierarchy

Transoceanic links are a part of long-range networks with high bandwidth capacity – the core, or long-haul networks – spanning across continents and oceans, they are the highest level in network hierarchy. One level below the core networks are metropolitan area networks, often referred to as MANs or metro networks. Metro networks are directing the data streams from the core networks across large areas covering cities (thus the name) and sometimes even small countries. The next level of network hierarchy is the access networks, distributing the traffic directed by the metro nodes among the individual users. One way to represent this hierarchical division would be the following: core networks serve as highways for the data streams, while metro networks rout those streams at the termination points, and access networks perform the last mile distribution.

While core networks, as was mentioned above, have been initially built with great bandwidth capacities in mind, metro and access networks have been always somewhat lacking behind. There are several reasons for that, for instance, unlike core networks, metro networks also have to perform routing of the data streams, which increases the complexity of network equipment by an order of magnitude. Over the course of telecommunications history, data streams routing was first performed in form of circuit switching

(similar to that in mid-XX-century telephone exchanges), later replaced by a more promising technology – packet switching, which has gained great popularity in form of IP packet switching for Internet needs due to significant simplification of switching [6,7]. Another important issue of the metro networks is their cost sensitivity.

Cost considerations are even more prominent for the access networks – these networks are connecting subscribers to the global network, which means that the end user will have to pay for the line termination equipment (LTE) in form of subscription fee or connection fee. Cost of a given access system here determines whether it will be competitive or not, so service providers are interested in access systems cost reduction in one way or another. This issue is preventing the most advanced technologies from being implemented in the access networks: even now, access networks are considered a bottleneck on the trail from the end user to the core network [8].

1.2. Brief problem formulation

One way or another, both access systems and metro systems are following the direction of satisfying the demands for broadband connectivity by employing fiber-optics. This means that eventually the bare numbers of bandwidth per link and bandwidth per user (for metro and access networks, respectively) will achieve the desired values. But even if those values are achieved, two fundamental issues remain unresolved: access networks have to be linked to the metro networks, and metro networks have to be linked to the core networks.

Indeed, let us consider a medium-sized European city like Copenhagen with its suburbs, that is about 1.7 million people, or about 0.5 million households. Considering a central office (CO) serving 12 32-user segments at 10 Gb/s each (i.e., as per IEEE 10G-EPON standard [9]), which is not unrealistic for a densely populated area, taking both upstream and downstream into consideration, the total

bandwidth would be 240 Gb/s per CO. The total bandwidth demand of the region with an area of 2,561 km^2 will be 312.5 Tb/s: even considering some 100 metropolitan nodes serving the region, that is over 3 Tb/s per metropolitan node. Even for a lower bit rate ITU-T GPON standard supporting 1 Gb/s synchronous transmission [10] that is 24 Gb/s per metropolitan node: for a WDM-based 10 Gb/s access network, it would reach 10 Tb/s per node for the same scenario.

The purpose of the work reported in this thesis was to formulate, evaluate and research the solutions for the former issue. Indeed, as metro networks and access networks have different primary objectives they have to fulfill, the technological solutions they are based on also differ. This difference manifests in form of differing signal bit-rates, signal formats, principles of achieving multi-channel transmission etc. The conventional approach overlooks those aspects: interfacing is performed by terminating the data stream from the access network, processing it in the electrical form and then transmitting it into the metro network. The low efficiency of this approach was the main motivation to look into the issues of interfacing between the metropolitan area networks and the access networks.

1.3. Thesis contributions

During the course of this PhD project, six separate issues playing significant role in shaping the interface between the access and the metro networks have been looked into. As the network interfacing problem has been divided into sub-problems, it became possible to address different aspects of metro and access networks, developing solutions which would simplify the interfacing between the two. The papers included in this thesis are marked with the letters A to K and their main contributions are summarized below.

Paper A A novel concept for a colorless differential quaternary phase-shift keying (DQPSK) receiver is proposed. Wavelength

inflexibility of a conventional one bit delay interferometer-based DQPSK receivers is overcome through introduction of wavelength conversion of various wavelengths to a single wavelength.

Contributions of the author: provided practical assistance during setup assembly and results acquisition, provided expertise in wavelength conversion, proposed interleaving of pump wavelengths in order to ensure wavelength resources re-use, contributed with practical aspects of DQPSK-based network scenarios. Participated in manuscript preparation, made graphical representation of the results.

Paper B This paper proposes an optical crossconnect structure for metropolitan networks based on a colorless DQPSK receiver. Equipment reduction by the reuse of the wavelength conversion pump lasers for signal transmission and smart wavelength allocation is achieved.

Contributions of the author: proposed the concept of DQPSK optical crossconnects based on a colorless DQPSK receiver, provided practical assistance during setup assembly and results acquisition. Provided expertise in wavelength conversion, proposed interleaving of pump wavelengths in order to ensure wavelength resources re-use, analyzed the practical aspects of DQPSK-based network scenarios, coordinated manuscript preparation and submission.

Paper C A novel metropolitan access network architecture based on hybrid time-wavelength interleaving operation is proposed. The proposed architecture provides transparent transport of a fraction of upstream data through the metropolitan network, leading to network node equipment reduction. Network performance for the proposed architecture is assessed with the aid of custom traffic analyzing software and compared to that of a reference wavelength division multiplexed (WDM) network.

Contributions of the author: proposed the concept of transparent time-wavelength access network architecture. Formulated network functioning principles, provided expertise in network topologies and structure. Provided practical assistance during simulation results analyisis and participated in manuscript preparation.

Paper D Novel SOA-based gain transient compensation technique is proposed. Gain transient are due to the inherent nature of burst/time slotted operation of access networks, mainly on the upstream direction. The performance of the proposed technique is assessed experimentally. This technique appears to be more promising for field installation compared to the previously proposed highly-nonlinear fiber (HNLF)-based gain transient control technique [11] due to use of compact low-power semiconductor optical amplifier (SOA).

Contributions of the author: contributed expertise in practical assessments. Consulted on laboratory equipment operation, provided practical assistance in results acquisition and analysis. Consulted on gain transient applications in practical network scenarios and participated in manuscript preparation.

Paper E This paper introduces a novel concept of using DSP-assisted coherent detection for access networks. The use of tunable optical local oscillator simplifies end-user equipment unification as well as provides high flexibility for dynamic wavelength rearrangement. Introduction of broadcast channels allows for unified transport of user-specific and broadcast services over a single fiber and their reception in a single end-user device. Additionally, as coherent detection provides improved receiver sensitivity and high spectral selectivity, the splitting ratio may be increased to as high as 1:128 and beyond, reducing the fiber cable infrastructure.

Contributions of the author: proposed a solution for convergence in form of coherent detection-based PONs. Analyzed the coherent access scenario and performed preliminary analysis through modeling. Performed experimental validation of the concept. Made manuscript preparation and submission, collected feedback from experiment participants.

Paper F Converged transport of Worldwide Interoperability for Microwave Access (WiMAX) and wireline signals over an extended reach passive access network is proposed. Experimental demonstration of such converged mixed signal transport is performed, with the focus on maximum fiber link length as well as maximum provided wireless bandwidth capacity.

Contributions of the author: contributed expertise in practical assessments, consulted on WiMAX transmission. Coordinated the manuscript preparation and submission process.

Paper G Converged transport of various services over long-reach access networks is assessed. Experimental demonstration of converged transport of wireless and wireline signals is performed over a 78-km deployed fiber link.

Contributions of the author: provided expertise on wireless-over-fiber transport. Assembled the WiMAX-over-fiber setup and performed results acquisition and evaluation, consulted on wireless-over-fiber transport and access network scenarios. Participated in manuscript preparation, provided expertise in graphical results representation.

Paper H Novel method for spectral amplitude coded (SAC) optical label detection is proposed. The proposed method relying on coherent detection and digital signal processing (DSP) is described. Main advantage of the proposed label detection method is the flexibility for labeling system adjustment it provides. The basic principle is experimentally validated.

Contributions of the author: proposed novel concept for flexible SAC label recognition. Provided preliminary comparison of the technique to the existing techniques, performed a proof of concept experiment. Coordinated manuscript preparation and submission.

Paper I Novel method for SAC optical label detection is assessed. Simulation of optical fiber propagation of SAC-labeled signals is performed in order to estimate the method's performance.

Contributions of the author: proposed novel concept for flexible SAC label recognition. Provided preliminary comparison of the technique to the existing techniques. Contributed expertise in simulation and results assessments, provided consultation during manuscript preparation and submission.

Paper J A novel label detection method for SAC-labeled DQPSK signals for metropolitan networks is proposed. Experimental assessment of the proposed method is performed, demonstrating its good performance and compatibility with DQPSK payload signals. Flexibility of the label detection method along with its compatibility with DQPSK signals makes it a good candidate for high-bit rate DQPSK-based packet switched metropolitan networks.

Contributions of the author: proposed novel concept for flexible SAC label recognition. Provided preliminary comparison of the technique to the existing techniques. Performed a proof of concept experiment, coordinated manuscript preparation and submission.

Paper K A novel architecture of metropolitan access networks is proposed. The architecture relies on transparent transport within metropolitan and access network segments based on optical packet routing. Such network configuration allows for large coverage area of a single network node with the aid of simplified remote routing cabinets. The main goal of such a hybrid network is maximization of

coverage area with the minimal amount of equipment and distribution of various services to their respective users.

Contributions of the author: Proposed novel concept for flexible SAC label recognition. Proposed SAC labeling of UWB signals for simplified access systems and wireless signal distribution. Performed the first demonstration of SAC labeling and label detection for UWB signals. Coordinated manuscript preparation and submission.

1.4. Thesis outline

The next chapter, Chapter 2, provides a brief historical discourse introducing the concepts connected to metro networks, access networks, key differences between them and some historical trends playing significant role in the evolution of those systems. This chapter also contains definitions of key concepts and access network configurations.

Chapter 3 contains an overview of solutions to the issues associated with the metropolitan area networks and aiming at equipment complexity reduction. A colorless DQPSK receiver and an optical crossconnect (OXC) utilizing it are introduced as a means to reduce the QPSK-based metropolitan network equipment complexity. A transparent metropolitan access network employing colorless reflective modulators at the user end and time-wavelength slot based operation is introduced as a means to reduce both CO and metropolitan network equipment by creating an optical bypass for high-priority traffic.

Chapter 4 concentrates on the issues existing in the access networks. A technique for multi-channel amplification gain balancing is introduced – gain transients caused by burst-like traffic characteristic on the upstream direction of access networks are controlled in an SOA. This simplifies the upstream signal detection process. Coherent

detection based passive access network architecture is introduced as a means to increase the access link length and the number of subscribers supported by a single CO. Other means of increasing the access link range are discussed, and long-reach access network architecture supporting transport of wireless signals over optical fiber is proposed.

An evolution of metro and access network level solutions into a general system simplification concept is discussed in Chapter 5. Packet switching is regarded as the main opportunity for such a simplification at the level of metro networks. One of the optical labeling techniques for optical packet switching – spectral amplitude coding (SAC) – is considered, and a technique for label detection is proposed. This technique is then investigated for possible implementation in access systems for simplified data distribution between the access service subscribers.

The concluding chapter considers possible evolution scenarios and points at the future work that needs to be done in order to make such evolution possible.

2. Background

This chapter contains basic definitions of key concepts and technologies used in metropolitan and access networks. It also presents key features of metropolitan and access networks and some technologies used with networks. The aim of this chapter is to provide an introduction to the characteristic for metropolitan and access networks, required to outline the technological challenges associated with the signal and routing and the interfacing between them.

2.1. Metropolitan area networks

Metropolitan area networks, often referred to as “metro networks”, or abbreviated to MANs, are the link connecting the transport-centric core network to the user-centric access networks [12]. The main task of metro networks is to implement disaggregation of high-bandwidth data streams from the core networks and their distribution between the access networks. Metro networks usually contain a moderate number of network nodes, and their coverage usually varies from campus and village areas to large metropolitan agglomerates and even country regions or small countries.

Due to the metropolitan networks task range, several types of metro nodes can be distinguished within the MAN structure. Edge nodes can technically be considered a part of both core and metro networks; they perform interfacing between the core network and the metro network. A typical core network usually only has a few of those. Ideally, each

metro network should only have one interfacing point, however for the reason of network security and load balancing the number of such nodes in the real-life MANs is greater; furthermore, sometimes different edge nodes are interfacing the MAN to different segments of the core network.

While edge nodes connecting the MAN to the core network are necessary, the same is true for the other network junction: interfacing nodes are bridging access networks to the MAN. Unlike the metro-core interfacing case, the number of such interfacing nodes is much greater: sometimes it comprises the majority of the nodes in the MAN. The reason for such difference is the necessity to distribute the data streams between the access networks across the MAN coverage area.

Additionally to performing interfacing functions, most (if not all) metro nodes perform routing – direction of the data streams to particular destination nodes. In addition to performing routing in their nodes, large-scale MANs may also have balancing nodes or balancing functionality added to the generic routing node. Traffic load balancing is used for improving network performance, especially in the scenarios where current traffic load exceeds 50% of the maximum traffic capacity of the network.

Metro networks have different topologies, varying from tree and star topologies to mesh and ring ones. But since metro networks affect great numbers of users, reliability and ability to function even if several links have been severed is a priority. For this reason it is uncommon to see hybrid ring or mesh topologies with a number of bypass and redundancy links, double rings and other high-reliability topologies.

2.2. Access networks

Access networks are the networks bringing connectivity to the end user. A typical access network provides connectivity to a number of users concentrated in a relatively small area – a small town, a rural area community or a block of buildings in a densely populated city. While being the final link on the way from the core network to the user, access networks are the networks with the highest cost sensitivity which is dictated by a much greater concurrence than on the other network layers. The investments required to enter the field are much lower due to lower equipment complexity and cost, but at the same time the necessity of being more competitive enforces lower retail prices, which in turn reduces the returns [13]. At the same time access networks consist of multiple distribution links and are operating significant data streams obtained from the users and going to the users. This requires large amounts of equipment and infrastructure, so different approaches aiming to reduce the capital costs of the access networks have been proposed over the course of optical access systems development.

2.2.1. Active networks

One of the more straight-forward implementations of an optical access network is an active network. The name – active – comes from the fact that there are active components (components that require electrical powering, back-up, cooling, etc.) in the link between the CO and the end user. An example of such an active network would be a fiber link from the CO to a cabinet located in a block of flats. The link from the CO is terminated at the cabinet and the signal is then distributed from a multi-port router to the end users.

2.2.2. Passive optical networks

Passive optical networks do not have any active components in the link between the CO and the end user. The main reason for such a network configuration is the optimization of the economic aspects: active equipment consumes much power, has relatively low reliability and requires housing and maintenance, all of which contributes to the network costs. First passive access network development attempts can be dated back to 1980's [14,15], but until recently installation of optical fiber for access was not too widespread. In a passive optical network (PON), end user connectivity is provided via a common fiber infrastructure, consisting of common fiber, splitting device and individual distribution fibers, delivering the connectivity to the end users. In the last decade, PONs have become a very attractive network topology, and since then have been widely implemented around the World [16,17].

The key feature of PONs is the use of a physical point-to-multipoint configuration, where one fiber is shared by multiple users. In order to do so, certain measures need to be taken in order to ensure that the user-specific signals can coexist in the same fiber infrastructure without collisions and interference. Various channel multiplexing technologies serve this purpose.

2.2.2.1. PON technologies overview

Initially TDM was used as a means for channel multiplexing in passive optical access networks [18], but since the technology has proven to possess a number of disadvantages, alternative multiplexing techniques have been proposed. One of the first PON standards, the APON (ITU-T G.983.1 [19]) included support for ATM transmission, similar to that used in the TDM-based core networks. APON systems operated with two separate wavelength (λ) ranges – 1260 to 1360 nm

and 1480 to 1580 nm, for upstream and downstream transmission, respectively, although dual-fiber operation was also possible. This type of access networks was mainly used for business applications (thus the ATM support).

A more advanced version of APON, BPON – Broadband PON (ITU-T G.983.4 [20]) was a standard based on APON. It added support for WDM, dynamic bandwidth allocation, video overlay support and increased survivability. BPON was succeeded by Gigabit PON (G-PON, ITU-T 984 [21-25]) that provided support for Ethernet packet transport and compatibility with Gigabit Ethernet. Another standard with similar characteristics, Ethernet PON (EPON, IEEE 802.3ah [26]) was an Ethernet-based standard. Over 25 million EPON subscribers have been installed worldwide.

A 10 Gb/s-capable upgrade for EPON is now being developed as 10G-PON (IEEE 802.3av [27,28]): providing partial compatibility with EPON, it is supposed to become commercially available in 2010. Additionally, attempts to formulate the requirements and parameters required to implement 100 Gb/s-capable passive access networks are being made [29].

2.3. Multiplexing technologies

Both metropolitan and access networks operate at high bit-rates. Multi-fiber links between network nodes are often used in metropolitan networks, but in order to provide sufficient bandwidth, various techniques for transmitting multiple channels over a single fiber are required. The most common technology for this is wavelength division multiplexing (WDM) [30] where a number of channels is transmitted on different wavelengths. Other multiplexing techniques being considered for implementation include time division multiplexing (TDM) [31] – a technology employing interleaving the channels in time domain, and optical code division multiplexing

(OCDM), in which [32-33] special keys are used to extract user-specific data.

2.3.1. Time division multiplexing (TDM)

The principle of TDM is quite simple: each channel in the system has a time slot within which it can transmit data. While one channel is being transmitted, the remaining channels are being idle. While being quite a common technology for various conventional applications, optical version of TDM is sometimes considered an outdated technology [34] which has an array of characteristic issues that prevent it from becoming widespread.

In order to transmit N channels with a bit-rate of B bits per second (b/s) in a TDM-based system, each channel has to be compressed by N times, which turns it into a channel with a bit-rate of $N \times B$ b/s. This leads to another issue: a receiver has to have a bandwidth sufficient to receive signals at a bit-rate of $N \times B$ b/s in order to receive an individual channel with the original bit-rate of B b/s.

Indeed, if we consider a metro network covering the area of an average city, a figure of 64 10-Gb/s channels per fiber would not be too far from reality. Applying the statement from above, this gives us an actual bit-rate of 640 Gb/s per channel: this makes a receiver for such a signal a complex system: current commercially available photodetectors are capable of receiving up to 40 Gb/s [35] and 120-Gb/s photodetectors are at their development stage [36]. An alternate approach to this issue is de-multiplexing the TDM channel by employing special techniques and de-compressing the obtained signal to convert it to its original bit-rate [37]. While this may be acceptable for some core network systems, this is barely an option for the metro networks due to complexity and cost considerations.

Another issue characteristic to the TDM-based systems is the upstream signal power level variation at the receiver: it is caused by signals originating from different sources and experiencing different transmission losses. Such a variation introduces additional degree of complexity for a multichannel TDM receiver – specific measures have to be taken to enable different threshold profiles for each individual channel and dynamic switching between those profiles.

2.3.2. Wavelength division multiplexing (WDM)

WDM technology employs channel multiplexing by arranging the channels in spectral domain. The main advantage of WDM systems comes from the fact that an optical fiber has a tremendous bandwidth capacity – about 50 THz [38], although only about 10 THz of frequency range lying in the wavelength region between 1490 nm to 1635 nm range is being commonly used. This limitation of the frequency range available for use in current-generation fiber-optic systems is caused by several limiting factors, such as silica absorption peaks [39], availability of sources and receivers and availability and technology maturity of the optical amplifiers [40-42].

Initially channel selection was performed on the receiving end of the transmission link by employing a technology commonly used in the wireless systems adapted to the fiber-optic systems – coherent detection. Much research was conducted in this area in 80's [43], but certain challenges associated with the nature of optical sources made those systems unreasonably complex and prevented them from ever leaving the labs.

WDM technology became popular again in early 90's when a simple planar waveguide structure – an arrayed waveguide grating (AWG) – has been proposed as a channel multiplexing/de-multiplexing device

[44]. While being a (de-)multiplexer, an AWG can also be produced in a configuration allowing it to be used as a wavelength routing device [45]. WDM-based systems have penetrated all levels of network hierarchy as WDM has become a mature technology.

2.3.3. Code division multiple access (OCDM)

OCDM technology relies on correlation-based extraction of channels from a super-channel which is a polynomial superposition of individual channels and has noise-like properties making it robust against transmission impairments [32]. This technology became popular for implementation for cellular systems and other wireless systems where there is a need to support a large number of channels in presence of stringent spectrum limitations. The technology is making its way into optical communications in form of OCDMA [33], but is still far from being a mature technology.

2.4. Conclusions

In the last few decades it became obvious that use of fiber infrastructure exclusively for the transmission of baseband data is prodigal and unreasonable: an average end user uses voice and/or audiovisual communication services (ranging from phone to voice over (internet protocol) IP (VoIP [46])), broadcast services (like television broadcasting), file sharing (BitTorrent [47] etc.) with similar up- and download rates. Additionally, interest in wireless signal distribution over fiber is growing and bandwidth-demanding services such as IP television (IPTV [48]) are appearing. In the light of those events, introduction of high bandwidth capacity optical access networks becomes inevitable, but it also has a prospect of greatly increasing the load put on COs and metropolitan networks. This

creates a need for high-efficiency metropolitan to access network interfacing solutions as well as solutions in metropolitan and access network layers which would help balance the load on network nodes and simplify the overall network configuration.

3. *Metropolitan network level solutions*

Metropolitan area networks [49] usually contain a moderate number of network nodes, and the main task of such nodes is the distribution of data streams that flow through the metropolitan network. One of the main challenges encountered at this level of the network hierarchy is the need for vast amounts of data processing required to route the data packets to their respective destinations, and this issue becomes more complex when interfacing with adjacent access and core network segments is taken into account.

The increased amounts of data processing in turn means that the MAN equipment becomes more and more complex: transport, processing and buffering massive volumes of data requires power-hungry bulky equipment, and consequently, both installation cost and maintenance cost of such equipment additionally scales up with growing network scale and bit rates. This means that the main direction of research capable of solving the spectrum of issues associated with metropolitan networks should aim for a common goal – equipment complexity reduction.

3.1. Colorless operation of DQPSK receivers

As metropolitan area networks usually cover significant areas – like towns or cities – and the number of network nodes is not so large, the distances between adjacent metropolitan area nodes usually are within the 40-60 km region and may occasionally reach 120 km. At the same time, the bit rates typical for metropolitan networks are quite high and are usually 10-40 Gb/s [50], and current research in that area is aiming to reach 100 Gb/s in the near future [51]. Additionally, multi-channel operation is required in order to accommodate for the significant data streams typical for the access network segment as single-channel systems are incapable of providing sufficient bandwidth capacity.

Key requirements applied in the selection of signal format used for metropolitan networks include high spectral efficiency; compatibility with the International Telecommunication Union (ITU) grid for WDM systems, specifically the 50 GHz grid and low signal degradation after several cascaded WDM filtering stages.. Over the decades of research in optical communications, it has been proven that phase modulation formats provide high robustness against transmission impairments [52]. Additionally, multi-level phase modulation formats provide improved spectral efficiency.

Quaternary phase-shift keying (QPSK) is a four-level phase modulation format which is considered to be the preferred candidate for scenarios typical for the metropolitan networks; each QPSK symbol carries 2 bits [53]. However, multiple wavelengths in conjunction with wavelength routing are used in metropolitan networks. This means that signal bursts with different wavelengths may arrive at a given network node at different moments of time and

have to be received and processed in order to be forwarded to the adjacent access and/or core network segments.

In contrast to intensity-modulated signals, phase-modulated signals may not be received with a simple photodetector: they require self-homodyne or coherent detection in order to extract the information carried by the phase of the signal; one-bit delay self-homodyne demodulator is one option. The delay demodulator relies on an interferometric structure [52] to create a phase off-set in order to detect the signal. The phase off-set of such a delay interferometer is wavelength dependent, which dictates use of multiple receivers, one for each wavelength in order to receive all the channels supported by the network node.

However, as mentioned in the introduction of this chapter, the main goal supporting the efficient interfacing between metropolitan and access networks is the overall equipment simplification and reduction. This therefore encourages the development of a solution that would help reduce the amount of equipment used to support multi-wavelength burst-mode reception. Tuning of the demodulator at the burst arrival rate requires fast control and feedback which would prove difficult to realize in practice. A more promising solution to the problem, would be to wavelength convert all incoming packets to one common wavelength.

Such a solution is proposed in ***Paper A***: three differential quaternary phase-shift keying (DQPSK) signals are converted to a single wavelength. Conversion to the receiver wavelength was achieved through the use of a four-wave mixing (FWM) process. Wavelength conversion was performed in two different media: highly-nonlinear fiber (HNLF) [54] and semiconductor optical amplifier (SOA) [42]. The spectra of the signals, pumps and their respective FWM products are presented in Fig. 1.

As demonstrated in ***Paper A***, the converted signal can be received error-free, and the power penalty on any single channel from wavelength conversion was observed to be between 0.7 dB and 1.6 dB for the HNLF case and between 4.1 dB and 5.6 dB for the SOA case. The colorless DQPSK receiver presented in ***Paper A*** has to become a part of a more complex structure in order to become a useful part of a metropolitan network. ***Paper B*** is considering a metropolitan access network scenario where DQPSK-modulated signals are used in a packet-switched network.

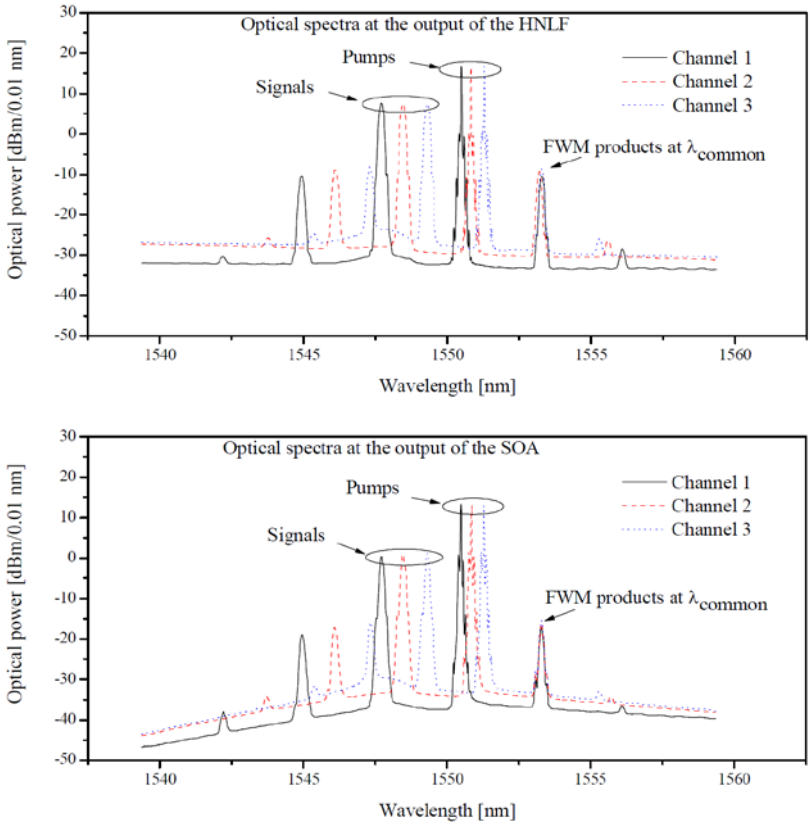

Fig. 1. Optical spectra at the output of the HNLF and SOA-based wavelength converters: pumps, signals and their FWM products used for detection for all 3 channels are marked with arrows.

Modern optical telecommunication networks are foreseen to rely on packet switching as a method of routing data streams between end users [55]. This trend is supported by the continued implementation of TCP/IP support for reliable delivery of data-intensive media delivery services including voice-over-IP, video streaming and peer-to-peer file transfer. Previous-generations of circuit switched solutions will not efficiently support this emerging need for the handling of packet oriented traffic. Therefore, optical packet switching solutions are believed to better exploit the optical network bandwidth, to give higher throughput and to offer greater flexibility [56].

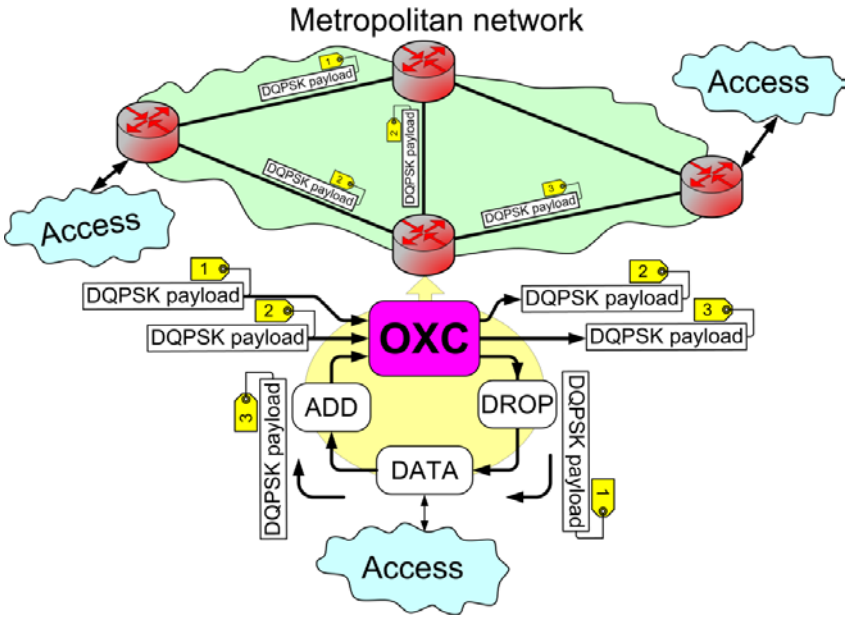

Fig. 2. Network scenario: DATA – Data storage and processing block.

Fig. 2 presents an optical packet switched network scenario: DQPSK-modulated payload signals are used for data transport, optical packet switching is performed in optical crossconnects (OXC): payload signals are labeled optically, and the label information is extracted in

order to perform payload routing. In case the destination of given packet is the access network adjacent to the OXC, the packet is routed to the colorless receiver in the ADD/DROP block.

Pump and signal wavelength allocation across the system allowed the pump lasers needed for the colorless DQPSK receiver in the DROP to be reused for DQPSK signal transmission in the ADD part of the OXC (Fig. 3) which helps reduce the number of active components used at the network node.

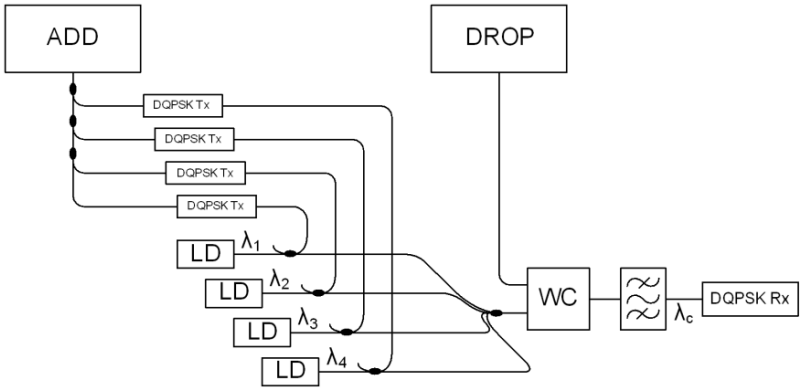

Fig. 3. Reuse of pump lasers.

3.2. Transparent metropolitan access topology

The conventional arrangement of the Metro and access networks includes a significant amount of terminations. Each termination involves signal being amplified (to a sufficient power level for detection), detected, processed for error correction and stored in an electronic buffer. In practice, this often occurs in situations, where the packet would then be retransmitted in the network with a similar signaling standard (for instance, from an optical network unit (ONU)

at one CO to an ONU at another CO), or it would be forwarded through metropolitan network to the edge node for transport in the core network.

In this case, the retransmission operations – optical-to-electrical-to-optical (O-E-O) conversions – are not justified: each O-E-O operation comprises of signal detection, processing and retransmission, requires a significant amount of equipment, and also demands massive amounts of energy.

This issue can be resolved by introducing partial transparency to the metropolitan access network: certain portions of the network traffic would thus be forwarded to the destination without intermediate processing. ***Paper C*** presents a realization of such transparent network architecture. The concept of the architecture is based on the fact that in most cases, there are only a small number of destinations which contribute to the most of traffic generated by the ONU can be distinguished: is most cases, 3-4 destinations contribute 80-95% traffic generated [57].

Transparent routes are created for such dominating destinations: by utilizing reflective semiconductor optical amplifier (RSOA) based colorless transmitters [58] at the ONUs and time-interleaved CO-generated seed light, ONUs are operating in a time-wavelength fashion, modulating the seed light at a particular wavelength with the packets that have a destination associated with that wavelength. The time-wavelength slots are then rearranged at the CO to form continuous WDM channels. Certain channels containing the packets going to the dominating destinations are routed through the metropolitan network transparently, while the remainder of wavelengths is treated normally.

Paper C also contains performance analysis results obtained by modeling various scenarios for network architectures and comparing

the results to the reference WDM PON performance. For a 3-wavelength system, the proposed time-wavelength architecture exhibited better performance than the reference WDM PON, and the performance improvement grew with the network load, and for full load comprised 20% for ring topology and 15% for star topology.

The number of wavelengths used in the system is a matter of discussion and optimization: usually the first (by the amount of traffic going to it) destination comprises up to 50-70% of the overall traffic, with each subsequent destination comprising less and less, and the first 3-4 destinations cumulatively comprising 80-95% of total traffic load. When only 2 wavelengths are available, 50% of the ONU's bandwidth will be dedicated to the transparent transport, which may be good in certain situations, but traffic pattern variation may lead to situations where the ONU effectively loses 50% of its bandwidth. To avoid this problem, wavelength number has to be selected carefully: when more wavelengths are used, a lower percentage of ONU bandwidth may be dedicated to a single wavelength. The solution to this issue would be dedicating about 15-25% of total bandwidth to the dominating destination (4-6 wavelengths) and redistributing excess portions of traffic to this destination between the common wavelengths.

3.3. Conclusions

One of the main limiting factors for interfacing between high-bit rate access networks and metropolitan networks is the high complexity of the equipment which is required in order to convert massive data streams generated in the access networks to the signaling format of the metropolitan networks and vice versa; and the complexity of the equipment required in order to distribute the data streams in the metropolitan networks.

Two solutions were presented in this chapter. The first solution addresses the wavelength dependence of DQPSK receivers. DQPSK is the signal format typical for metropolitan networks, which makes this dependence a sensitive issue. A colorless DQPSK receiver concept based on wavelength conversion to a common wavelength is proposed in ***Paper A*** as a means to reduce the complexity of metropolitan node equipment. The colorless receiver concept is then applied to a typical optical packet switched metropolitan network scenario and an OXC structure using such colorless receiver was proposed and discussed in ***Paper B***. The equipment reduction provided by the colorless DQPSK receiver concept is reinforced in the OXC concept by reusing pump lasers for transmission of locally-generated data.

The second solution discussed in this chapter was the transparent network architecture presented in ***Paper C***: the proposed architecture utilized smart time-wavelength slot based operation that allows transparent transport of some portion of traffic through the access and metropolitan networks. Such transparent transport provides an optical bypass of intermediate nodes between the data source and its destination. In terms of network node equipment this means reduced number of equipment at the intermediate nodes as no O-E-O conversion is involved.

This makes both proposed solutions promising steps towards overall reduction of network equipment and its complexity; nearing the ultimate goal of low-cost effective interfacing between metropolitan and access networks. However, access networks also present challenges on that path: there is much space for additional optimizations, and further investigation of the possibilities to extend the access network range and functionality is required. The converged transport of baseband and wireless services over a common long-range fiber infrastructure is expected to help reduce the overall network complexity.

4. Access-level issue solutions

The main purpose of access networks is to facilitate the distribution of data streams originating at the COs and destined for end user equipment – the optical network units (ONUs) – and collection of the data streams from them. This influences the challenges associated with them: network reach, services provision and cost optimization.

4.1. Multi-channel amplification for extended-reach access networks

Access networks support large numbers of end users at the customer premises: they may be realized in different topologies but the most common one is a point-to-multipoint links in which a single distribution fiber originating at the CO is connected to an intermediate splitting point from where a number of individual fibers connect the end users. Each individual fiber is then terminated at an ONU. Such a configuration helps optimize the fiber infrastructure: it requires less cabling then a point-to-point configuration directly from the central office to the end users. The weak point of such an approach is the additional losses which are incurred in the use of optical power splitters: passive power splitters are used for TDM-based systems, while WDM-based systems use arrayed waveguide grating (AWG) multiplexers/demultiplexers to distribute different wavelength channels along separate output fibers. The losses at the splitting point therefore limit the maximum split ratio of the access network: a

typical split ratio for EPON systems is 1:16 [26], and 1:32 for BPON and G-PON systems [20, 21] (1:64 ratio may be available at the expense of network reach).

At the same time, the range of optical access networking system will invariably affect the viability of commercial implementations; system developers are therefore motivated to maximize the coverage area supported in any given scheme in order to provide services to a reasonably large number of users, and minimize the number of Cos, in order for network installations to provide an attractive return on investment. In order to achieve greater range, the network has to be engineered to accommodate increased optical power losses. There are several options for compensating transmission losses and power splitting: increased transmitter power, increased receiver sensitivity, link amplification, reduced fiber losses etc.

It should however be noted that additional expenses are associated with implementing high-sensitivity receivers; high-power transmitters require more sophisticated thermal control systems which also leads to increased equipment cost; additionally high signal power induces non-linear effects in the transmission link, which causes degradation of the overall system performance. Using the same transmission fiber to provide link amplification turns out to be an economically viable solution: all the channels are simultaneously amplified by a single simultaneously. Raman amplifier-based distributed amplification [59] or EDFA-based localized amplification [60] schemes may be employed in case of WDM systems where multiple wavelength channels have to be amplified simultaneously.

However, in the upstream direction the optical power level of the signals aggregated at the AWG-based splitting (coupling) point from the various ONUs will differ considerably. This is caused by the differences in link length-induced optical power losses, coupling losses, as well as non-uniform power splitter losses and launch power

variations [61] experienced by the signals from different users. This introduces severe upstream gain transients due to sudden variation of optical power at the input of the backhaul EDFA or Raman amplifier.

Such optical power level transients are a strong degrading factor for the system operation as they introduce errors in the signals received at the CO: power overshoots induce non-linear effects and insufficient receiver power results in a degraded optical signal-to-noise ratio [62]. This dictates the need for gain transient control of some sort. ***Paper D*** presents a demonstration of gain transient control for WDM access networks. In the proposed setup, a semiconductor optical amplifier (SOA) integrated with the WDM receiver is used not just as a pre-detection amplifier [63], but also is used to restore the signal in the presence of such gain transients.

While a number of gain transient control methods have been proposed in the past [64-68], the scheme proposed in ***Paper D*** was the first demonstration of BER results obtained for 10 Gb/s fiber transmission with a near-saturated SOA based gain transient control applied. Successful use of an SOA to restore the system performance after its degradation due to gain transients makes the implementation of such a scheme in WDM access systems attractive: the gain transient-induced penalty was reduced from 2.3 dB to mere 0.2 dB when a holding beam was used to optimize the SOA performance; although it was demonstrated in a 1550 nm band SOA, this solution can also be implemented for the 1310 nm band.

4.2. Converged delivery of services for access networks: wireline and wireless signal transport over fiber

Numerous services relying on physical infrastructure to deliver signals are being used on regular basis. An average access network subscriber typically uses a multitude of telecommunication services: copper-wire telephone connections are not uncommon; television services are received via decimeter-wave (dm-wave) television antennae, satellite dishes or cable television (CATV) coaxial cables and so on. Additionally, the demand for bandwidth from the individual access network user is being stimulated by novel bandwidth-intensive network services like high-definition television (HDTV), high-definition (HD) video-on-demand, peer-to-peer file sharing, telecommuting, remote backup and storage services etc.

This trend has also reached the wireless access networks, causing an increase in supported bit rates. Multiple broadband data transport-oriented wireless technologies have recently been developed. Such wireless access technologies include Worldwide Interoperability for Microwave access (WiMAX) [69-72] and 3rd Generation Partnership Project long-term evolution (3GPP LTE) [73]. These broadband wireless access technologies gain interest and popularity due to the fact that they provide a degree of mobility to the end user, allowing for real-time functioning of information-sensitive applications – both for business and for entertainment.

While support for fixed and mobile wireless access provided by WiMAX technology makes its use very attractive for the operators and the subscribers, it also poses a challenge: massive data streams generated by and destined to customer premises equipment (CPE) and hot spot base stations have to be distributed to and from the COs.

On the other hand, optical fiber-based communications systems are capable of providing significant data bandwidth; they also support multi-channel broadband operation by employing WDM. This makes fiber infrastructure an ideal platform for the converged delivery of various user-specific and broadcast, baseband and wireless services to the end user.

Fig. 4 shows an experimental setup featured in ***Paper G***: such a converged delivery was performed for wavelength-multiplexed channels over existing deployed fiber infrastructure. Simultaneous transport was performed for four 21.4 Gb/s baseband DQPSK channels; two radio-over-fiber (RoF) channels modulated with 250 Mb/s binary phase-shift keying (BPSK) on a 5-GHz RF carrier; a 3.125 Gb/s impulse radio ultrawideband (UWB) [74] channel; and a WiMAX standard compliant RoF channel modulated with a 12 Mbaud 256-position quadratic-amplitude modulation (256-QAM) on a 5.8-GHz carrier. All the channels were successfully received after a 78-km deployed fiber transmission; the 12 Mbaud 256-QAM WiMAX signal was transmitted in an air link after fiber transmission prior to detection, validating the long-reach access network and the converged concept declared as the main goal of the experiment described in ***Paper G***.

Paper F features a successful demonstration of converged transport of 100 Mb/s WiMAX signals over 118.8 km of single-mode fiber (SMF): an additional 40-km SMF distribution link was added to the experimental setup used in ***Paper G*** without additional optical amplification. The featured PON link length exceeded all the previous demonstrations at the moment of publication [75].

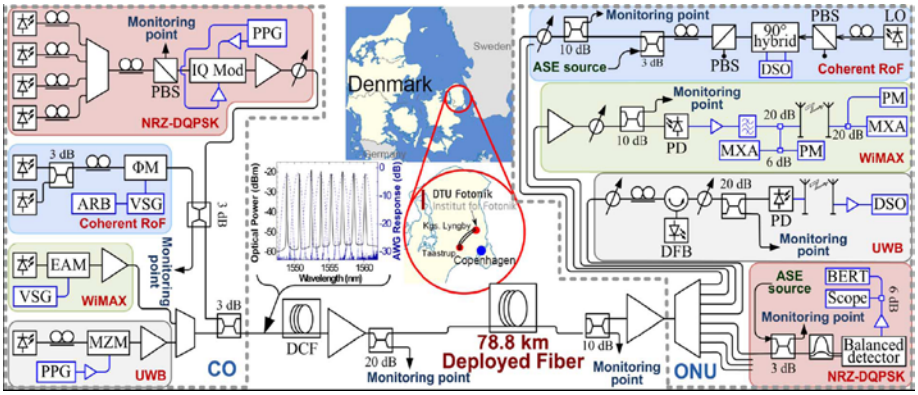

Fig. 4. Detail of the experimental setup. PPG: pulse pattern generator; PBS: polarization beam splitter; PM: optical phase modulator; ARB: arbitrary waveform generator; VOA: variable optical attenuator. ASE added to evaluate system OSNR sensitivity for phase-modulated signals: precompensating DCF-implemented decorrelation of RoF and NRZ-DQPSK signals. (Inset) Spectra of launched WDM optical signal (solid line) and AWG response (dashed line).

Bi-directional transmission of 256-QAM modulated WiMAX-compliant signals in the unlicensed 2.4 GHz band over 35-km and 80-km non-zero dispersion-shifted fiber (NDSF) PON links was also reported in ***Paper F***. Successful 64 Mb/s synchronous bidirectional transmission of WiMAX signals over an 80-km NZDSF access fiber with subsequent air transmission was achieved; additionally, asynchronous 100/64 Mb/s transmission (for uplink and downlink directions, respectively) was successfully performed for the same experimental setup, which is presented in Fig. 5.

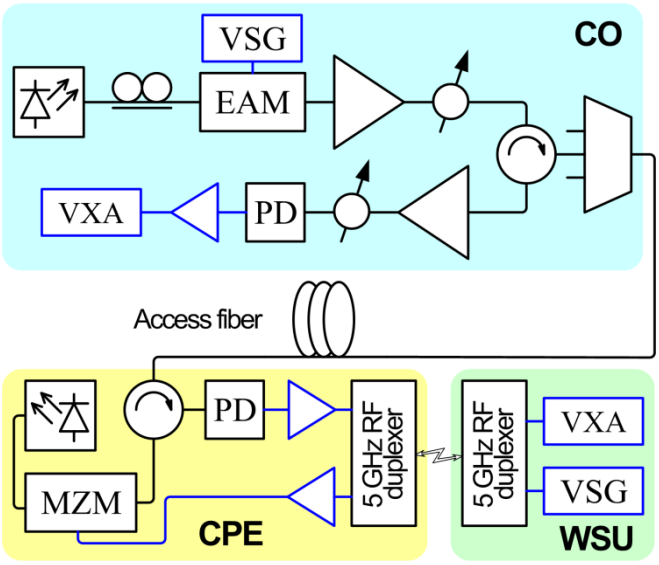

Fig. 5. Long-reach PON link with bi-directional WiMAX transmission. CO – central office; CPE – customer premises equipment; WSU – wireless subscriber unit; VSG – vector signal generator; EAM – electro-absorption modulator; VXA – signal analyzer; MZM – Mach–Zehnder Modulator; and PD – photodiode.

4.3. Coherent detection for broadcasting enabled passive access networks

The idea to use coherent detection for optical fiber transmission appeared in the late 70's. Such an attempt to adopt a mature wireless technology for optical communication was caused by the fact that it provides certain advantages that make its use promising for long-range transmission of wavelength-multiplexed optical signals. Following is a basic explanation of the optical coherent detection principle: the transmitted optical signal can be expressed in complex notation as follows:

$$E_S = \sqrt{P_S} exp(\omega_S t + \varphi_S) \quad (1)$$

In this equation (1), P_S represents the optical power in the signal, ω_S is the angular frequency of the optical signal, φ_S represents the phase-encoded information. In order to perform coherent detection, a local oscillator (LO) is required; the light from the LO can be expressed in complex notation as:

$$E_{LO} = \sqrt{P_{LO}} exp(\omega_{LO} t + \varphi_{LO}) \quad (2)$$

The two are mixed, and the mixing products are received with a photodetector. Since a photodetector responds to the optical intensity, the optical power incident at the photodetector can be expressed as: $P \sim |E_S + E_{LO}|^2$ and comprises:

$$P(t) = P_S + P_{LO} + 2\sqrt{P_S P_{LO}} exp(\Delta\omega t + \varphi_S - \varphi_{LO}) \quad (3)$$

In equation (3), P_S and P_{LO} represent the input optical powers of the signal and the LO respectively, and $\Delta\omega$ is the angular frequency difference between the optical signal and the LO, and the difference frequency is expressed as $\Delta\omega = \omega_S - \omega_{LO}$.

If we analyze the expression in equation (3), we can see that there are two types of mixing products – constant ones which manifest in form of a DC bias in the photodiode, and the one that carries signal information. The first advantage comes from the fact that the LO optical power can be significantly higher than that of the received signal, providing improved sensitivity to the coherent receiver. The second advantage is the spectral selectivity innate to the coherent detection-based receivers: by adjusting the LO frequency, the frequency of the signal received by the photodetector can be selected.

An immense amount of research was conducted in this area in the 80's [43] as optical coherent detection was considered the main candidate

technology for long-range multi-channel transmission. Unfortunately, the level of technological development of that time was insufficient to create commercial-grade optical coherent detection-based systems: linewidth, phase noise and wavelength instability of the laser sources (both LO and signal sources) are significant contributors to signal quality degradation. The parameters of laser sources of that time were not satisfactory – to the point where such systems would be impractical. The emergence of optical amplifiers and AWG-based WDM systems in the 90's put the development of coherent detection-based systems on hold.

A new stimulus for development of coherent detection-based systems was given in the beginning of the XXI century: laser source fabrication technology reached sufficient maturity to allow low phase noise narrow-linewidth sources to become commercially available at reasonable cost [76]; major advances in microelectronics components made high-speed digital signal processing (DSP) [77] possible. High-quality sources with reduced phase noise, wavelength instability and linewidth significantly reduced the amount of impairments to be taken care of, and high-speed DSP relying on sophisticated prediction algorithms became capable of compensating for such impairments [78]: compensation of transmission impairments with no in-line dispersion compensation has been demonstrated [79].

Such advances in optical coherent detection suggest that the technology will reach its maturity in the foreseeable future: mass production of one of the key components of optical coherent receivers – the optical hybrid [80] – will cause its price to drop, stimulating subsequent system cost reduction. Additionally, coherent detection based systems are capable of detecting the full spectrum of optical modulation formats, and DSP allows detection of all those formats after necessary detection software adjustment. This makes coherent detection an attractive technology even for access networks of the

foreseeable future. While having several advantages over conventional WDM systems – increased receiver sensitivity and localized wavelength selectivity – coherent detection based systems have also a disadvantage: in order to use localized wavelength selectivity, power splitters have to be used at the splitting point: splitting losses are proportional to the split ratio of the systems, each multiple of 2 adding 3 dB losses: for a 1:32 splitting point it will comprise 15 dB and for a 1:128 splitting point – 21 dB; AWG-based WDM demultiplexer's losses are only about 8 dB.

However, as mentioned above, coherent detection-based systems have improved receiver sensitivity, which to some extent compensates for the increased splitting losses, but what is more important – with the use of a tunable LO source, any wavelength channel may be selected. This makes network reconfiguration much simpler: unified optical network units (ONUs) could then possibly be installed at the customer premises, these could then be tuned to the desired wavelength channels by software programming. Current generation tunable laser sources have very high tuning rates [81,82], making multi-channel broadcast service receivers possible.

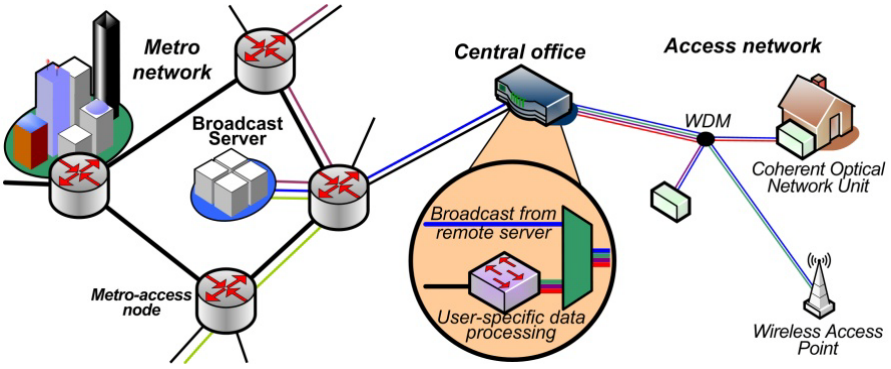

Fig. 6. Coherent detection based PON with broadcast service support.

Paper E features a concept of a passive access network supporting broadcast service distribution from a remote broadcast server (Fig. 6).

The broadcast stream in a network with such architecture is distributed from the broadcast server and is multiplexed with the user-specific data streams at the CO; common stream is then distributed between the end users normally. A passive optical power splitter is used to deliver a duplicate of the common stream to each user. Channel selection is made possible through the use of tunable LO based coherent receivers in an ONU: dynamic switching between the broadcast channels greatly extends the spectrum of services available to the subscriber.

The experiment presented in ***Paper E*** simulates such a scenario: multiple channels with different signal formats and of different nature (baseband and wireless) are transmitted in a common stream and are received with the coherent receiver. Four 10 Gb/s amplitude shift keying (ASK) and four 250 Mb/s PSK RoF channels with the radio frequency (RF) carriers at 5 GHz were representing the user-specific channels, and four 10 Gbaud DQPSK channels represented remotely-generated broadcast channels.

In order to represent the remote distribution of the broadcast services, the DQPSK signals were transmitted over 78.8 km of deployed SMF fiber representing the broadcast distribution link, and then multiplexed with the user-specific channels. The common stream was then transmitted over 34 km of SMF representing the distribution fiber with the user-specific fiber link. Coherent detection with off-line DSP support was applied to all signals, and successful detection of all the channels transmitted this way was observed. This validated the concept of a coherent detection based PON with distributed broadcast support.

4.4. Conclusions

Access network-based solutions have been introduced in this Chapter: extended range PONs, converged transport of services, transport of wireless signals over PONs and coherent detection based PONs with broadcast service support have been presented. Each of those solutions provide access networks with benefits that reduce the overall access network cost in the end: PON range extension helps reduce the amount of COs by increasing the area served by one CO; converged transport of various services including the wireless signal transport helps reuse common fiber infrastructure to satisfy a wider spectrum of user needs at a lower cost; and coherent detection helps add broadcast services to this spectrum of services sharing the infrastructure.

While simplified solutions both for metropolitan and access networks have been proposed, an approach which treats metropolitan and access networks as a common entity is required to maximize the network simplification. Such an approach will be discussed in the following Chapter.

5. *Unified approach: metropolitan access networks*

As it was mentioned in the previous Chapter, treating the metropolitan network and the access networks connected to it as a single entity can help achieve maximal optimization of the overall network complexity. On the other hand, treating them as independent and isolated entities solves only existing issues without addressing the underlying root causes and could be called ‘symptomatic treatment’. This Chapter attempts to address these two networks with significantly different properties and tasks as one common entity, and uses the holistic approach to develop and propose solutions for improved network interfacing.

5.1. Optical packet switching

Packet switching has become a widely implemented in electronic communication systems: it turned out that packet switching became a very effective way of distributing data streams in communications networks [6,7]. With the recent growth of net bandwidths implemented in data transport networks, interest to introducing packet switching for optical fiber communications systems has been developed. This is motivated by the fact that a major portion of the data traffic circulating in data transport networks is packet-based. Therefore, the introduction of packet-based transmission and switching in fiber optical networks was inevitable. However, until

recently, such packet-based operation took the form of electrical packet switches with optical front-ends.

Conventional packet switching in optical networks assumes that, the data stream would be terminated, packets stored in an electrical buffer, have their headers analyzed, and then would be re-aggregated into a new data stream composed of packets with the same destination for the next hop and be transmitted towards that hop. This implies that an optical-to-electrical-to-optical (OEO) conversion is performed for each node on packet's path to its final destination. As data transmission bandwidth demand keeps growing of communication networks kept growing over the last two decades, the cost of packet routing based optical systems with such configuration is growing at an ever-increasing rate with its associated high cost of high-speed electronics and increased power consumption.

Optical packet switching (OPS) [56] presents an interesting alternative for this issue: it implements an optical label with each transmitted packet; this label contains sufficient information for correct routing to be performed for the packet. The advantage of such an approach is that only a low-speed label is being processed, which substantially simplifies the optical router electronics: OPS is very attractive for all types of optical networks [55]. The data-carrying portion of the signal – its payload – is routed onto an optical delay line (usually just a spool of fiber) while the label is being processed and switching plane is preparing a lightpath for the packet. There are multiple ways of labeling an optical packet [83,84] such as using a low-bit rate preamble, separate signaling channel, or a sequence of spectral tones.

The third option – use of spectral tones – is commonly referred to as spectral amplitude coding (SAC) [85-87]. The basic principle of this method is quite simple: the data payload is transmitted normally, but a number of optical tones are present within the payload channel, slightly off-set from the payload band: amplitude of such tones may

have two states – “low” and “high”, representing one bit of the label – “zero” or “one”, respectively. The power of such tones is high compared to the power of the neighboring spectral components belonging to the payload to make the label tone easily distinguishable. Due to this power being concentrated in a very narrow spectral range (ideally – tens of Hz, but in practice it may be several MHz) and a multi-gigahertz off-set from the payload band, SAC labels have very limited effect on the payload. I have assessed this characteristic, and have reported confirmation in ***Paper I***.

5.2. Coherent detection of SAC labels

There are several realizations of SAC label detection schemes, one of them utilizes an optical correlator [88,84]: in this scheme an optical correlator is used to determine the presence of an amplitude tone – depending on the power of the spectral components at a particular spectral position, such correlators produce either a very powerful or a very weak output signal which can be subsequently detected in order to form an electrical label. Depending on the configuration of the label detection block, single tones or complete label combinations can be detected. However, this approach has several significant disadvantages: first of all, as optical correlators are integral wavelength-dependent devices, tuning them to accommodate for varying label structure is impossible. They are additionally associated with quite high insertion losses, which in conjunction with power splitting required to detect the full spectrum of possible label tone combinations, implies the use of optical pre-amplification in practical implementations.

In ***Paper H*** and ***Paper I*** a different approach is proposed for SAC label detection: instead of having selective optical components to detect each individual wavelength tone, the whole label-containing wavelength range is scanned in order to detect the labels. A

configuration presented in Fig, 7 is employed: the signal – payload with its label – is connected to a mixer (a 90-degree optical hybrid was used for the experiments presented in this Chapter), a local oscillator (LO) is connected to the other input of the mixer. The mixer output is a waveform containing the full spectrum of mixing products. This resultant waveform is digitized in analogue to digital signal converter. In the frequency spectrum of the resultant samples of the mixing product-containing waveform I observed results similar to those presented in Fig. 8.

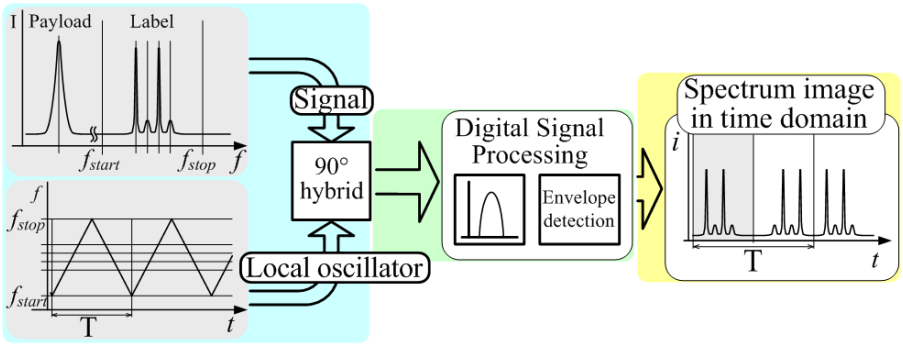

Fig. 7. Proposed label detector configuration.

In this case a label with 4 tones spaced at 500 MHz was used: at the output, there was a DC component, three products of cross-mixing between the label tones – at 500 MHz, 1 GHz and 1.5 GHz; and a cluster of four products resulting from the mixing between the LO and the label – a cluster of four tones centered around 2.8 GHz: the tones are positioned at approximately 2.1, 2.6, 3.1 and 3.6 GHz. The cluster location is determined by the LO laser being off-set (relative to the central wavelength of the label tone cluster, or, in other words, relative to the label center); such an offset was deliberately introduced in order to separate the self-mixing products from the label-LO mixing products.

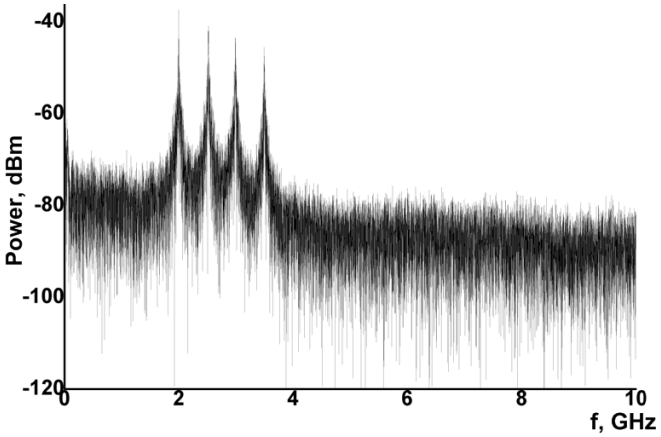

*Fig. 8. Label-LO mixing product, as observed in **Paper K**.*

In order to recover the label, the LO has to be tuned across the wavelength range containing the label: a series of product samples with different LO wavelength offsets is then obtained. Digital signal processing (DSP) was applied to the obtained samples, in order to extract the label tone information contained in them: When applied around the center of the label, a narrow pass-band digital filter will perform conversion of the immediate total powers of the spectral components located within the filter's pass-band into a time-domain sample for each initial sample. Serializing the samples obtained in this manner allows reconstruction of the optical spectrum of the label within the LO tuning range. However, linear and continuous tuning of the LO is required in order to enable long-term label detector operation. A realization of such a sweep is presented in Fig. 7.

A basic demonstration of such label detection technique is featured in ***Paper H***, demonstrating how the label tones can be recovered; ***Paper I*** features analytical evaluations of systems operating with SAC labeling and employing the proposed approach. This label detection technique can be considered an enabling technology for flexible packet-switched hybrid metropolitan access networks.

5.3. Packet-switched hybrid metropolitan access networks

Metropolitan networks benefit the most from packet-switching transmission architectures, as their main task is to distribute data streams between the network nodes; implementing OPS for optical metropolitan networks would boost their performance and reduce the overall network installation and upkeep costs.

5.3.1. Differential quaternary phase-shift keying for packet switching

Differential quaternary phase-shift keying (DQPSK) is one of the signal formats being considered for implementation in metropolitan networks. The DQPSK modulated signal is robust and has high spectral efficiency and survives multiple arrayed waveguide grating (AWG) based routers and (de-)multiplexers [89]: it can be used for long-range transmission of 100 Gb/s signals within the standard 100 GHz ITU-T grid, and polarization division multiplexing (PDM) technique is capable of doubling the bit rate. But in order to reliably receive DQPSK signals at such high data rates, coherent detection with the aid of DSP is required: phase information has to be reliably recovered in presence of signal-to-noise ratio (SNR) degrading factors such as chromatic dispersion, source and LO wavelength and phase instability, phase rotation and others.

Additionally, detection of PDM-DQPSK bursts with DSP-assisted coherent receivers has been demonstrated for 112 Gb/s per polarization (for a total of 224 Gb/s) [51] which implies that this signal format may yet find application in future broadband optical communications schemes. The effect from introduction of OPS for such a high-bit rate solution will be significant: without it, extremely

complex electronics will be required to process such signals at each intermediate node. The possibility of SAC labeling and consequent label detection for DQPSK packets has been demonstrated in ***Paper J***. However, its use should not be restricted exclusively for application with metropolitan networks.

5.3.2. Impulse radio ultra-wideband signal transport for packet switching

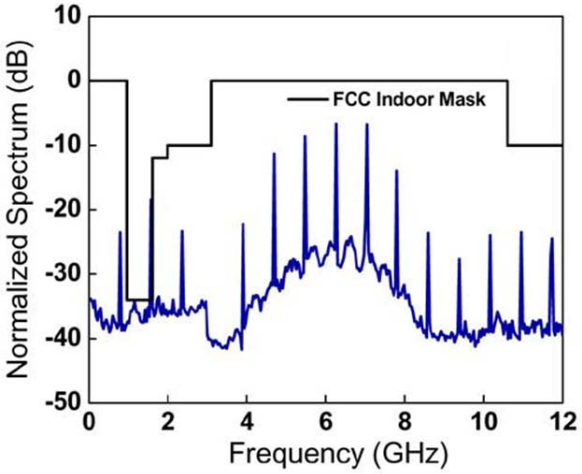

Fig. 9. Spectrum of an optically-generated UWB signals [91].

Impulse radio ultra-wideband (IR UWB) signaling, a specialization of more generalized ultra-wideband (UWB) transmission systems, is a wireless signal format finding increased application in wireless communications. Short-range indoor UWB signaling has been defined by Part 15 rules of the Federal Communications Commission (FCC): such signals may occupy a frequency range from 3.1 GHz to 10.6 GHz, and has the maximum power of each individual spectral

component limited by -42 dBi [90]. UWB-based systems may coexist with conventional wireless systems occupying the aforementioned frequency range as due to their low power; low power also means that the range of UWB-based systems will be quite short – they will provide something referred to as ‘pico-cell’ or ‘in-room’ connectivity. In order to cover a large area – for instance, an office building – a large number of such cells may be implemented, each requiring a UWB wireless access point (WAP) to support service provisioning.

Transport of UWB signals over fiber allows for more effective, centralized signal processing with simple antenna units for WAPs while using a common optical fiber infrastructure with the access networks [90]. Additionally, UWB signals can be generated optically, which is even simpler than conventional generation with the electronics (an example of the spectrum of such an optically-generated UWB signal is presented in Fig. 9) [91,92]. ***Paper K*** demonstrates feasibility of SAC labeling of such optically-generated UWB signals and subsequent detection thereof.

5.3.3. Packet-switched hybrid network paradigm

Fig. 10 features conventional optical network architecture: access network relies on a central office (CO) to provide connectivity to the end users. Each CO features the following equipment: two optical front-ends, terminating data streams both from the metropolitan network (MAN) and from the end users; a required number of optical amplifiers to maintain power levels sufficient to meet the power budget prerequisite; electronic equipment required to detect and store optical packets, analyze their labels and forward them to the respective optical port in order to forward them to their destination. As soon as a transition towards access technologies supporting 10 Gb/s

and higher is made, such network architecture becomes very expensive and complex as the data streams to be processed electronically scales up.

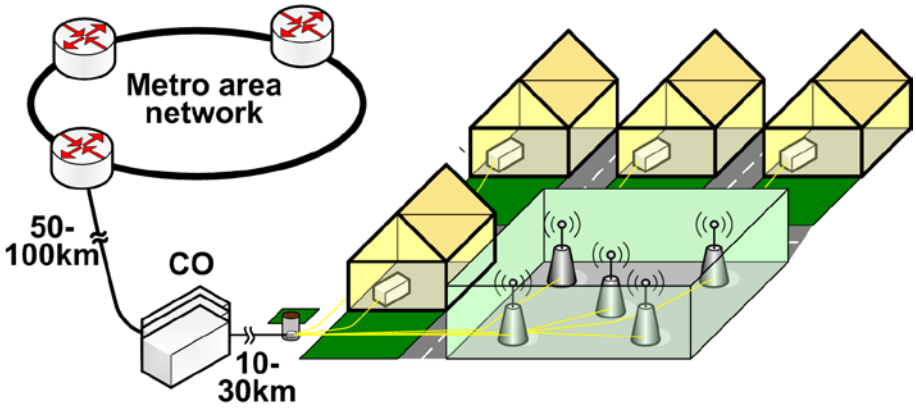

Fig. 10. Conventional network architecture.

An architecture relying on a completely different paradigm was proposed in ***Paper K***. In this report, the metropolitan network and the access networks attached to it are considered as a single entity, removing the border between them (see Fig. 11). In order to do so, bulky expensive electronics-filled COs would have to be replaced with some other structure taking its functions – (de-)aggregation of the data streams between the end users and the metropolitan network. A concept of a local routing cabinet (LRC) is proposed in ***Paper K*** as a solution for this challenge: OPS is employed on the downstream direction, providing optimized use of the resources for MAN-LRC data transport. A sequence of SAC-labeled packets is transmitted with minimal interval, to minimize the negative effects from burst-mode transmission, which allows for maximized transmission link length.

At the LRC, the received optical signal is amplified and compensated for dispersion. The data streams are optically routed to their respective destinations – arranged by wavelength and output distribution fiber.

User-end equipment – the ONUs – employs DSP-assisted coherent receivers for signal detection and compensation of transmission impairments. This allows for increased reach of the distribution link, which has a positive impact on the overall system cost.

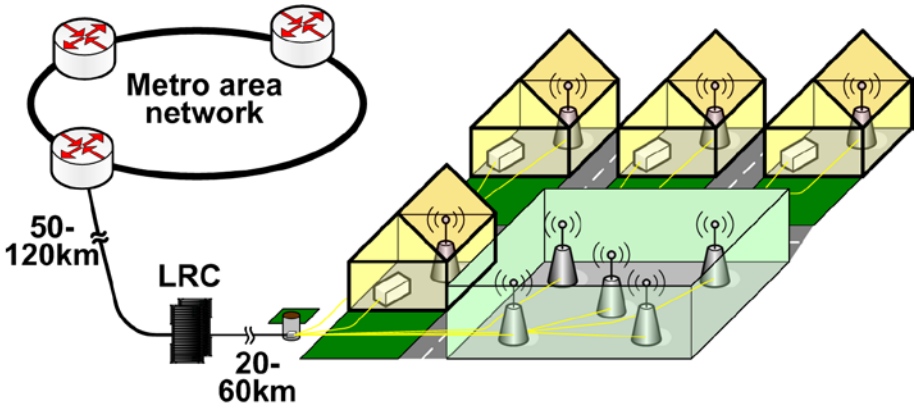

Fig. 11. Proposed hybrid metropolitan access architecture.

In the downstream direction, simple multiplexing of the channels is employed at the LRC; but a more complex process can be employed at the LRC: primitive router-based compression of the data stream is performed – to optimize the transmission link utilization, the upstream packets are re-aggregated into a continuous data stream.

The main advantage of this approach is that it is transparent to signal formats and bit rates because only label processing and packet switching is performed at the LRC. This process requires less intensive data processing and avoids the use of complex high-speed electronics; as the data streams are not terminated at the LRC, it may be considered an extension of a metropolitan network node, allowing it to directly work with the end users.

5.4. Conclusions

In this Chapter, a new network paradigm has been proposed. SAC label-based optical packet switching was used to achieve significant simplification of the intermediate node between the metropolitan network and the access network. This leads to the replacement of the CO with a LRC – a simpler, less bulky intermediate point, which enables direct interaction between the end user and the metropolitan network. Such an approach effectively creates a hybrid metropolitan access network: by extending the array of services to broadcast and wireless-over-fiber services, such a hybrid network is made even more attractive – both for the operators and the users, as it can support the transmission of several data services over a common fiber infrastructure.

6. Conclusion

During my doctoral studies I have analyzed the challenges associated with the interfacing between metropolitan and access levels in a communication network hierarchy. This allowed me to identify the key issues that need to be resolved in order to develop solutions that would allow for more effective interfacing between metropolitan and access networks. The issues identified were: excessive complexity of the network equipment – especially due to routing performed in electrical form; short range of the access systems inducing the need for a large number of central offices in order to provide connectivity to the users in a given area; need for high-bandwidth services; need for wireless and broadcast service support.

A colorless DQPSK receiver concept for metropolitan networks has been developed: the proposed receiver reduces the complexity of equipment required at metropolitan network nodes by reusing a single interferometer-based receiver for multiple wavelengths. The concept was then expanded to a crossconnect for metropolitan networks: this concept explained how and why the colorless DQPSK receivers would be used; concise wavelength arrangement and components reuse ensured further equipment reduction.

A transparent metropolitan-access architecture based on reflective end-user equipment has been proposed: by employing multiple wavelengths, it became possible to establish transparent lightpaths for a fraction of data packets generated at the customer premises, partially

reducing the data stream to be terminated at the central office. In this simulation we have observed an improvement in network performance relative to a conventional WDM-PON.

A technique for gain transient control with the use of semiconductor optical amplifiers and highly-nonlinear fibers has been proposed: this technique reduces signal degradation in wavelength-multiplexed systems by moderating gain transients occurring in the fiber amplifiers, allowing for longer link range.

Coherent detection provides some significant advantages, such as improved receiver sensitivity and wavelength selectivity; a coherent detection based passive optical network architecture supporting broadcasting and wireless services has been proposed.

Systems for transport of wireless signals over long-range access links have been developed: converged transport of broadband wireless service together with several wireless and baseband services has been demonstrated for 78.8 km of single-mode fiber; bi-directional transport of 100/64 Mb/s WiMAX signals has been demonstrated for 78.8 km of single-mode fiber and 40 km of non-zero dispersion shifted fiber, exceeding all the previously demonstrated results both in terms of bandwidth and range.

Finally, a SAC label detection method based on coherent detection has been proposed to enable cost-effective optical packet switching: this novel technique allows for flexible and reliable label detection thanks to use of DSP algorithms. This technique was applied to detect the labels for wireless and baseband signals.

SAC labeling-based optical packet switching was proposed as a means to enable transparent interaction between the metropolitan network node and the end user: this approach greatly simplifies the intermediate node, and I believe that the use of previously developed range extension and converged service delivery techniques would

form a new paradigm of hybrid metropolitan access networks. When applied on massive scale it would revolutionize metropolitan and access networks by allowing for seamless operation of such networks via a flexible packet switching based hybrid network architecture; the complexity of such a hybrid network would be reduced compared to networks with a conventional approach even if some of the aforementioned solutions are implemented for them.

6.1. Outlook

While considering the proposed hybrid metropolitan access network very attractive for implementation, I believe that it may be eventually developed to support labeled upstream packet transmission. With the use of certain techniques (such as packet compression for bit rate conversion), optical packet switching approach could be extended to include not just metropolitan and access networks, but also to support transparent transport between the metropolitan and core networks. Eventually, this approach would help reduce the network complexity and provide economies to the network operators and subsequently the users.

I also believe that some issues associated with SAC label propagation over long-range fiber links should be investigated: high-power SAC label tones will be gaining more and more power as they propagate over a cascade of amplifiers in a fiber link which may trigger four-wave mixing and other nonlinear effects in the transmission fiber.

Paper A

Jesper Bevensee Jensen, Alexey V. Osadchiy, Idelfonso Tafur Monroy, Palle Jeppesen, "Colorless DQPSK Receiver for Wavelength Routed Packet-Switched Networks," **IEEE Photonics Technology Letters**, 20, no. 22, pp 1839-1841 (2008)

Colorless DQPSK Receiver for Wavelength Routed Packet-Switched Networks

Jesper Bevensee Jensen, Alexey V. Osadchiy, Idelfonso Tafur Monroy, and Palle Jeppesen

***Abstract*—We propose and demonstrate experimentally a scheme for the demodulation of 21.4-Gb/s return-to-zero differential quaternary phase-shift keying signals in packet-switched wavelength routed networks where packets at different wavelengths are arriving to the same demodulator. The idea is based on wavelength conversion, and in the demonstration, all channels were received error-free after wavelength conversion. In a packet arrival emulation, the ability of handling incoming packets at different wavelengths were successfully demonstrated.**

***Index Terms*—Packet-switched, 060.2310 fiber optics, 060.4259 networks, 060.5060 phase modulation.**

I. Introduction

In packet-switched networks using wavelength routing, packets at different wavelengths will arrive to the same receiver at different times. For phase-modulated signals using delay demodulation, this is a problem due to the wavelength-dependent phase off-set in the demodulator. Using one demodulator for each incoming wavelength is a complex and costly, and therefore, undesirable solution. Tuning of the demodulator on a packet by packet rate requires fast control and feedback which would prove difficult to realize in practice. A more promising solution to the problem, would be to wavelength convert all incoming packets to one common wavelength.

In this letter, we propose and investigate experimentally, a method of converting a number of incoming phase-modulated signals to one common wavelength to which the receiver is optimized. The modulation format used in the experiments was 21.4-Gb/s return-to-zero (RZ) differential quaternary phase-shift keying (DQPSK), and the proposed scheme was demonstrated for three channels. The wavelength conversion was done through degenerate four-wave mixing (FWM) in nonlinear media. Experiments using highly nonlinear fiber (HNLF) as well as semiconductor optical amplifier (SOA) were performed. In both cases, error-free performance after wavelength conversion was achieved.

In order to add network functionality such as the routing information to an optical add–drop multiplexer to the scheme, a simple 1-bit optical label was added to the signal in the form of a weak sinusoidal amplitude modulation at a frequency equal to half the symbol rate. The use of the half-clock frequency for labelling ensures minimum label-induced signal degradation [1].

Manuscript received April 22, 2008; revised June 27, 2008. First published August 22, 2008; current version published October 31, 2008.

The authors are with the DTU Fotonik, Department of Photonics Engineering, Technical University of Denmark, Dk-2800 Kgs. Lyngby, Denmark (e-mail: jj@com.dtu.dk).

Color versions of one or more of the figures in this letter are available online at http://ieeexplore.ieee.org.

Digital Object Identifier 10.1109/LPT.2008.2004694

The proposed scheme is based on wavelength conversion by degenerate FWM with one pump laser for each signal laser. Appropriate allocation of pump and signal wavelengths ensures that the lasers which act as pumps for the wavelength conversion at the receiver side can be used as signal lasers for transmission to other network nodes. This can be seen by the following argument.

For degenerate FWM with $\omega_s > \omega_p$, where ω_s and ω_p are the angular frequencies of the pump and signal, the relations between the frequencies of the pump, signal, and FWM products are $\omega_+ = 2\omega_s - \omega_p$ and $\omega_- = 2\omega_p - \omega_s$, where ω_+ and ω_- are the angular frequencies of the up- and down-converted signals. If $\omega_s < \omega_p$, the relations become $\omega_+ = 2\omega_p - \omega_s$ and $\omega_- = 2\omega_s - \omega_p$ [2]. For the phase, the corresponding relations become $\phi_+ = 2\phi_s - \phi_p$ and $\phi_- = 2\phi_p - \phi_s$ for $\omega_s > \omega_p$, and $\phi_- = 2\phi_s - \phi_p$ and $\phi_+ = 2\phi_p - \phi_s$ for $\omega_s < \omega_p$. Here, ϕ_s, ϕ_p, ϕ_+, and ϕ_- are the phases of the signal, pump up-converted and down-converted signals, respectively, and a common phase off-set has been omitted for clarity since only the differential phase between adjacent symbols is important due to the delay demodulation [2]. From the phase relations, it is seen that for $\omega_s > \omega_p$, apart from an inversion the data information contained in ω_s is preserved for the down-converted FWM product, whereas for $\omega_s < \omega_p$ the data information is preserved (apart from an inversion) for the up-converted FWM product. From the relation between the frequencies, it is seen that if the signal spacing is twice the pump spacing, the desired wavelength conversion of all signals to one common receiver wavelength can be achieved. If, on the other hand, two receiver wavelengths, and hence the requirement of two receivers are accepted, a double set can be constructed, where the pumps and signals have the same spacing. In this way, the possibility of re-using all lasers as both pumps and signals has been achieved, and no extra lasers have been added to the system due to the wavelength conversion. A double-set which would fit the 50-GHz ITU grid is illustrated in Fig. 1.

II. Experimental Setup

A simplified block diagram of the setup used in the experiment is shown in Fig. 2. Three distributed-feedback (DFB) lasers (tunable in 0.01-nm steps) were used for the signal and three external cavity lasers (ECLs) (tunable in 0.001-nm steps) were used as pumps for the wavelength conversion. As it is assumed that only packets at a single wavelength will be present at a given time, only one signal pump pair is active at the same time. Continuous-wave (CW) light from the three signal lasers were coupled into a Mach–Zehnder modulator (MZM) driven by an electrical clock signal at the pulse rate of 10.7 GHz for pulse carving, and by a weak sinusoidal modulation at half the symbol rate (5.35 GHz) for the label. After pulse-carving, 21.4-Gb/s DQPSK modulation was applied by

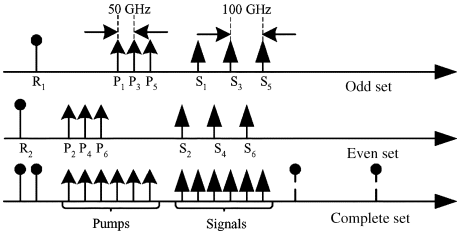

Fig. 1. Pump/signal allocation scheme in frequency domain. The dashed lines display the receiver frequencies in the case where pumps and signals are interchanged.

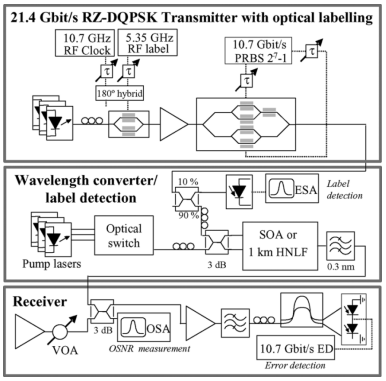

Fig. 2. Simplified block diagram of the setup used in the experiments.

a parallel MZM superstructure driven by two decorrelated 127-bit-long 10.7-Gb/s pseudorandom bit sequences (PRBS). Modulator loss was compensated by an erbium-doped fiber amplifier (EDFA). The 5.35-GHz labelling tone was detected by a photo diode and an electrical spectrum analyzer. This was done before the wavelength conversion, in order for the label to be used to control an optical add–drop multiplexer (OADM). In a real implementation, label processing could be performed by narrow electrical filtering around 5.35 GHz followed by decision gating.

Before detection, conversion to the receiver wavelength was performed by FWM in either 1 km of HNLF or in an SOA. The pump laser corresponding to the wavelength of the incoming signal was selected by a fiber-optic switch (crosstalk $\simeq$ -80 dB, switching-time $\simeq$300 ms). Pump and signal powers at the input of the HNLF were 14.0 and 12.5 dBm, respectively. For the SOA, 12.0 dBm was used for the pump and 9.0 dBm for the signal. The signal was detected by a preamplified receiver setup, where the signal was loaded with noise from an open-ended EDFA before optical signal-to-noise ratio (OSNR) measurement by an optical spectrum analyzer, and data recovery by a one-symbol delay interferometer and a pair of balanced photodiodes. Bit-error ratio (BER) was

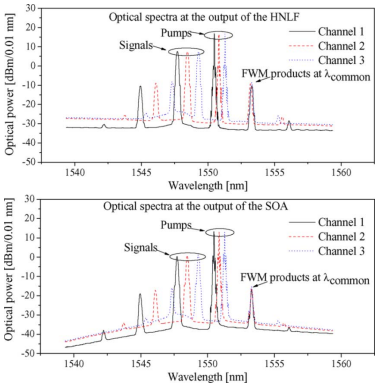

Fig. 3. Optical spectrum at the output of the HNLF and SOA showing pumps, signals, and FWM products for all three channels.

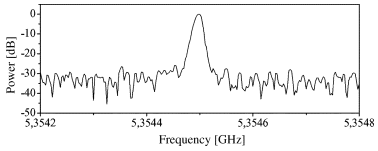

Fig. 4. Electrical spectrum (normalized to peak power) showing the label-tone at 5.35 GHz.

counted using an error detector programmed with the expected DQPSK tributary. In order to detect the two DQPSK tributaries simultaneously, two sets of delay interferometers and balanced photodiodes are required. In the laboratory implementation, the two tributaries were measured one at a time, and the total BER was calculated as the average of the two.

III. Results

The optical power spectra at the output of the HNLF and SOA, respectively, are plotted in Fig. 3 for all three channels. As expected, the up-converted FWM product for all channels coincide on the same wavelength, thus verifying the wavelength conversion of three channels to one receiver wavelength. The nonflat noise floor in the SOA case is due to the nonflat gain spectrum of the SOA.

The electrical spectrum around 5.35 GHz showing the optical label is plotted in Fig. 4, indicating a better than 20-dB electrical signal-to-noise ratio for the label.

The measured BER of all channels with and without label is plotted in Fig. 5 before (a) and after wavelength conversion in the HNLF (b) and the SOA (c). In neither case was an indication of an error-floor observed, and the label induced no degradation of the BER. The required OSNR for a BER of 10^{-9} in the case without the label are given in Table I. After wavelength conversion in the HNLF, a small OSNR penalty of 0.7 dB for Channels 1 and 2, and 1.6 dB for Channel 3 is observed. For the SOA, the measured conversion penalties were 5.4, 5.6, and

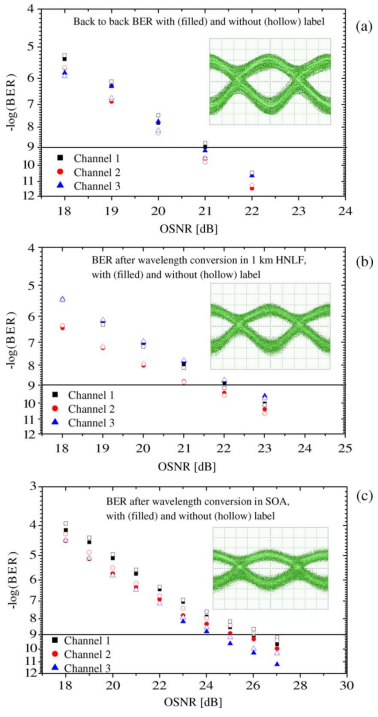

Fig. 5. BER versus OSNR (a) before, (b) after wavelength conversion in 1-km HNLF, and (c) after wavelength conversion in an SOA. Insets show the demodulated eye diagrams.

TABLE I
OSNR REQUIREMENTS FOR A BER OF 10^{-9} BACK-TO-BACK (B2B), AND AFTER WAVELENGTH CONVERSION IN HNLF AND SOA, RESPECTIVELY

	Channel 1	Channel 2	Channel 3
B2B	21.1 dBm	20.5 dBm	20.6 dBm
HNLF	21.8 dBm	21.2 dBm	22.2 dBm
SOA	26.5 dBm	26.1 dBm	24.7 dBm

4.1 dB for the three channels, respectively. The higher penalty for the SOA compared to the HNLF is confirmed by the eye diagram, which has a lower amplitude for the SOA. This is in good agreement with Fig. 3, which shows a lower OSNR for the signal after wavelength conversion in the SOA than in the HNLF. The SOA used in the experiment was a Mach–Zehnder structure chosen for availability rather than good FWM performance. Since only one arm of the device was used, but the noise generated in the other arm still degrades the signal, better performance would be expected from a device specifically designed for wavelength conversion. In order to emulate the scenario of

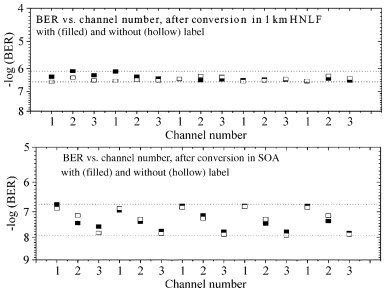

Fig. 6. Monitored BER in the packet arrival emulation experiment.

packets from different channels arriving to the same receiver at different times, an experiment was carried out where the active signal and pump pair was cyclically switched through the three channels, while monitoring the BER. The OSNR into the receiver was kept at 19 dB for the HNLF and at 23 dB for the SOA. The results are plotted in Fig. 6. For the SOA as well as for the HNLF, the variations in BER were very small. For the SOA, BER between 2×10^{-7} and 3×10^{-8} was measured, and for the HNLF between 9×10^{-7} and 4×10^{-7}. Again, no degradation was observed from the label.

The method of wavelength conversion of packets with different wavelengths to one common wavelength has thus been demonstrated as a candidate for mitigation of the problem of wavelength-dependent receiver for phase-modulated signals. Fine-tuning of the wavelength of the pump lasers is required. It was found that 0.01-nm steps for the signal lasers and 0.001-nm steps for the pump lasers were sufficient to achieve error-free performance after wavelength conversion.

IV. CONCLUSION

A receiver setup capable of coping with the problem of phase-modulated signals with different wavelengths arriving to the same receiver at different times in packet-switched networks using phase modulation has been investigated experimentally. Wavelength conversion of three incoming 21.4-Gb/s RZ-DQPSK signals at different wavelengths to one common wavelength was achieved with error-free reception of the wavelength converted signal. The wavelength conversion was performed by FWM in HNLF and in SOA. A small OSNR penalty of 0.7–1.6 dB was measured after conversion in the HNLF, 4.1- to 5.6-dB OSNR penalty was found after conversion in the SOA. A simple 1-bit optical label was added to the signal with no additional penalty.

REFERENCES

[1] I. T. Monroy, J. V. Olmos, M. G. Larrode, T. Koonen, and C. D. Jimnez, "In-band 16-QAM and multi-carrier SCM modulation to label DPSK payload signals for IP packet routing," *Opt. Express*, vol. 14, pp. 1000–1005, 2006.

[2] G. T. Zhou, K. Xu, C. Yan, Y. Su, and J. T. Lin, "Self-pumping wavelength conversion for DPSK signals and DQPSK generation through four-wave mixing in highly nonlinear optical fiber," *IEEE Photon. Technol. Lett.*, vol. 18, no. 22, pp. 2389–2391, Nov. 15, 2006.

Paper B

Alexey V. Osadchiy, Jesper Bevensee Jensen, Palle Jeppesen, Idelfonso Tafur Monroy, "Crossconnect architecture for colorless detection of DQPSK modulated payload signals in packet switched networks," **Optical Switching and Networking** (UNDER REVIEW) (2010)

Crossconnect architecture for colorless detection of DQPSK modulated payload signals in packet switched networks

Alexey V. Osadchiy[1,*], Jesper B. Jensen[1], Palle Jeppesen[1], Idelfonso Tafur Monroy[1]

[1] DTU Fotonik, Technical University of Denmark, Oersteds Plads 343, DTU Campus, 2800 Kgs. Lyngby, Denmark

** Alexey V. Osadchiy*

DTU Fotonik, Technical University of Denmark

Oersteds Plads 343, DTU campus, Office 214

2800 Kgs. Lyngby, Denmark

Tel.: +45 4525 3657

Email: avos@fotonik.dtu.dk

Abstract: We propose a crossconnect architecture capable of detecting DQPSK modulated payload signals for packet switched networks. The DQPSK modulation format is considered a promising candidate for signal transmission due to the high spectral efficiency and tolerance towards transmission impairments. However, receivers employing a Mach-Zehnder delay interferometer (MZI for demodulation require exact phase matching between the two arms of the MZI for each incoming wavelength. Our proposed crossconnect architecture incorporates a colorless DQPSK receiver, based on wavelength conversion to a common wavelength to handle packets arriving from different destinations on different wavelengths. We demonstrate its feasibility in an experiment with three DQPSK modulated channels operating at 21.4 Gbit/s, all of which were received error free after wavelength conversion. Moreover, the system is tested in an emulated packet arrival scenario.

Keywords: optical routing; wavelength conversion; add-drop multiplexing

1. Introduction

Modern optical telecommunication networks are foreseen to rely on packet switching as a method of routing data streams between end users. This trend is supported by the emerging growth of services such as voice-over-IP, video streaming and peer-to-peer file transfer. Conventional optical circuit switched solution will not efficiently support this emerging need for the handling of packet oriented telecommunication traffic. Therefore, optical packet switching solutions are believed to better exploit the optical network bandwidth, to give higher throughput and to offer greater flexibility [1].

Several approaches to implement IP transport over optical networks have being proposed ranging from optical burst switching (OBS), optical label switching (OLS) and all-optical packet (AOPS) switching [2]. While OBS relies on complex electronic control mechanisms to establish end-to-end transparent optical paths and in this way avoid optical buffering at the intermediate nodes, AOPS attempts to implement packet switching entirely in the optical domain. However, buffering and memory functionalities required to implement native packet switching entirely in the optical domain are not mature at the present time. OLS is an intermediate approach where short, fixed length labels are associated with high-speed payload data. These simple labels can be processed electronically at routing nodes to control optical switching matrices, performing routing of high-bit-rate payload data without conversion to the electrical domain [3].

We consider in this article the case of optically labeled payload data encoded in Differential Quadrature Phase-Shift Keying (DQPSK) modulation format [4]. DQPSK format has several advantages compared to intensity modulation formats, amongst those are higher receiver sensitivity, higher spectral efficiency, higher tolerance towards chromatic and polarization mode dispersion, and higher compatibility with a DWDM 50 GHz spacing grid [5-7]. However, to correctly demodulate a DQPSK signal employing a one symbol delay interferometer, the phase of the two signal paths inside the delay interferometer need to be fine tuned to match the signal wavelength. These delay intereferometers can be implemented by several technologies, for instance, fiber-based or free-space [8,9]. In an optical packet switched networking scenario, DQPSK payload signals may arrive at different wavelengths to the same receiver, which in turn raises a requirement for a dedicated DQPSK demodulator for each wavelength used in the network. In this article we present an optical crossconnect architecture for label-controlled DQPSK metropolitan networks employing a colorless multi-wavelength receiver. We experimentally demonstrate the feasibility of such colorless DQPSK receiver operating at 10.7 Gbaud.

2. Architecture of a label controlled crossconnect for DQPSK payload signals

A current challenge in modern optical telecommunication systems is finding the most efficient realization of the signal routing and interfacing between the Metropolitan and the Access network segments. These two network segments usually operate at different bitrates, use different signal formats, and possibly even different wavelengths bands (1310 nm, 1540 nm, 1550 nm, etc.). One of the possible approaches to the interfacing is to

perform electrical-to-optical (E/O) and optical-to-electrical (O/E) conversion of all signals at the routing nodes. Routing nodes will then be equipped with electronic packet handling functionalities from and to access network segments, including signal dropping to the access network and re-injection/adding into the metro network. However, considering the pressure put on the routing efficiency and speed of Metro-Access interface nodes due to the introduction of high capacity access networks, such as Wavelength Division Multiplexing Passive Optical Networks (WDM PONs) with capacity of 10 Gb/s [10], a much more reasonable approach is required. An example of such an approach is to use an optical cross-connect (OXC) supporting both transparent payload routing (optical bypass of payload signals) and signal termination capabilities.

Fig. 1 shows a label-switched metropolitan network architecture employing DQPSK payloads and label-controlled crossconnects for metro-to-access interfacing.

The block diagram of an OXC is presented in Fig. 2. It consists of a label processing block, processing the labels of inbound packets, a routing block, handling the switching of the light paths for individual packets, a contention resolution block with an optical buffer to queue packets in such a way that they do not collide, and an ADD/DROP block, responsible for extraction and injection of packets originating from the local access network and having that network as their destination. One of the major challenges associated with the development of such an OXC is the necessity to devise a way to realize on-the-fly optical routing and contention resolution functionalities. One of the possible approaches is accompanying the high bit rate packet payloads with low bit rate optical labels which are

detected and processed electronically to control the switching of the payload. Different techniques exist to introduce an optical label into optical payload signals, such as outband or inband labeling. In case of inband labeling, the label can be filtered out from the payload signal. In the case of outband labels, the label is inserted by exploiting a different domain of the optical carrier than that used for the payload signal (phase, frequency, intensity, polarization) or by employing Time Division Multiplexing (TDM) of the label ahead of the payload signal [11]. Using low bit rate optical labels reduces the bitrates of the control signals required to perform routing, which reduces the cost of the routing nodes and the system as a whole (by enabling the use of cheaper low bit rate receivers), at the same time reducing the packet processing time – the high bit rate part of the packet (payload) is kept in the optical domain.

Routing information retrieved from the optical labels is used to control the optical switching plane, which is the major part of the routing block in Fig. 2. The switching plane can be realized in a number of ways [12], for instance, by utilizing MZI switches, optical gates, or by a combination of cyclic Arrayed Waveguide Gratings (AWG) and tunable wavelength conversion. The contention resolution block can be realized, for instance, in the form of an array of fixed or variable optical delay lines, connected to the switching plane; see Fig. 2.

Optical crossconnects serve as interfacing and routing nodes at the same time: they can realize the interfacing between the metropolitan networks and the access networks, as well as the routing of metropolitan network traffic. The ADD/DROP subsystem shown in Fig. 2

is the key building block for realizing such interfacing. Optical packets with a local destination are directed to the DROP block of the crossconnect. At the DROP block, optical packets are transformed into the electrical form, and forwarded to the data storage and processing block. At the same time, packets originating from the local access network are handled by the data storage and processing block and transmitted to the ADD block. Thereafter those packets are injected into the metropolitan segment by the routing block of the OXC. Connectivity from the metropolitan routing node and the customer premises can be implemented by several optical access architectures such as passive optical networks (PONs) or wavelength division multiplexing PONs [13].

3. Colorless receiver for DQPSK payload signals

Although several architectures for label controlled routing nodes have been proposed, they address predominantly the case of optical intensity modulated payload data rather than payload data encoded in phase modulated formats [14]. An optical DPSK or DQPSK receiver based on direct detection [15] employs an optical interferometer detector, fine tuned to the wavelength of the optical signal to be received. In an optical labeled routed network, packets may be directed to a drop port at an intermediate node or arrive at the end-user receiver, at different wavelengths as they may originate from different sources. In order to have a flexible network, a receiver should support reception of packets from any destination arriving at any wavelength; however it may imply dedicating an individual DPSK or DQPSK detector for each wavelength supported by the network. Therefore, it is of interest to conceive a solution for a colorless DPSK or DQPSK receiver.

Fig. 3 shows our proposed architecture for a DQPSK OXC which is capable of receiving packets at multiple wavelengths with one detector-receiver combo: several wavelengths are converted to one common wavelength and are detected by one common set of receiving equipment. Wavelength conversion to a common wavelength has to be phase-maintaining to make this operation possible. Therefore we propose [16] to exploit four-wave mixing (FWM) to realize wavelength conversion to a common wavelength, with a number of pump sources whose wavelengths are arranged to match each of the incoming signal wavelengths. Moreover, the wavelengths are allocated in such a way, that the pump sources used to wavelength convert the received signals can be used as light sources for the transmission of the outgoing packets. Fig. 3 shows the way a single wavelengths subgroup is handled: the group of wavelengths is converted to a common wavelength and detected with a single receiver, while the lasers used for pumps are also used for transmission of the outgoing packets.

Fig. 4 shows an example of wavelength allocation for the case of 16 channels, arranged in 2 matching groups, each formed by a pair of subgroups of 4 wavelengths. Such an allocation enables reuse of the light source for packet detection and transmission as mentioned above. A stack of light sources (4 for the considered OXC example) is used both as pump for wavelength conversion (converting 4 incoming wavelengths, or one subgroup, to 1 common wavelength) and as wavelengths for outgoing packet transmission.

In the example presented in Fig. 4, a continuous grid of incoming wavelengths (g) and pumps (h) is formed by matching 4 subgroups of wavelengths (a), (b), (c) and (d), filling

the gaps in the grid. The light sources used as pumps can simultaneously be used as light sources for outgoing packets transmission. This approach allows for designing an OXC to be fully compliant with an ITU wavelength grid allocation and therefore does not introduce any wavelength use inefficiency – it is capable of transmitting outgoing packets at any of the wavelengths used for colorless DQPSK packet detection.

An important feature of the proposed architecture is that it is assumed that only one wavelength is present at the receiver belonging to each group at a given moment of time. This assumption puts up an interesting design issue relating the amount of channels allocated to one wavelength group (or, to be more specific, the amount of wavelengths received by one detector-receiver combo) and the justification of introducing wavelength conversion or any other contention resolution scheme. On one hand, the more channels one can receive with one detector-receiver combo the better its resource efficiency. This means fewer components are required to receive the same amount of wavelengths: the amount of light sources remains the same, while the amount of demodulators and receivers decreases. On the other hand, the more wavelengths rely on a single detector-receiver combo, the fewer packets per individual wavelength can be processed over a given period of time which may indicate the need for contention resolution. We consider the case of 3-4 channels per group being a rather reasonable trade-off, however further evaluation is required to confirm this choice. The assumption is – with such an amount of channels per detector-receiver combo one can, considering the explosive type of network traffic, handle the receiver sharing with only a slight drop in performance by delaying contending packets in the feedback delay line block presented in Fig. 2.

Our proposed OXC has an advantage in compactness compared to OXC architecture for DQPSK encoded packets which does not rely on wavelength conversion to a common wavelength, because using a detector-receiver combo for every channel makes the equipment rather bulky and potentially costly when it comes to introduction of DQPSK signal format in WDM metro networks.

4. Experimental demonstration

In this section, we present an experimental demonstration of our proposed colorless DQPSK receiver. We also demonstrate its successful operation when a packet by packet arrival scenario is emulated by switching among the three implemented WDM channels.

The modulation format used in the experiment was 21.4 Gbit/s return to zero (RZ) DQPSK. The wavelength conversion was done through degenerate four wave mixing (FWM) using a semiconductor optical amplifier (SOA) as the non-linear medium. The SOA was selected due to its structure allowing it to be built as a part of compact optical circuits, which is important for building optical crossconnects. 1 km of highly non-linear fibre (HNLF) has also been used for performing the required wavelength conversion and the authors have demonstrated its feasibility for a three channel system whose results are presented in [16]. In both cases, error-free performance after wavelength conversion from 3 WDM channels to a common wavelength was achieved. In addition to our proposed colorless DQPSK receiver, a simple 1-bit optical label was added to the signal in the form of a weak

sinusoidal amplitude modulation at a frequency equal to half the symbol rate, which ensures minimum label-induced signal degradation.

The wavelength conversion principle is based on degenerate FWM with one pump laser for each signal wavelength. Appropriate allocation of pump and signal wavelengths enables the re-usage of the lasers used as pumps and also as light source for packet transmission. This can be seen from the following argument. For degenerate FWM, if ωs is the angular frequency of the signal, and ωp is that of the pump, for $\omega_s > \omega_p$, the relations between the frequency of the pump, signal and FWM products are $\omega_+ = 2\omega_s - \omega_p$ and $\omega_- = 2\omega_p - \omega_s$, where ω_+ and ω_- are the angular frequencies of the up- and down-converted signals. In case of $\omega_s < \omega_p$, the relations become $\omega_+ = 2\omega_p - \omega_s$ and $\omega_- = 2\omega_s - \omega_p$ [17]. For the phase, the corresponding relations become $\Phi_+ = 2\Phi_s - \Phi_p$ and $\Phi_- = 2\Phi_p - \Phi_s$ for $\omega_s > \omega_p$, and $\Phi_- = 2\Phi_s - \Phi_p$ and $\Phi_+ = 2\Phi_p - \Phi_s$ for $\omega_s < \omega_p$. This means, that for $\omega_s > \omega_p$, $\omega_- = 2\omega_p - \omega_s$ should be used, and for $\omega_s < \omega_p$, $\omega_+ = 2\omega_p - \omega_s$ respectively [15]. In this way we avoid multiplying the phase by a factor of 2 and the change of sign for the phase does not matter in the delayed detection scheme. This means that if the signal spectral spacing is twice the pump spacing, wavelength conversion of all signal channels to a common receiver wavelength can be achieved. By introducing a complimentary set of signal channels and pumps, one can achieve a continuous 50 GHz ITU grid [18] as shown in Fig. 5 where R_1 and R_2 denote the common wavelength conversion products for the odd set and the even set, respectively. Following the argument above, we can see that the pump signals can also be used as transmitter light sources by mirroring the signal and pump wavelength allocation at the other receiver end.

A simplified block diagram of the experimental setup is shown in Fig. 6. Three distributed feedback (DFB) lasers were used for the signals and three external cavity lasers (ECLs) were used as pumps for the wavelength conversion. It was assumed that only packets at a single wavelength will be present at any given time, and that only one signal-pump pair is active at the same time. Continuous wave (CW) light from the three signal lasers was coupled into a Mach-Zehnder modulator (MZM) by polarization maintaining (PM) directional couplers.

The MZM was driven by an electrical clock signal at the symbol rate of 10.7 GHz for pulse carving, and by a weak sinusoidal modulation at half the symbol rate (5.35 GHz) for the label. After pulse-carving, 21.4 Gbit/s DQPSK modulation was applied by a parallel MZM superstructure. Modulator loss was compensated by an erbium doped fiber amplifier (EDFA). The 5.35 GHz labelling tone was detected by a photodiode and an electrical spectrum analyzer (ESA). This was done before the wavelength conversion, as the presence of the label would determine if the signal should be routed on in the network or if it should be send to the receiver. In a real implementation, label processing could be performed by narrow electrical filtering around 5.35 GHz followed by decision gating.

Before detection, conversion to the receiver common wavelength was performed by FWM in a semiconductor optical amplifier (SOA). The SOA used in the experiment was an SOA integrated in a double MZI structure, originally intended for other applications such as optical signal processing. 70 mA current was applied to the SOA. The pump laser corresponding to the wavelength of the incoming signal was selected by a fiber-optic

switch. Pump and signal powers at the input of the SOA were 12.0 dBm for the pump and 9.0 dBm for the signal. The signal was detected by a pre-amplified receiver, where amplified spontaneous emission noise generated by an open-ended EDFA was added to the signal in a 3-dB fiber coupler. One output from the 3-dB coupler was used for optical signal to noise ratio (OSNR) measurement by an optical spectrum analyzer (OSA), and the other output of the 3-dB coupler was used for data recovery by a one-symbol delay interferometer and a pair of balanced photodiodes. Bit error ratio (BER) was measured using an error detector programmed with the expected DQPSK tributary. In order to detect the two DQPSK tributaries simultaneously, two sets of delay interferometers and balanced photodiodes would be required. In the laboratory implementation, the two tributaries were measured one at a time, and the total BER was calculated as the average of the two.

4. Results of the experimental demonstration

Bit error ratio (BER) versus OSNR of the signal before wavelength conversion is plotted in Fig. 7. Results with and without the label are plotted. Eye diagram of the signal after demodulation is shown in Fig. 8. A clear eye-opening is seen, and there is no indication of error-floor on any of the channels. Required OSNR for a BER of 10-9 was 22.1 dB, 21.3 dB and 22.3 dB for channels 1, 2 and 3 respectively. No measurable signal degradation was observed from the label. In Fig 9, the electrical spectrum around 5.35 GHz is plotted, showing the 1-bit label.

An SNR of 25 dB for the label can be observed on Fig. 9, indicating that the label can be clearly detected. The possibility of more complex labels used with the DQPSK signals requires further investigation.

The optical power spectrum at the output of the SOA is shown in Fig. 10 for all three channels. As expected, one of the FWM products is at the same wavelength for all three channels. The shape of the gain spectrum of the SOA shows as a "hillshaping" of the noise floor. The measured BER of all channels after wavelength conversion, with and without label, is shown in Fig. 11. As for the back to back case, there were no indications of error-floor in either case. In the case of wavelength conversion in the SOA, the measured OSNR requirements for a BER of 10-9 was 26.0 dB, 25.3 dB and 24.3 dB for channels 1, 2 and 3 respectively, corresponding to OSNR penalties after wavelength conversion equal to 3.9 dB, 4.0 dB and 3.0 dB respectively.

In order to emulate the scenario of packets from different channels arriving to the same receiver at different times, an experiment was carried out where the active signal and pump pair was cyclically switched through the three channels, and the BER was monitored without any tuning of the delay interferometer phase off-set or the center wavelength of the optical band-pass filter in the receiver. The OSNR into the receiver was kept at 23 dB.

The results are plotted in Fig 13. The variations in BER turned out to be very small: BER between 2×10^{-7} and 3×10^{-8} were measured. Again, no degradation was observed from the label, which proves the feasibility of implementing the label control with DQPSK signals.

This experiment has demonstrated the feasibility of the method of wavelength conversion of several channels to a single wavelength as a way to overcome the wavelength dependency of the MZI based DQPSK signal receivers in multichannel optical telecommunication systems.

5. Conclusion

We have proposed an OXC architecture that incorporates a colorless DQPSK receiver capable of reducing the amount of MZIs required for demodulation of incoming packets on different wavelengths. Colorless operation was achieved by wavelength conversion to a common wavelength in an SOA; a solution chosen for its ease of photonic integration. The employed wavelength allocation scheme also enables the reuse of pump light sources as light sources for data transmission, thus improving the device and power efficiency of the crossconnect and enables the construction of compact modular OXCs.

In an experimental demonstration, error-free reception of all channels was performed after wavelength conversion with conversion penalties of 2.3 to 4.0 dB. Packet arrival emulation with channel switching demonstrated the stability of the BER after wavelength conversion. Furthermore, an optical label added to the signal was successfully detected after wavelength conversion. These results show that this new scheme can be used in scenarios where packets arrive at different wavelengths randomly, and where optical labeling is employed. The experiment validates the proof of operation of the architecture proposed,

however there are still issues to investigate further, such as scalability, content resolution, label detection etc.

References

[1]P. Gambini et al., “Transparent optical packet switching: network architecture and demonstrators in the KEOPS project,” in IEEE J.S.A. Comm., vol. 16, no. 7 , pp. 1245-1259, 1998

[2]Rajat Kumar Singh and Yatindra Nath Singh, “An overview of photonic packet switching architectures,” in IETE Tech. Review, vol. 23, no. 1, pp. 15-34., 2006

[3]I.Tafur. Monroy et al , “Optical label switched networks: laboratory trial and network emulator in the IST-STOLAS project,” in IEEE Comm. Magazine, vol. 44, no. 8 , pp. 43-51, 2006

[4]R. A. Griffin, A. C. Carter, “Optical differential quadrature phase-shift key (DQPSK) for high capacity optical transmission,” in OSA OFC procs., 2002.

[5]K. Mishina et al., “All-optical modulation format conversion from on-off-keying to multiple-level phase-shift-keying based on nonlinearity in optical fiber,” in Optics Express, vol. 15, no. 13, pp. 8444-8453, 2007

[6]P.J. Winzer and R.-J. Essiambre, “Advanced Modulation Formats for High-Capacity Optical Transport Networks,” in IEEE/OSA JLT, vol. 24, no. 12, pp. 4711-4728, 2006

[7]M. Rohde et al., “Robustness of DPSK direct detection transmission format in standard fibre WDM systems,” in Elec. Letters, vol. 36, no. 17, pp. 1483-1484, (2000)

[8]Y.K. Lize, B. Kuhlmey, R. Kashyap, "Broadband Mach-Zehnder interferometer design using microstructured optical fibers for multi-channel DPSK demodulation," in Optical Fiber Technology, vol. 13, no. 1, pp. 85-90, 2007

[9]X. Liu et al., "Athermal optical demodulator for OC-768 DPSK and RZ-DPSK signals," in IEEE Photon. Technol. Lett., vol. 17, no. 12, pp. 2610-2612, 2005

[10] H. Rohde and S. Randel, “Project PIEMAN: A European approach to a symmetrical 10 Gbit/s, 100 km, 32 lambda and 512 split PON,” in Procs of SPIE, vol. 6353 I, p. 635304, 2006

[11] A.M.J. Koonen et al., “Label-Controlled Optical Packet Routing—Technologies and Applications,” in IEEE J.S.T. in Quantum Electronics, vol. 13, no. 5, pp. 1540-1550, 2007

[12] G. Bennett, “All-Optical Switching Tutorial,” in Light Reading, 2001, http://www.lightreading.com/document.asp?doc_id=9017&print=true

[13] A. Banerjee, “Wavelength-division-multiplexed passive optical network (WDM-PON) technologies for broadband access: A review,” in JON, vol. 4, no. 11, pp. 737-758, 2005

[14] J. Cheyns et al., “Routing in an AWG-Based Optical Packet Switch,” in Photonic Network Communications, vol. 5, no. 1, pp. 69-80, 2003

[15] G. Bosco and P. Poggiolini, “On the joint effect of receiver impairments on direct-detection DQPSK systems,” in IEEE/OSA JLT, vol. 24, no. 3, pp. 1323-1333, 2006

[16] J. B. Jensen et al., “Colorless DQPSK Receiver for Wavelength Routed Packet Switched Networks,” in IEEE Photon. Technol. Lett. (submitted for publication)

[17] G. T. Zhou et al., “Self-Pumping Wavelength Conversion for DPSK Signals and DQPSK Generation Through Fourwave Mixing in Highly Nonlinear Optical Fiber,” in IEEE Photon. Technol. Lett., vol. 18, no. 22, pp. 2389-2391, 2006

[18] ITU-T G.694.1 (2002) – Spectral grids for WDM applications: DWDM frequency grid. See e.g. http://www.bayspec.com/pdf/ITUDWDM.pdf

Biography

Alexey V. Osadchiy received the M.Sc. degree in fiber optical communications from the Bonch-Bruyevich State University of Communications, Saint-Petersburg, Russia, in 2006. He is currently pursuing a Ph.D. in optical communications engineering at DTU Fotonik, Technical University of Denmark, with main focus on access networks and interaction between access networks and higher level of network hierarchy networks, namely, metro-access interfacing.

Idelfonso Tafur Monroy received the M.Sc. degree in multichannel telecommunications from the Bonch-Bruevitch Institute of Communications, St. Petersburg, Russia, in 1992, the Technology Licenciate degree in telecommunications theory from the Royal Institute of Technology, Stockholm, Sweden, and the Ph.D. degree from the Electrical Engineering Department, Eindhoven University of Technology, The Netherlands, in 1999.

He is currently Head of the metro-access and short range communications group of the Department of Photonics Engineering, Technical University of Denmark. He was an Assistant Professor until 2006 at the Eindhoven University of Technology. Currently, he is an Associate Professor at the Technical University of Denmark. He has participated in several European research projects, including the ACTS, FP6, and FP7 frameworks (APEX, STOLAS, LSAGNE, MUFINS). At the moment, he is in involved the ICT European projects Gi-GaWaM, ALPHA, BONE, and EURO-FOS. His research interests

are in hybrid optical-wireless communication systems, coherent detection technologies and digital signal processing receivers for baseband and radio-over-fiber links, optical switching, nanophotonic technologies, and systems for integrated metro and access networks, short range optical links, and communication theory.

Figures

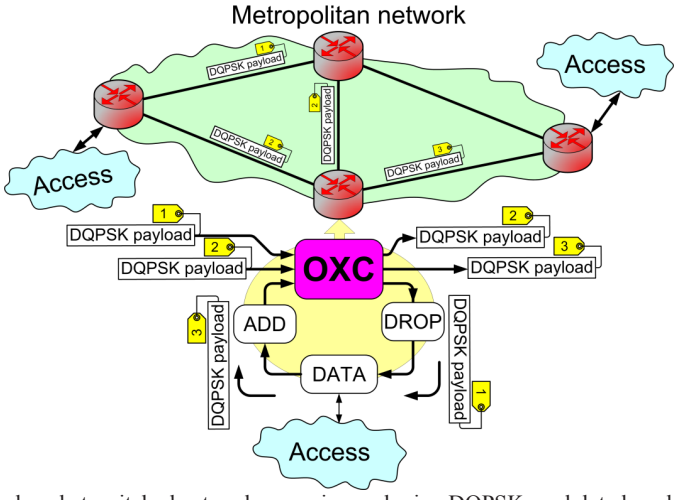

Fig. 1. Optical packet switched network scenario employing DQPSK modulated payload signals and optical label controlled crossconnets and interface between the metropolitan and access network segments. DATA=Data storage and processing block.

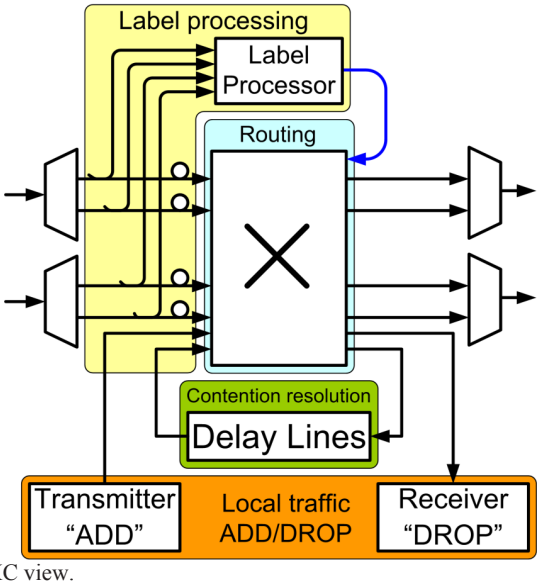

Fig. 2. Detailed OXC view.

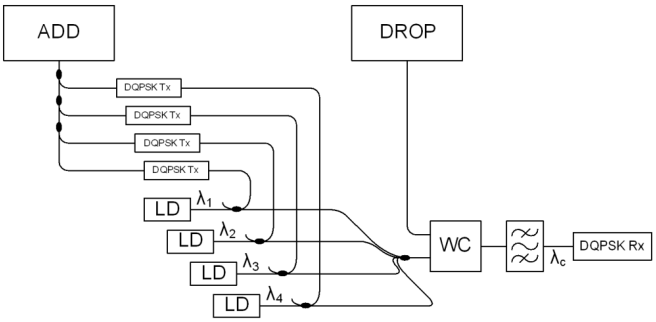

Fig. 3. Interaction between the ADD and DROP parts of the optical cross-connect (OXC).

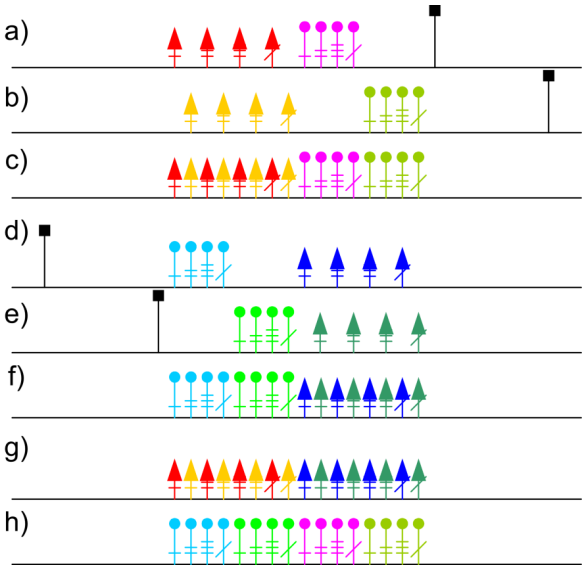

Fig. 4. Wavelengths allocation: (a) and (b) represents two subgroups, forming a group (c). Subgroups (d) and (e) form a group (f), matching group (c) in such a way that a full grid of signals (g) and pumps (f) match each other. Arrow-ended lines represent signal wavelengths, pin-head-ended ones represent pumps, and square ended lines represent common wavelengths.

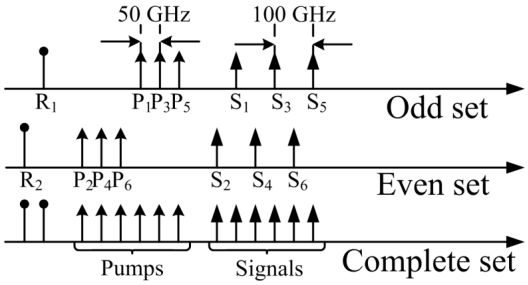

Fig. 5. Experimental setup pump/signal allocation scheme for the receiving part in frequency domain. R1 – common wavelength conversion product for the odd set, R2 – for the even set.

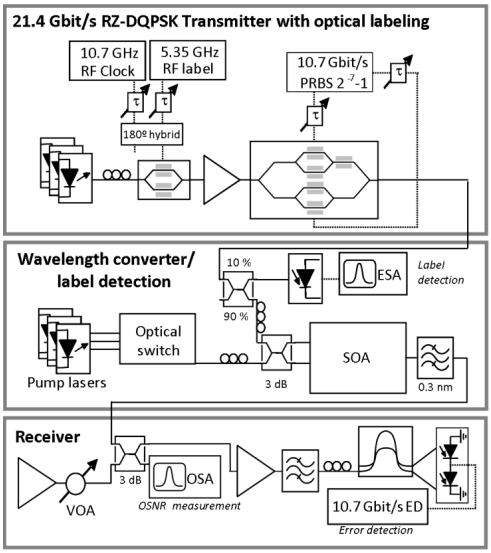

Fig. 6. Experimental setup.

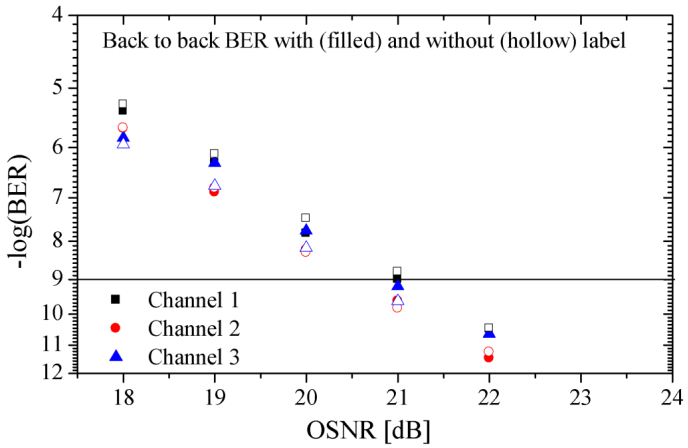

Fig. 7. Signal and label back-to-back BER measurement.

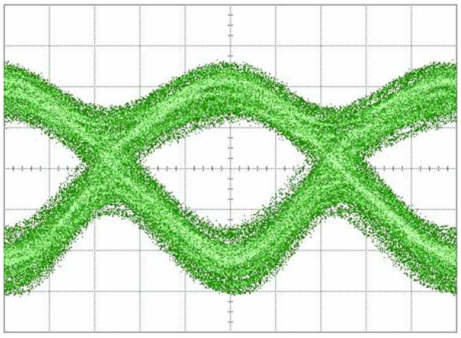

Fig. 8. Signal with a label eye back-to-back.

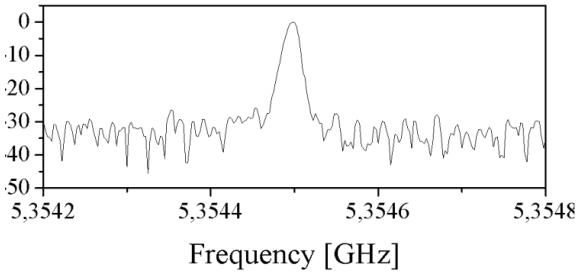

Fig. 9. Detected label signal electrical spectrum.

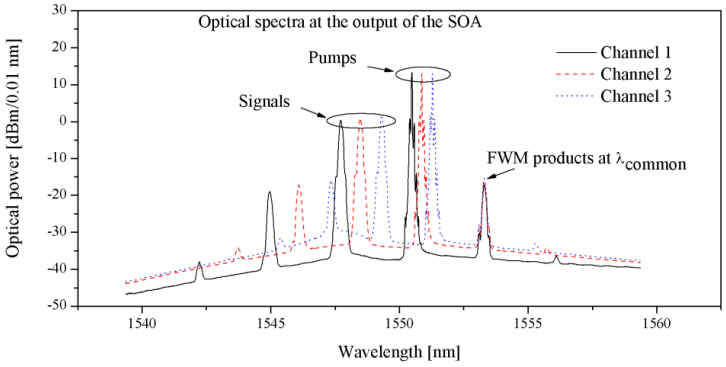

Fig. 10. Optical spectrum for the case 3 WDM channels.

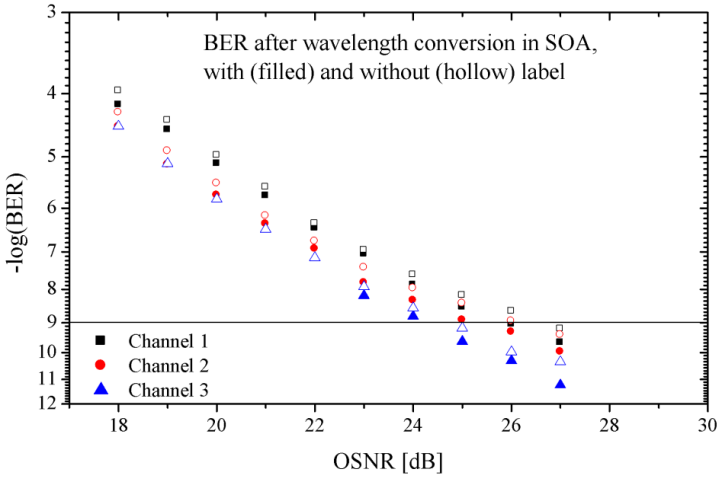

Fig. 11. Signal and label BER after wavelength conversion.

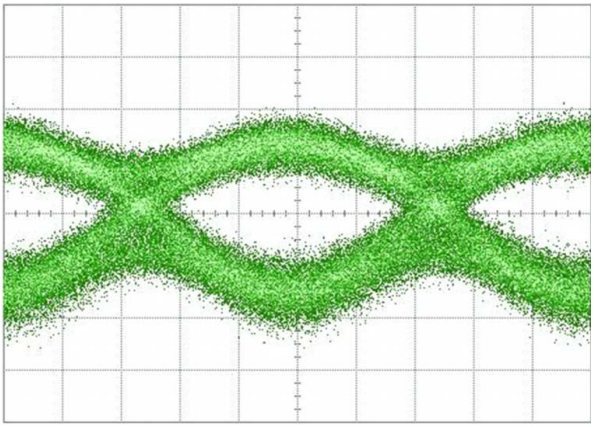

Fig. 12. Signal and label eye after wavelength conversion.

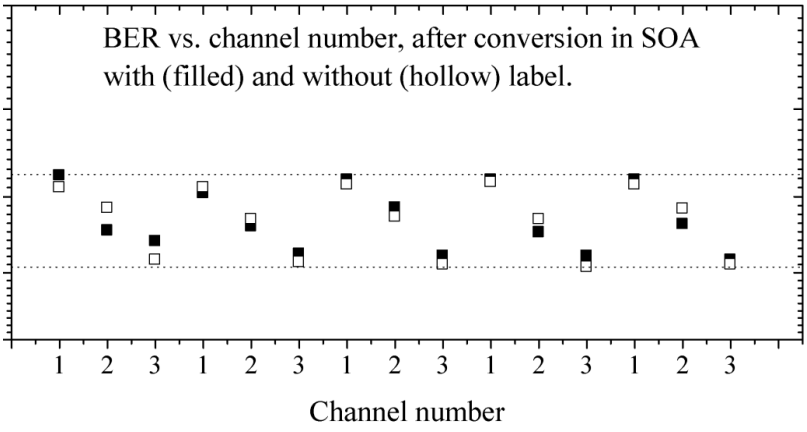

Fig. 13. Monitored BER after switching experiment with SOA.

Paper C

Marcin Wieckowski, Alexey V. Osadchiy, Jarek P. Turkiewicz, Idelfonso Tafur Monroy, "Performance assessment of flexible time-wavelength routing for a self-aggregating transparent Metro-access interface," *35th European Conference on Optical Communication*, Paper P6.16 (2009)

Performance Assessment of Flexible Time-Wavelength Routing for a Self-aggregating Transparent Metro-Access Interface

M. Więckowski[(1)], A. V. Osadchiy [(2)], J. P. Turkiewicz[(1)], I. Tafur Monroy[(2)]

[(1)] Institute of Telecommunication, Warsaw University of Technology, m.wieckowski@stud.elka.pw.edu.pl
[(2)] DTU Fotonik, Technical University of Denmark, 2800 Kgs. Lyngby, Denmark, idtm@ fotonik.dtu.dk

Abstract. *A time-WDM architecture with on-the-fly wavelength routing and traffic self-aggregation is proposed. Metro-accesss ligthpaths are established using ONUs with reflective modulators. Simulations results show the advantages of the proposed architecture over WDM-PONs.*

Introduction

It is foreseen, that FTTH networks will migrate towards multi-Gbit/s transmission speed utilizing WDM technology to meet growing demands for capacity[1,2]. This scenario implies that central offices, supporting hundred-to-thousands of end-users will need to perform aggregation and de-aggregation of traffic in volumes reaching Tbit/s. In particular, there will be a large pressure on the interface between the access and the metropolitan network layer to cope with the requirements on low latency, flexibility and reliability that will be expected from future broadband networks. At the same time, cost and energy efficiency has to be seriously taken into account.

We propose, based on the traffic profile of access networks, a novel optical access network architecture based on time-wavelength routing for transparent, self-aggregating metro-access interface architecture. In this paper, we evaluate by extensive computer simulations the performance of the proposed architecture.

Metro-access node architecture

It has been observed at IP routing nodes, that the majority of the network traffic (80%-95%) goes from the router to the same 4-5 destinations[3]. This kind of traffic characteristic could be exploited by setting a permanent (with reconfiguration capabilities) passively-routed lightpath from the other destinations to those 'major' destinations. That way, up to 80% of the traffic could go all the way from the originating user (access) to major destinations without the need of re-aggregation or any other routing processing. Traffic would be processed only when leaving the network segment capable of handling it in its form (e.g. interfacing between Metro and Access networks). Based on that observation, we are proposing a novel solution. The architecture proposed is a time-wavelength (*t-λ*) routed access network, shown schematically in Fig. 1.

Optical network units (ONUs) are considered to use a reflective modulator to implement the upstream channel towards the central office (CO). Time-wavelength slots are generated at the CO and send to the ONUs. The provided continuous wave (CW) slots are used by each ONU to modulate its data to be sent upstream. A certain wavelength can be therefore associated with a destination and/or services. The t-λ slots are arranged so that at the passive combining point no slot overlapping takes place and therefore avoiding conflicts. In this way, at the CO each wavelength will contain data from several ONUs performing self-aggregation of traffic to the same destination. Thus on-the-fly routing is possible at the CO by proper wavelength path pre-assignments.

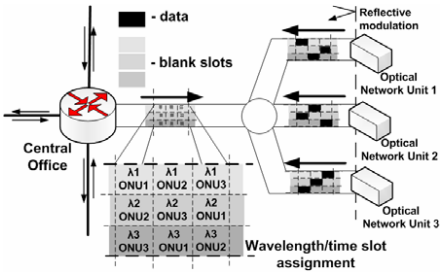

Fig. 1 Description of a time-wavelength routed access network; ONU-optical network unit; All ONUs with reflective electro-absorption modulator

Performance evaluation

Two network topologies were studied: a ring and a star configuration. Fig. 2 shows the diagram of the ring topology.

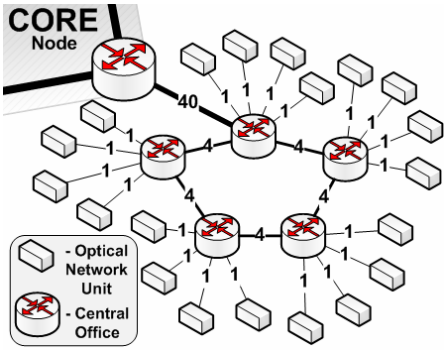

Fig. 2 Simulated network topology based on a ring interconnection of the COs. Numbers on the connection lines indicate their throughputs

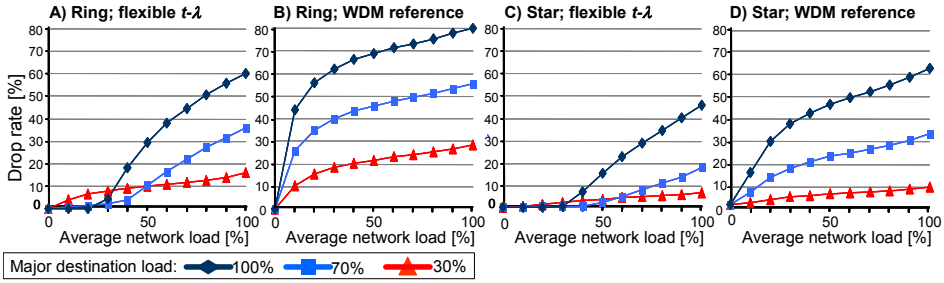

Fig. 3 Simulations result for the packet drop probability. Ring topology; a) t-λ and b) WDM reference. Star topology: c) t-λ and d) WDM reference.

The evaluated network consisted of five COs with four ONUs connected to each of them and a Core Node (CN) as a major destination, see Fig 2. The COs were connected to each other in a ring or star arrangement. One CO was connected to the CN. Totally, each topology consisted of 5 COs, 20 ONUs and one CN. As a reference, we considered a conventional WDM-PON, where each ONU had its own λ assigned to it, which is terminated at the CO, i.e. no WDM signal transparency provided. In the proposed solution, *t-λ* slots were assigned in such a way that wavelengths were associated with the CN and the COs, where the CN was our denoted 'major destination'. A 10-packet buffer was assigned to each ONU, while the COs used no buffering. The numbers shown on the connecting lines (Fig. 2) represent the link throughput. The applied traffic model followed a Poisson distribution. The goal of the performance analysis was to quantify the packet drop probability when a part of the overall traffic - 'major destination load' - was assigned to the CN and the rest equally distributed among the other destinations.

A dedicated computer simulation program was developed to evaluate the performance of the proposed metro-access interface. Each simulation starts with a warm-up period long enough to ensure a stable network condition and accuracy of the final results.

Simulation results

Fig. 3 shows the results for our *t-λ* and its comparison with a WDM reference case. Each scenario utilizes 4 wavelengths for a CO-ONUs communication. Moreover, in our simulations, one wavelength is dedicated to the major destination, i.e. CN and the others serve the other destinations.

In a pure WDM PON, each ONUs connected to the CO has its own wavelength, while in our proposed architecture those wavelengths are time-shared among ONUs. We can observe from Fig. 3a and Fig. 3b (ring topology) that the overall packet drop probability is higher for a WDM scenario compared to *t-λ* scenario. Fig. 3c and Fig. 3d, show the comparative results for a star configuration. Also for this case, the simulation results indicates the superiority of the proposed *t-λ* routing architecture

It can be seen in Fig. 3 that for both ring and star configurations in *t-λ* routing the very low floor in drop rate performance. For the average network load up to 30% regardless the major destination load the drop rate is below 10%. For reference WDM based routing the drop rate, taking into account the same conditions, is between 20-60% in a ring configuration. When increasing the average network load the drop rate increases. For the average network load 50% the maximal drop rates are 30% and 70% for the ring in t-λ and WDM reference respectively and 15% and 45% for star topology. With full network load the maximal drop rates are 60% and 80% for the ring in t-λ and WDM reference respectively and 45% and 60% for star topology. Overall, the star topology show slightly better performance.

Conclusions

We present simulation results showing the advantages of using a novel, flexible time-wavelength routed access interface for metro-access networks. ONUs with colourless reflective modulators are used to allow self-aggregation of traffic at the central office by establishing transparent lightpaths to certain destinations. Comparing to a WDM-PON scenario, our simulation results show the superiority of proposed architecture for both a ring and a start network topology. Although, our traffic model is Poisson and more sophisticated traffic models need yet to be implemented, our results indicate that a *t-λ* routing has potential application for flexible metro-access interface exploiting colourless reflective modulation based ONUs.

References

1 F.-T. An et al., IEEE Journal of Lightwave Technology, **22**, 2557 (2004)
2 A.M.J. Koonen, Proc. of the IEEE, 94, 911 (2006)
3 P.-L Tsai et al., Computer Communications, **16**, 456 (2006)

Paper D

Timothy Braidwood Gibbon, Alexey V. Osadchiy, Rasmus Kjær, Jesper Bevensee Jensen, Idelfonso Tafur Monroy, "Gain transient control for wavelength division multiplexed access networks using semiconductor optical amplifiers," Optical **Fiber Technology**, 15, no. 3, pp 279-282 (2009)

Optical Fiber Technology 15 (2009) 279–282

Contents lists available at ScienceDirect

Optical Fiber Technology

www.elsevier.com/locate/yofte

Gain transient control for wavelength division multiplexed access networks using semiconductor optical amplifiers

T.B. Gibbon *, A.V. Osadchiy, R. Kjær, J.B. Jensen, I. Tafur Monroy

DTU Fotonik, Department of Photonics Engineering, Technical University of Denmark, Ørsteds Plads 343, DK-2800 Kgs. Lyngby, Denmark

ARTICLE INFO

Article history:
Received 13 October 2008
Revised 8 December 2008
Available online 23 January 2009

Keywords:
Transient control
Semiconductor optical amplifier
Wavelength division multiplexed access networks

ABSTRACT

Gain transients can severely hamper the upstream network performance in wavelength division multiplexed (WDM) access networks featuring erbium doped fiber amplifiers (EDFAs) or Raman amplification. We experimentally demonstrate for the first time using 10 Gb/s fiber transmission bit error rate measurements how a near-saturated semiconductor optical amplifier (SOA) can be used to control these gain transients. An SOA is shown to reduce the penalty of transients originating in an EDFA from 2.3 dB to 0.2 dB for 10 Gb/s transmission over standard single mode fiber using a $2^{31}-1$ PRBS pattern. The results suggest that a single SOA integrated within a WDM receiver at the metro node could offer a convenient all-optical solution for upstream transient control in WDM access networks.

1. Introduction

The implementation of a typical wavelength division multiplexed (WDM) access network is shown in Fig. 1. For such systems both erbium doped fiber amplification [1] and Raman amplification [2] has been proposed for the backhaul link in order to increase the network reach and/or splitting ratio. The signal power aggregated at the array waveguide grating (AWG) from the various optical network units (ONUs) will differ considerably due to factors such as differences in path loss, power splitter non-uniform loss and non-uniform launch power levels [3]. This will introduce severe upstream gain transients as the input optical power to the backhaul erbium doped fiber amplifier (EDFA) or Raman amplifier is suddenly changed. Such transients will introduce burst errors at the metro node by means of strong non-linearity at the power overshoots, and degraded signal-to-noise ratio at the power undershoots [4]. Transient control in such a scenario is thus crucial.

Dense WDM receiver technology featuring a single integrated SOA functioning as a pre-detection amplifier for up to 40 channels simultaneously has been demonstrated by Nagarajan et al. [5]. We propose that the benefits of an SOA integrated within a WDM receiver at the metro node could be extended beyond pre-detection amplification to include signal restoration in the presence of transients. In the past a number of general transient control methods have already been proposed, including EDFA gain clamping using an optical feedback loop [6,7], electrical feedforward/feedback control of the pump power [8,9], clamping the EDFA with a holding beam to limit the variance in the total optical input power [10], and the use of saturated or near-saturated semiconductor optical amplifiers [11–15]. To the best of our knowledge however, we are the first to present 10 Gb/s fiber transmission bit error rate (BER) measurement results illustrating transient control using a near-saturated SOA.

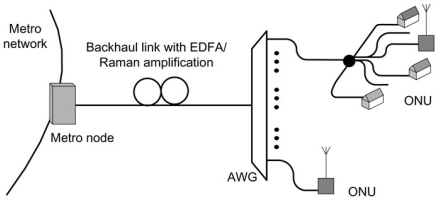

Fig. 1. The configuration of a typical WDM access network.

2. Experimental setup

The experimental setup is shown in Fig. 2. An acousto-optic modulator operating at 500 Hz was used to generate a 1548 nm transient pump lightwave, similar to a transient signal arriving at the remote node AWG from the ONUs. Transient effects of the 10 Gb/s non-return-to-zero (NRZ) signal at 1550 nm were generated in an EDFA due to cross-gain saturation between the information carrying signal and the 1548 nm co-propagating transient pump lightwave modulated at 500 Hz by the acousto-optic modulator. A 1550 nm band-pass filter (BPF) positioned after the EDFA

* Corresponding author at: DTU Fotonik, Technical University of Denmark, Ørsteds Plads, Building 343, room 218, 2800 Kgs. Lyngby, Denmark. Fax: +45 4593 6581.
E-mail address: tbgi@fotonik.dtu.dk (T.B. Gibbon).

1068-5200/$ – see front matter
doi:10.1016/j.yofte.2008.12.004

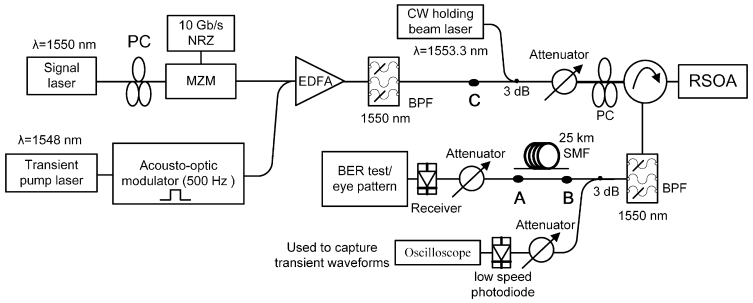

Fig. 2. Schematic of the experimental set-up used to demonstrate SOA transient suppression.

was used to remove the transient pump lightwave. In order to demonstrate the suppression of signal power transients by an SOA operated close to saturation, we used a reflective semiconductor optical amplifier (RSOA) and circulator. The RSOA was a commercially available device designed for the wavelength range 1530 to 1570 nm, with a maximum noise figure specification of 11 dB. The performance of the RSOA in terms of transient suppression and signal amplification depends on both the state of polarization and the intensity of the light entering the device. The 1553.3 nm continuous wave (CW) holding beam laser, attenuator and polarization controller (PC) before the circulator were thus used to optimize the RSOA performance. A second BPF centered at 1550 nm was used to filter out the holding beam and suppress amplified spontaneous emission noise before the signal was detected and the transient waveforms, bit error rate (BER) and the eye patterns were measured.

3. Experimental results

Fig. 3 shows the RSOA output power at 1550 nm for different input optical power, both with and without the holding beam. The SOA begins saturating at optical input powers above around −20 dBm in both cases. The holding beam does thus not considerably alter the gain curve profile in terms of shifting the saturation point, but it was used since holding beams have been shown to improve SOA performance. Gain recovery in an SOA is limited by the carrier lifetime. A holding beam causes a higher optical intensity in the active layer of the SOA. This increases the stimulated recombination rate and shortens the carrier lifetime, thereby improving the device performance [16–18]. Initially we investigated the transient suppression performance of the SOA as a function of the SOA optical input power. With the 10 Gb/s signal power into the EDFA set to −1.0 dBm, the transient pump power set to 1.4 dBm, the EDFA set to give a fixed output power of 14 dBm, and the holding beam switched off, a series of transient waveforms such as those shown in Fig. 4a were measured at the low speed photodiode. The SOA optical input power was adjusted using the attenuator before the circulator, and the power at the low speed photodiode was kept constant throughout. Fig. 4b shows the modulation indexes ($V_{pp}/2V_{average}$) obtained from transient waveforms for three different transient pump powers corresponding to three different transient magnitudes. From Fig. 4b it is evident that for SOA input power greater than around −2.5 dBm the modulation index approaches zero, an indication that the transients are almost completely removed. Operating this deeply within the saturated region of the gain curve will however not only remove the transients, but also erase the intensity modulation carrying the data.

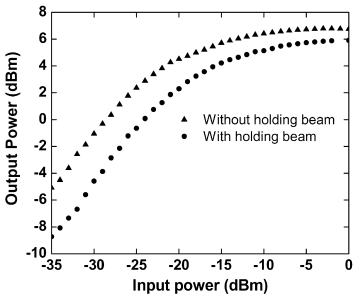

Fig. 3. RSOA output power at 1550 nm as a function of input optical power.

There is thus a trade-off between transient removal and the signal extinction ratio.

In order to determine the optimal SOA operation point for transient suppression without erasing the signal, BER measurements of the 10 Gb/s NRZ modulated signal as a function of SOA input power between −22 dBm and −10 dBm. Fig. 5 shows the BER curves for the back-to-back case (without the SOA, i.e. with points C and A in Fig. 2 connected by a patchcord) both with and without transients. Also shown in Fig. 5 are the BER curves for SOA input powers of −10 dBm and −14 dBm with the SOA connected. All measurements were performed using a 2^7–1 PRBS pattern with a 1.4 dBm transient pump power and the holding beam off.

The SOA was found to reduce the transient penalty by a maximum margin of 1.5 dB for an optimal SOA input power of −14 dBm. The SOA transient suppression in terms of eye reopening is clearly evident. The overshoots in the −10 dBm and −14 dBm eyes are attributed to preferential gain experienced by the leading edge of the pulse as it encounters a non-depleted carrier density. After this the carrier density is lowered and the remainder of the pulse experiences less amplification. For SOA input powers above −14 dBm, the BER is degraded by the introduction of excessive zero-level noise into the eye. From the manufacturer specification the noise figure of the SOA used was rather high (up to 11 dB) and better performance is expected from an SOA with a lower noise figure.

To demonstrate SOA transient control under field conditions, such as for PON links where transmission distances from the remote node to the ONU is in the order of 20 km are typical, 25 km

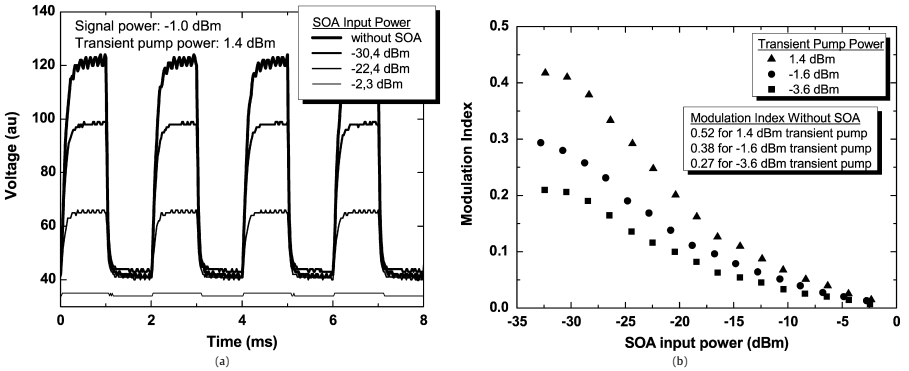

Fig. 4. (a) Transient waveforms at different SOA input powers for a 1.4 dBm transient pump power. (b) Transient modulation index as a function of the SOA input power for three different transient pump powers. For transient pump powers of 1.4 dB, −1.6 dBm and −3.6 dBm, the corresponding modulation indexes without the SOA were 0.52, 0.38 and 0.27, respectively.

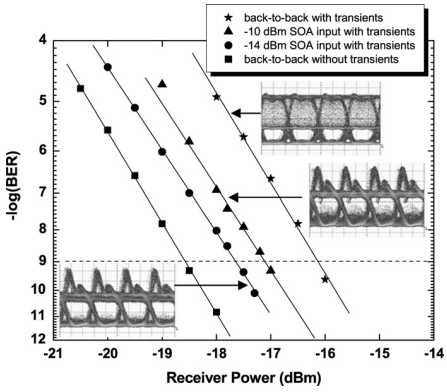

Fig. 5. BER curves and corresponding eye diagrams for various SOA input powers with a 1.4 dBm transient pump and a 2^7-1 PRBS pattern. Eye diagram scales: X: 40 ps/div; Y: 297 μW/div.

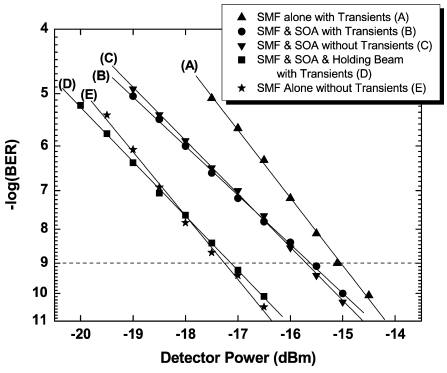

Fig. 6. Transmission over 25 km of standard SMF for a $2^{31}-1$ PRBS pattern.

of standard single mode fiber (SMF) was inserted after the SOA between points A and B in Fig. 2. A transient pump power of 1.4 dBm was used, corresponding to a transient modulation index of 0.52. More challenging test conditions in terms of SOA patterning effects were introduced by using a $2^{31}-1$ PRBS pattern instead of the shorter 2^7-1 PRBS pattern used previously. All measurements were performed with the previously determined optimal SOA input signal power of −14 dBm, and the BER results are summarized in Fig. 6 and Table 1.

From a comparison between BER curves A and E in Fig. 6, it is found that for the case of the SMF alone without the SOA (i.e. with the SMF inserted between points B and C in Fig. 2) the transient caused a 2.3 dB penalty at a BER of 10^{-9}. The introduction of the SOA reduced the penalty to 1.7 dB, shifting curve A to curve B. Comparison between curves B and C reveal that with the inclusion of the SOA, the BER performance is almost identical with and without transients. From this we can conclude that the SOA almost completely suppresses the transient-related penalty. The SOA however introduces some additional penalty through eye patterning and noise, hence curves B and E do not coincide. In general, for pattern lengths longer than 2^7-1 we observed that patterning significantly degraded the BER performance when the SOA was used. Holding beams have been shown to reduce patterning associated with longer pattern lengths by improving SOA performance through inducing a higher stimulated recombination rate and shortening the carrier lifetime [16,17]. We thus used a holding beam at 1553.3 nm with a power of around −2.3 dBm to improve the SOA performance. This shifted curve B to curve D in Fig. 6, reducing the penalty at a BER of 10^{-9} to a mere 0.2 dB as measured using a $2^{31}-1$ PRBS pattern. The SOA when used with the holding beam thus almost completely restored the system performance to that of the SMF alone without the transients.

4. Summary

We have demonstrated how an SOA can be used to restore system performance for upstream WDM access network transients

Table 1
Receiver sensitivities and power penalties measured using a $2^{31}-1$ PRBS pattern for the transmission results over 25 km of SMF shown in Fig. 5.

	Curve in Fig. 6	Receiver sensitivity at a BER of 10^{-9}	Penalty relative to case of SMF alone without transient
SMF alone without transient	E	−17.3 dBm	–
SMF alone with transient	A	−15.0 dBm	2.3 dB
SMF & SOA with transient	B	−15.6 dBm	1.7 dB
SMF & SOA without transient	C	−15.7 dBm	1.6 dB
SMF & SOA & holding beam with transient	D	−17.1 dBm	0.2 dB

originating in EDFAs and Raman amplifiers. The effectiveness of transient suppression was shown to depend strongly on the SOA optical input power, where optimum suppression occurs in the vicinity of the saturation region of the gain curve. For a 10 Gb/s signal disturbed by transients with modulation index of 0.52 and transmitted over 25 km of standard SMF, the introduction of an SOA was shown to reduce the transient penalty from 2.3 dB to 1.7 dB. The overall transmission penalty was further reduced to a mere 0.2 dBm when a holding beam was used to improve the SOA performance by improving the carrier dynamics and reducing patterning. The results presented in this paper suggest that an SOA incorporated within the metro node WDM receiver could offer a convenient all-optical solution for upstream transient control in WDM access networks.

Acknowledgments

The work described in this paper was carried out with the support of the BONE-project (Building the Future Optical Network in Europe), a Network of Excellence funded by the European Commission through the 7th ICT-Framework Programme.

References

[1] R.P. Davey, P. Healey, I. Hope, P. Watkinson, D.B. Payne, O. Marmur, WDM reach extension of a GPON to 135 km, J. Lightwave Technol. 24 (1) (2006) 29–31.
[2] I. Tafur Monroy, R. Kjaer, F. Ohman, K. Yvind, P. Jeppesen, Distributed fiber Raman amplification in long reach PON bidirectional access links, Opt. Fiber Technol. 14 (1) (2008) 41–44.
[3] S. Appathurai, D. Nesset, R. Davey, Measurement of tolerance to non-uniform burst powers in SOA amplified GPON systems, in: Proc. Optical Fiber Communication Conference, Anaheim, California, 2007, paper OWS2.
[4] C.-J. Chen, W.S. Wong, Transient effects in saturated Raman amplifiers, Electron. Lett. 37 (6) (2001) 371–372.
[5] R. Nagarajan, M. Kato, S. Hurtt, A. Dentai, J. Pleumeekers, P. Evans, M. Missey, R. Muthiah, A. Chen, D. Lambert, P. Chavarkar, A. Mathur, J. Bäck, S. Murthy, R. Salvatore, C. Joyner, J. Rossi, R. Schneider, M. Ziari, F. Kish, D. Welch, Monolithic 10 and 40 channel InP receiver photonic integrated circuits with on-chip amplification, in: Proc. Optical Fiber Communication Conference, San Diego, California, 2007, paper PDP32.
[6] M. Karasek, A. Bononi, L.A. Rusch, M. Menif, Gain stabilization in gain clamped EDFA cascades fed by WDM burst-mode packet traffic, J. Lightwave Technol. 18 (3) (2000) 308–313.
[7] M. Karasek, M. Menif, L.A. Rusch, Output power excursions in a cascade of EDFAs fed by multichannel burst-mode packet traffic: Experimentation and modeling, J. Lightwave Technol. 19 (7) (2001) 933–940.
[8] C. Tian, S. Kinoshita, Analysis and control of transient dynamics of EDFA pumped by 1480- and 980-nm lasers, J. Lightwave Technol. 21 (8) (2003) 1728–1733.
[9] T. Yoshikawa, K. Okamura, E. Otani, T. Okaniwa, T. Uchino, M. Fukushima, N. Kagi, WDM burst mode signal amplification by cascaded EDFAs with transient control, Opt. Express 14 (11) (2006) 4650–4655.
[10] T. Shiozaki, M. Fuse, S. Morikura, A study of gain dynamics of erbium-doped fiber amplifiers for burst optical signals, in: Proc. European Conference on Optical Communication, Copenhagen, Denmark, 2002, paper We.4.02.
[11] I. Hallax, D. Simeonidou, S.S. Sian, Patent No. WO 98/19416, Transient suppression in optical wavelength division multiplex network, World Intellectual Property Organization, 1998.
[12] F. Bruyere, A. Bisson, L. Noirie, J.-Y. Emery, A. Jourdan, Gain stabilization of EDFA cascade using clamped-gain SOA, in: Proc. Optical Fiber Communication Conference, San Jose, California, 1998, paper WJ5.
[13] R. Ibrahim, Y. Gottesman, B.-E. Benkelfat, Q. Zou, EDFA gain stabilization with fast transient behavior by use of a semiconductor optical amplifier, in: Proc. Quantum Electronics and Laser Science Conference, Baltimore, MD, 2007, paper JTuA84.
[14] T.B. Gibbon, A.V. Osadchiy, R. Kjær, J.B. Jensen, I. Tafur Monroy, Gain transient suppression for WDM PON networks using semiconductor optical amplifier, Electron. Lett. 44 (12) (2008) 756–758.
[15] T.B. Gibbon, I. Tafur Monroy, Multi-level burst power transient suppression using semiconductor optical amplifiers in gigabit access links, in: Proc. European Conference on Optical Communication, Brussels, Belgium, 2008, paper P. 6.13.
[16] J. Yu, P. Jeppesen, Improvement of cascaded semiconductor optical amplifier gates by using holding light injection, J. Lightwave Technol. 19 (5) (2001) 614–623.
[17] M. Amaya, A. Sharaiha, J. Le Bihan, Evaluation of BER and WDM crosstalk penalty at 2.5 Gb/s in an SOA by holding beam injection around transparency wavelength, in: Proc Information and Communication Technologies Conference, Cairo, Egypt, 2006, paper Mo.4.5.1.
[18] J.L. Pleumeekers, M. Kauer, K. Dreyer, C. Burrus, A.G. Dentai, S. Shunk, J. Leuthold, C.H. Joyner, Acceleration of gain recovery in semiconductor optical amplifiers by optical injection near transparency wavelength, Photon. Technol. Lett. 14 (1) (2002) 12–14.

Paper E

Alexey V. Osadchiy, Kamau Prince, Neil Guerrero Gonzalez, Antonio Caballero, Ferney Orlando Amaya, Jesper B. Jensen, Darko Zibar, Idelfonso Tafur Monroy, "Coherent Detection Passive Optical Access Network Enabling Converged Delivery of Broadcast and Dedicated Broadband Services," **Optical Fiber Technology** (ACCEPTED FOR PUBLICATION) (2010)

Coherent Detection Passive Optical Access Network Enabling Converged Delivery of Broadcast and Dedicated Broadband Services

Alexey V. Osadchiy[1,*], Kamau Prince[1], Neil Guerrero Gonzalez[1], Antonio Caballero[1], Ferney Orlando Amaya[1,2], Jesper B. Jensen[1], Darko Zibar[1], Idelfonso Tafur Monroy[1]

[1] *DTU Fotonik, Technical University of Denmark, Oersteds Plads 343, DTU Campus, 2800 Kgs. Lyngby, Denmark*

[2] *GIDATI Research Group Universidad Pontificia Bolivariana Medellín, Colombia*

* *Alexey V. Osadchiy*

DTU Fotonik, Technical University of Denmark

Oersteds Plads 343, DTU campus, Office 214

2800 Kgs. Lyngby, Denmark

Tel.: +45 4525 3657

Email: avos@fotonik.dtu.dk

Abstract: We propose a passive optical network architecture based on coherent detection for converged delivery of broadcast services from a dedicated remote broadcast server and user-specific services from a local central office. We experimentally demonstrate this architecture with mixed traffic types, wavelength division multiplexed, unicast channels composed of four radio-over-fiber channels operating at 5 GHz carrier frequency with 250 Mbaud phase shift keying modulation and four 10 Gb/s baseband amplitude shift keying channels; while the broadcast channels were four 10 Gbaud DQPSK channels. The broadcast channels were transmitted over 78 km of single mode fiber to a central office where they were multiplexed with the unicast channels for further fiber transmission over 34-km to reach the access network. Successful detection of all channels is demonstrated.

Keywords: coherent detection; optical broadcast; access networks; wireless-wireline convergence

1. Introduction

The bandwidth demands of an average end user have grown significantly over the last decade, mainly due to introduction of new bandwidth-intensive services, such as file sharing and high-definition TV (HDTV) [1]. Current trend suggests that bandwidth demands for optical fiber access are going to grow above 1 Gb/s per user in the near future [2]. Such a bandwidth capacity demand has caused an increase of interest in developing broadband access systems as in their current form, access networks form a 'bottleneck' between the high-speed metro and backbone networks and the high-speed local area networks.

Until recently, various fiber-to-the-customer premises solutions have been developed [3], however, the most common fiber based access network standards, ITU-T GPON and IEEE EPON [4,5], rely on time division multiplexing (TDM) of user data, and provide less than 100 Mbps per single user. Wavelength division multiplexing (WDM) based standards are now being introduced to enable higher bandwidth capacity per user [6]. One way to optimize bandwidth capacity of access systems is to differentiate the network traffic into unicast, or dedicated, and broadcast, or common traffic; and to treat the two traffic types separately. While the WDM schemes in development will provide much higher bandwidth per user [7], they do not support broadcast channels due to physical demultiplexing of channels into user-specific fibers.

Broadcasting is one of the ways to improve overall data transport efficiency of an access system: separate handling of unicast and broadcast services can provide guaranteed bandwidth capacity for both. Introduction of remote dedicated broadcast servers removes the broadcast traffic processing functionality from the central offices (COs), which makes them simpler. Combined with the existing trend for long-reach access systems [8], such a broadcast overlay will provide high-bandwidth broadcast and dedicated services to users in a large geographical area. This will decrease the number of COs required for full coverage and reduced complexity of individual COs, leading to a significant reduction in overall network complexity, and thus will offer substantial economies of scale.

In the following sections, we shall introduce our proposed overlay architecture to smoothly integrate both broadband broadcast and unicast services over a common passive optical fiber network and discuss the principles it is based on. Next, we elaborate on the experimental demonstration of our proposed approach, including the experimental setup description, listing of the results for different signal formats, and closing with a discussion of the obtained results. In the last section, we shall discuss the challenges and prospects associated with our proposed network architecture.

2. Proposed network architecture supporting broadcast

We propose a passive optical network (PON) design that provides high bandwidth per user and supports multiple broadcast channels. Fig. 1 shows the principle of remote broadcast server-based PON: a dedicated broadcast server provides broadcast traffic to multiple

central offices (COs) via a long-reach link. Broadcast traffic is then aggregated – wavelength multiplexed – with the local data traffic and cast into an access PON, relaying broadcast services to end-user equipment.

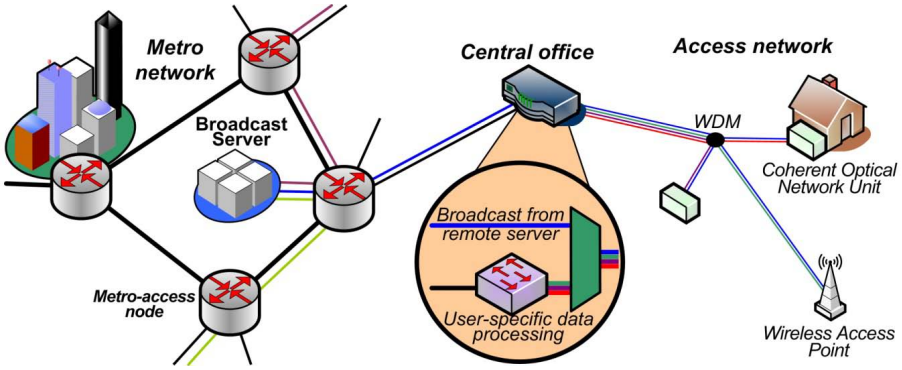

Fig. 1. Proposed remote broadcast server-based PON implementation.

Channel selection in the proposed PON design is achieved by employing coherent detection at the user end. This solution leads to increased receiver sensitivity and additionally enables high wavelength selectivity [9] of the optical network units (ONUs), thus enabling narrow channel spacing. Digital signal processing is used to compensate for transmission impairments and coherent detection imperfections.

2.1. Current PON architectures

TDM PON is the most wide-spread optical fiber access technology [10]. Capacity upgrade, including support for broadband broadcasting, of this topology is severely hampered by power budget limitations due to the use of power splitter/combiner to multiplex the end-user channels. Another disadvantage of this PON architecture is related to the shared channel capacity, which implies that all receiver units need to operate at the full system bandwidth, while the end-user only gets a fraction of that bandwidth. Moreover, due to time-slot based channel operation of the upstream channel, burst-mode detection, clock recovery and signal power equalization at the CO are all issues for capacity upgrades [7].

The WDM PON architecture was introduced as a more advanced PON technology to replace TDM PONs [6]. In WDM PONs, arrayed waveguide gratings (AWGs) are used to demultiplex the WDM channels into individual access fibers. Additionally, AWG's insertion loss is low, typically 4 dB per channel, and is independent of the number of wavelengths, which improves the system power budget compared to that of TDM PONs. This makes WDM PONs more appealing in terms of link reach and bit-rate per wavelength channel. However, WDM PON exhibit disadvantageous features for capacity upgrade and reconfiguration – this is caused by the nature of AWGs. Additional challenges are associated with the increased numbers of channels: in this case, AWGs with narrow channel spacing and low crosstalk values have to be used, which leads to the need for finer alignment of each wavelength to fit the AWG passband. Traditional WDM PONs are also incapable of efficiently providing broadcast services to the users due to the inherent

channel selectivity of the AWG making this approach incapable of supporting broadcast services, foreseen to play an important role in future services integration [11].

2.2. Coherent detection based receivers

Coherent receivers are attractive for practical application, as they allow improved power budget and simultaneous optical de-multiplexing and detection of optical signals [9]. However, until recently, optical coherent systems were considered too complex to implement due to high sensitivity to polarization mismatch between the incoming optical signal and the local oscillator and stringent requirements for low laser phase noise. Recent advances in digital signal processing (DSP) technology, combined with mature technology for narrow-linewidth semiconductor lasers and the prospect for photonic circuit integration have produced a revival of interest in optical coherent detection systems [12]. In particular, DSP is used to compensate for coherent detection imperfections and signal degradation due to transmission – through the use of various statistical and heuristic algorithms with the potential to be implemented in compact DSP chips. Coherent receiver-based optical systems are therefore becoming more attractive for both long-haul and access networks.

The basic operating principle of a coherent detection receiver is shown in Fig. 2: the incoming optical signal is mixed with the light from a local oscillator (LO) laser in an optical 90º hybrid combiner; after photodetection, Inphase and Quadrature component signals are obtained. These electrical signals are then processed by the DSP for

synchronization, clock-recovery and demodulation: compensation of transmission impairments may also be done.

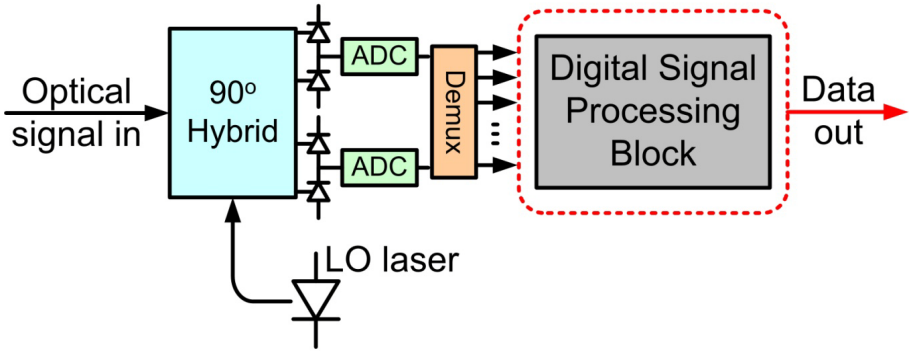

Fig. 2. Schematic diagram of a coherent receiver supported by DSP techniques, where LO laser is the local oscillator source, ADC – analogous-digital converters, and Demux is a parallelizing demultiplexer.

In a coherent detection setup as shown in Fig. 2, the receiver sensitivity is enhanced by up to 5-10 dB compared to a direct detection scheme [9], depending on the modulation format used. Such an increase in receiver sensitivity can be used to compensate for system losses and brings coherent system close in terms of power budget to WDM PONs as the number of users is increased. Moreover, any channel in the network can be selected by tuning LO wavelength, which is a requirement for broadcast services implementation. Simple filtering in electrical domain makes it possible to down-convert only the targeted channel to baseband during coherent detection, which enables narrow channel spacing.

3. Experimental setup

3.1. Experimental setup description

The experimental setup is presented on Fig. 3; it emulates a network scenario in which remotely generated broadcast channels are transmitted over a 78-km deployed SSMF, and are then combined with CO-generated unicast channels. The combined channels are then transmitted over 34-km distribution SMF.

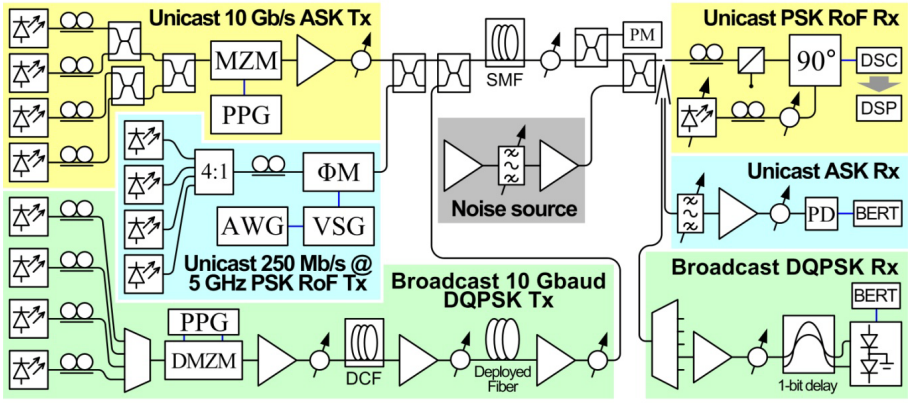

Fig. 3. Experimental setup. ΦM – phase modulator; MZM – Mach-Zehnder modulator; DMZM – dual Mach-Zehnder modulator; DCF – dispersion compensating fiber; SMF – distribution single mode fiber; DSC – digital sampling scope; PM – power monitor; 90° - 90-degree hybrid for coherent detection.

In the experiment, a group of four 10 Gb/s ASK-modulated data channels at 25 GHz spectral spacing represented user data channels generated at the central office (CO). Those channels were combined with four Radio-over-Fiber (RoF), 250 Mbaud, PSK channels

with a carrier frequency of 5 GHz, also spectrally spaced at 25 GHz, which represented CO-generated traffic for wireless access points. The third group of four 10 Gbaud DQPSK channels at 200 GHz spacing represented remotely generated broadcast traffic. The spacing between the groups was dictated by the available laser sources tunability ranges, and was as follows: 275 GHz between the ASK and PSK RoF channels, and 354 GHz (intended 350 GHz, mismatch due to the used arrayed waveguide grating (AWG) properties). The third group containing the DQPSK channels was transmitted over a span of 14 km of dispersion compensating fiber (DCF) and 78 km deployed SSMF simulating an inter-office distribution link from a remote broadcast server. Prior to injection into the 34-km distribution fiber, the channel powers were equalized within the groups, and the groups were amplified. The optical powers of each group were adjusted in order to provide optical signal-to-noise ratios (OSNR) sufficient for detection of all channels.

3.2. Results

3.2.1. 250 Mbaud 5 GHz carrier RoF PSK

The PSK channels were generated by combining a vector signal generator for frequency up-conversion and an arbitrary waveform generator for baseband generation. A 2^{7-1} PRBS pattern was used for the channels. The receiver configuration for this case is presented in Fig. 3. A 90-degree hybrid for coherent detection with a 100 kHz-linewidth external cavity tunable laser as a local oscillator (LO) was used to receive the inphase (I) and quadrature (Q) tributaries of the signals. The power of the PSK signals at the coherent receiver input

measured –18,5 dBm, while the power of the LO measured 4,5 dBm. An 8-bit real-time digital sampling scope was used to save samples of the received tributaries at 40 Gs/s. $2 \cdot 10^6$ symbols were processed for each measured point.

A DSP algorithm including a digital phase lock loop (DPLL) [13,14] was applied to the saved samples to perform phase matching, equalization, phase recovery and other operations required to compensate for transmission impairments of the signals. As a result of applying the algorithm, series of BER values of the signals were obtained. The BER for the recorded samples, both for the back-to-back and the fiber transmission case, was within 10^{-2} to 10^{-3} for OSNR values ranging within 2,5 to 6 dB, respectively. The BER curves are presented in Fig. 4. Bold and dashed lines represent approximation fits for back-to-back and transmission cases, respectively. BER of as low as 10^{-3} was obtained for each of the 4 channels for back-to-back and transmission cases. The scattering of the BER points observed in Fig. 4 is caused by the properties of the DSP algorithm and laser wavelength instability.

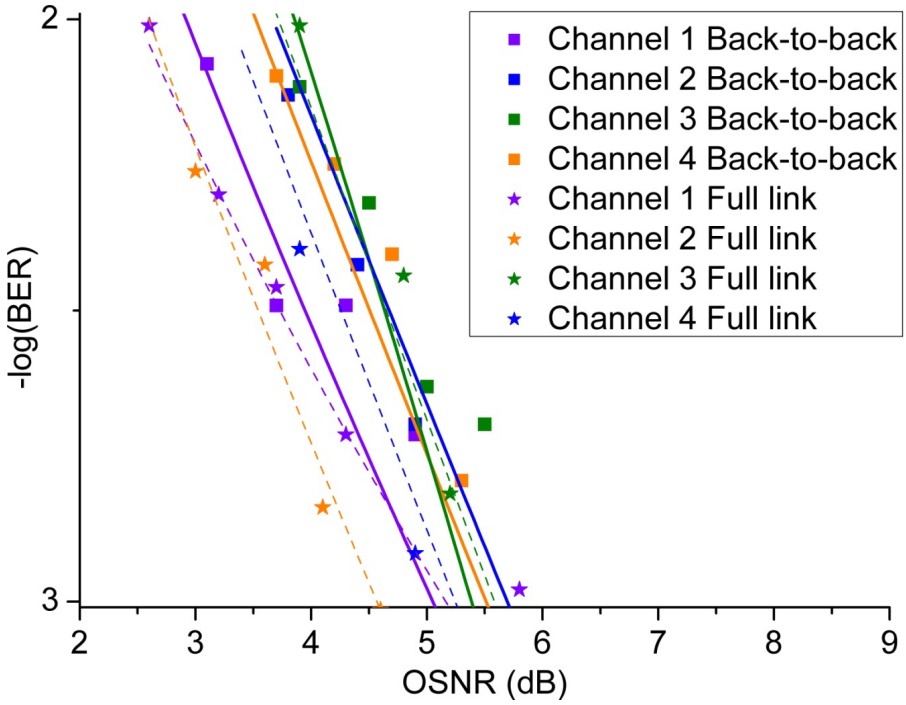

Fig. 4. PSK RoF channel BERs after digital signal processing.

3.2.2. 10 Gb/s ASK

Four separate laser sources were coupled together and intensity modulated by a Mach-Zehnder modulator (MZM); the modulating waveform was derived from pseudorandom binary sequence (PRBS) data, of length 2^{7-1} bits. The experimental setup is presented in Fig. 3. A narrow passband tunable optical filter was used to select the appropriate channel at the receiver side. A preamplified receiver was used to detect the ASK channels. The obtained BER curves are presented in Fig. 5; they show a 0.5 to 0.8 dB OSNR penalty for the signals transmitted through the system.

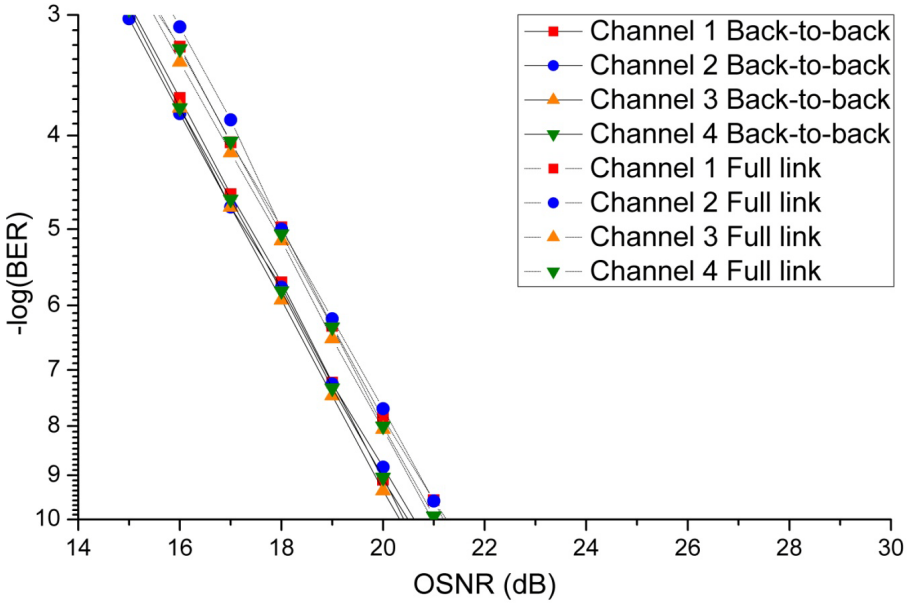

Fig. 5. ASK channel BERs.

3.2.3. 10 Gbaud DQPSK

The DQPSK signal was generated by modulating the continuous-wave (CW) output from four DFB lasers in a dual Mach-Zehnder IQ modulator (DMZM). A pulse pattern generator was used to create the PRBS signals: the resulting electrical waveform was split and then connected to both inputs of the DMZM. Decorrelation between the two inputs of the DMZM was secured by time delays between the two data signals.

The resulting channel group was transmitted over a 78-km SSMF deployed fiber link with a 14-km dispersion compensating fiber (DCF) configured as pre-compensation. After the

deployed fiber, the group was passively coupled with the other channels, emulating transmission over a long-reach distribution link from a remote broadcast server.

Two different approaches were used to detect the transmitted DQPSK signals: coherent detection with the use of Agilent N4391A Optical Modulation Analyzer and self-homodyne approach in a one-symbol delay interferometer.

3.2.3.1. Self-homodyne detection

Fig. 3 shows the receiver configuration for the self-homodyne case. The channel was demultiplexed with an arrayed waveguide grating (AWG) and was amplified in an EDFA to 5 dBm to reach the one-symbol delay-based detector's sensitivity range. Fig. 6 shows the BER curves versus OSNR plotted for each of the four DQPSK channels, for the back-to-back, remote distribution link and full transmission link cases. While the resulting curves are within 1 dB for each channel, most likely due to transmitter and receiver parameter drift over the course of measurements, error-free transmission is achieved for all of them, with no error floor is observed.

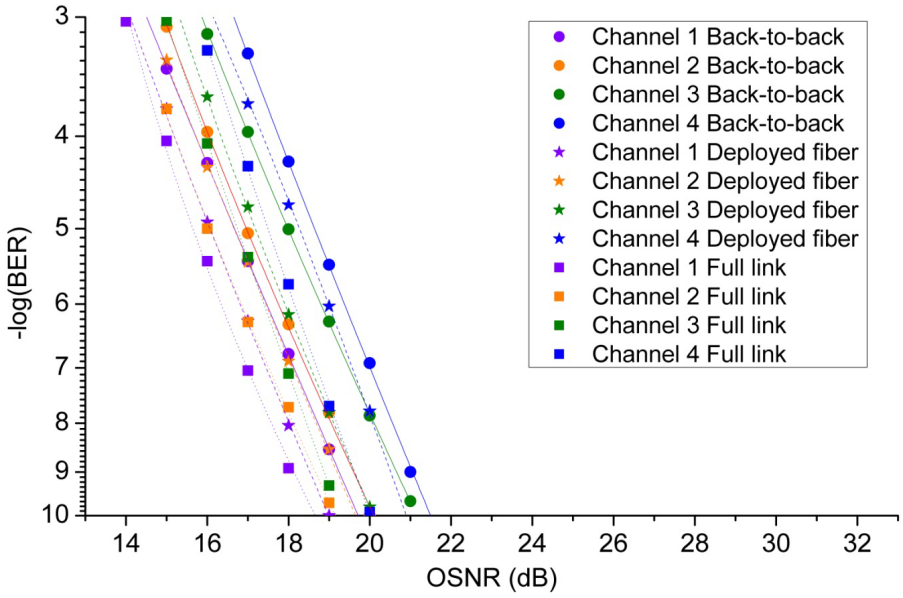

Fig. 6. BER curve obtained for the DQPSK channels.

3.2.3.2. Coherent detection

The coherent receiver setup was similar to that of Fig. 3 with the following differences: an optical polarization diversity coherent detector built into Agilent N4391A Optical Modulation Analyzer was used to detect the signal, and a built-in tunable local oscillator (LO) laser was used both as a signal laser and as a LO.

Obtained error vector magnitude (EVM) – the difference between actual received symbols and ideal symbols - versus OSNR curves for the coherent detection case are presented in Fig. 7. The inset shows an eye diagram for the worst case of measured EVM for full

transmission. We can observe an open eye for this case, which suggests that the signal can be reliably detected.

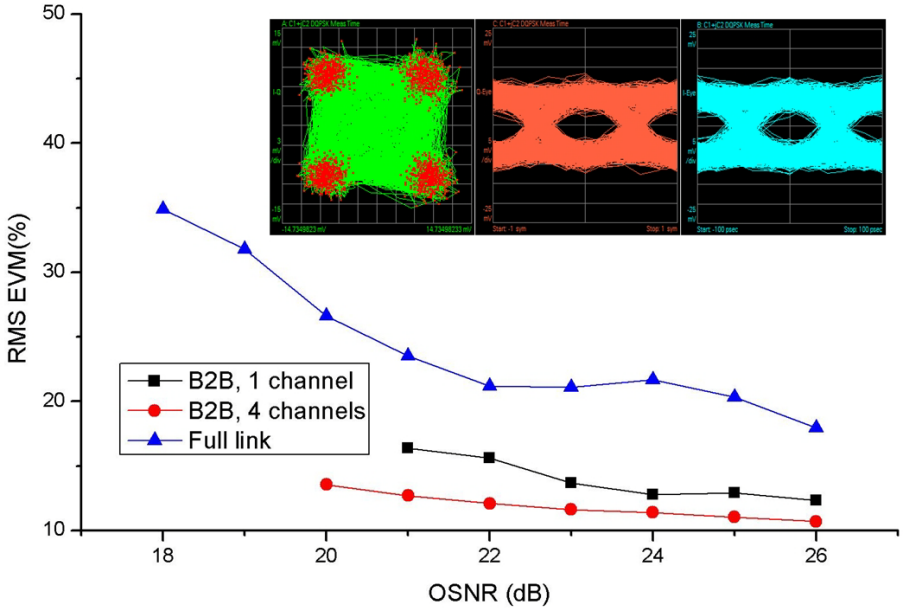

Fig. 7. EVM vs. OSNR curve obtained for the coherent-detected DQPSK channels. Inset shows the worst case for the full transmission link.

3.3. Discussion of results

These results demonstrate the feasibility of a narrow channel-spaced coherent detection based PON with the employment of DSP algorithms. We have shown how the two concepts complement each other: coherent detection makes it possible to receive long-reach and closely WDM-spaced channels, while dedicated broadcast servers substantially reduce the complexity, footprint and eventually power consumption of individual COs.

The proposed coherent detection based PON system is intended to improve the capacity and flexibility of TDM PONs while reusing their infrastructure. By exploiting the feature of high wavelength selectivity of coherent detection, higher bit-rate and higher spectral efficiency signal formats can be introduced. They may coexist with the legacy PON TDM system. The prospect of creation of multi-format any-bit-rate DSP-assisted coherent receivers is rather realistic in the light of current advances in the area of semiconductor electronics and digital signal processing, which makes the proposed network configuration even more promising in terms of gradual upgradeability.

Another beneficial feature of a coherent detection-based PON is the ability to tune to different wavelengths, which makes it possible to incorporate broadcast services – from IP TV to HD TV, to shared digital radio-over-fiber transport – into the conventional access links. This feature also allows a more flexible and efficient wavelength resource utilization by redistributing the downstream data channels dynamically between the users, depending on their demands. This would enable the service providers to supply the user with different types of information services and would enable the convergence between wireline and wireless networks, as well as enabling the all-in-one type of networks in the future, while still utilizing a common PON fiber infrastructure for signal transport.

4. Challenges and prospects

An important feature of any access system is its relatively limited accessibility and serviceability of the user-side equipment as maintenance costs and fault resolution times are

adversely affected by issues of access to ONU located inside customer premises. This imposes certain restriction on that equipment: it has to be reliable, easily replaceable and cost effective. A challenge associated with our proposed Coherent PONs is the use of tunable lasers LO in the user-side termination equipment. These are required to allow the receivers to tune to any of the broadcast channels or the correct data channel. However, the potential for cost efficiency and power consumption of the user-end termination modules lies in the prospects of availability of such components with improved characteristics and reduced production cost.

Another advantageous feature of the proposed system is the fact that coherent detection receiver can be DSP-assisted, and this means that the receiver can be built reconfigurably in order to receive a number of set signal formats at different bit-rates. Such a flexible receiver allows the service provider to remotely install and implement new services with different signal formats and bit-rates even after equipment deployment, allowing a path for future network development. This will enable gradual upgrades of a wide selection of services provided by the network.

The introduction of a dedicated server for broadcast services will require equipment for amplification and dispersion compensation to be located at each central office: the use of long-reach links (possibly spanning hundreds of kilometers) for broadcast traffic distribution also reduces overall network complexity. This will have a positive effect on CO maintenance cost and complexity, and will also reduce the power consumption of COs in the network.

5. Conclusion

In this paper we have proposed an access network architecture with distribution of broadcast traffic from a remote broadcast server. The proposed architecture relies on coherent detection for narrow channel spacing and improved reach of the distribution links. We have experimentally demonstrated the proposed architecture: the unicast data channels – the direct detection ASK baseband channels and the digitally-processed optical PSK modulated RoF channels were successfully detected, with the obtained BER values compliant with the requirements for signals without and with the use of FEC, respectively, for the transmission over 34 km of access SMF.

DQPSK broadcast channels were transmitted over a 78-km distribution SSMF and a 34-km access SMF, and were successfully detected by employing both self-homodyne and coherent detection. The proposed scheme has potential application for high-speed access networks with large channel density and high degree of service convergence.

Acknowledgement

This work was partly supported by the European Community's Seventh Framework Programme (FP7/2007-2013) within the project ICT ALPHA under grant agreement 212 352 and ICT GigaWAM under grant agreement 224 409. We would like to acknowledge Agilent Technologies Denmark for providing Agilent N4391A Optical Modulation Analyzer measurement equipment for this experiment.

References

[1]X. Yang, D. Xiaojiang, Z. Jingyuan, H. Fei, S. Guizani, "Internet Protocol Television (IPTV): The Killer Application for the Next-Generation Internet," IEEE Com. Mag., 45, no. 11, 126-134 (2007)

[2]S. Cherry, “Edholm's law of bandwidth,” IEEE Spectrum, 41, 58-60 (2004)

[3]P. W. Shumate, “Fiber-to-the-Home: 1977–2007,” OSA JLT 26, no. 9, 1093-1103 (2008)

[4]ITU-T G.984, http://www.itu.int

[5]IEEE 802.3, http://www.iee.org

[6]K. Grobe, J.-P. Elbers, "PON in adolescence: From TDMA to WDM-PON," IEEE Com. Mag., 46, no. 1, 26-34 (2008)

[7]Y. Hsueh, W. Shaw, L. G. Kazovsky, "Success PON demonstrator: experimental exploration of next-generation optical access networks," IEEE Com. Mag., 43, no. 8, S26 (2005)

[8]R.P. Davey, D.B. Grossman, M. Rasztovits-Wiech, D.B. Payne, D. Nesset, A.E. Kelly, A. Rafel, S. Appathurai, Yang Sheng-Hui, Long-Reach Passive Optical Networks, in: J. Light. Tech. 27 (2009), no. 3, 273-291

[9]T. Okoshi, K. Kikuchi, 'Coherent Optical Fiber Communications,' Springer (1988)

[10] IDATE for FTTH Council Europe, http://www.ftthcouncil.eu/documents/studies/Market_Data-December_2008.pdf

[11] S. Han, S. Lisle, G. Nehib, "IPTV Transport Architecture Alternatives and Economic Considerations," IEEE Com. Mag., 46, no. 2, 70-77 (2008)

[12] E. Ip, A. P. Tao Lau, D. J. F. Barros, J. M. Kahn, "Coherent detection in optical fiber systems," Opt. Express, 16, no. 2, 753-791 (2008)

[13] N. Guerrero, A. Caballero, F. Amaya, D. Zibar and I. Tafur Monroy, "Experimental 2.5 Gbit/s QPSK WDM Coherent Phase Modulated Radio-over-Fibre Link with Digital Demodulation by a K-means Algorithm," ECOC 2009, P3.15 (2009)

[14] D. Zibar, Xianbin Yu, C. Peucheret, P. Jeppesen, I.T. Monroy, "Digital Coherent Receiver for Phase-Modulated Radio-Over-Fiber Optical Links," IEEE PTL, 21, no. 3, 155-157 (2009)

Biography

Alexey V. Osadchiy received the M.Sc. degree in fiber optical communications from the Bonch-Bruyevich State University of Communications, Saint-Petersburg, Russia, in 2006. He is currently pursuing a Ph.D. in optical communications engineering at DTU Fotonik, Technical University of Denmark, with main focus on access networks and interaction between access networks and higher level of network hierarchy networks, namely, metro-access interfacing.

Kamau Prince received the B.Sc. degree (first class honours) in electrical engineering from the University of the West Indies, St. Augustine, Trinidad, in 1999; a Graduate Diploma in telecommunications engineering and M.Eng.Sci. degree from the University of Melbourne, Victoria, Australia, in 2003 and 2006, respectively. He is currently pursuing a Ph.D. in optical communications engineering at DTU Fotonik, Technical University of Denmark.

Antonio Caballero received the B.Sc. and M.Sc. degree in Telecommunications Engineering from Centro Politécnico Superior, Zaragoza, Spain, in 2008. He is currently pursuing a Ph.D. in optical communications engineering at DTU Fotonik, Technical University of Denmark.

 Ferney Amaya received the B.Sc. degree in electronics engineering from the Universidad de Antioquia, Colombia, in 1998; a Graduate Diploma in M.Eng.Sci. degree from the Universidad del Valle, Colombia, in 2006. He is currently pursuing a Ph.D. in Telecommunications at Universidad Pontificia Bolivariana, Colombia in the GIDATI research group.

 **Darko Zibar** was born on December 9th, 1978, in Belgrade former Yugoslavia. He received the M.Sc. degree in Telecommunication in 2004 from the Technical University of Denmark and the Ph.D. degree in 2007 from the Department of Communications, Optics and Materials, COM$\bullet$DTU within the field of optical communications. He was a Visiting Researcher with Optoelectronic Research Group led by Prof. John E. Bowers, at the University of California, Santa Barbara (UCSB) from January 2006 to August 2006, and January 2008 working on coherent receivers for phase-modulated analog optical links. From Febryaru 2009 until Luly 2009, he was Visiting Researcher with Nokia-Siemens Networks working on digital clock recovery for 112 Gb/s polarization multiplexed systems. Currently, he is employed at DTU Fotonik, Technical University of Denmark as the Assistant Professor. His research interests are in the area of coherent optical communication, with the emphasis on digital demodulation and compensation techniques.

Darko Zibar is a recipient of the Best Student Paper Award at the IEEE Microwave Photonics Conference (MWP) 2006, for his work on novel optical phase demodulator based

on a sampling phase-locked loop as well as Villum Kann Rasmussen postdoctoral research grant in 2007.

Idelfonso Tafur Monroy received the M.Sc. degree in multichannel telecommunications from the Bonch-Bruevitch Institute of Communications, St. Petersburg, Russia, in 1992, the Technology Licenciate degree in telecommunications theory from the Royal Institute of Technology, Stockholm, Sweden, and the Ph.D. degree from the Electrical Engineering Department, Eindhoven University of Technology, The Netherlands, in 1999.

He is currently Head of the metro-access and short range communications group of the Department of Photonics Engineering, Technical University of Denmark. He was an Assistant Professor until 2006 at the Eindhoven University of Technology. Currently, he is an Associate Professor at the Technical University of Denmark. He has participated in several European research projects, including the ACTS, FP6, and FP7 frameworks (APEX, STOLAS, LSAGNE, MUFINS). At the moment, he is in involved the ICT European projects Gi-GaWaM, ALPHA, BONE, and EURO-FOS. His research interests are in hybrid optical-wireless communication systems, coherent detection technologies and digital signal processing receivers for baseband and radio-over-fiber links, optical switching, nanophotonic technologies, and systems for integrated metro and access networks, short range optical links, and communication theory.

Biography

Alexey V. Osadchiy received the M.Sc. degree in fiber optical communications from the Bonch-Bruyevich State University of Communications, Saint-Petersburg, Russia, in 2006. He is currently pursuing a Ph.D. in optical communications engineering at DTU Fotonik, Technical University of Denmark, with main focus on access networks and interaction between access networks and higher level of network hierarchy networks, namely, metro-access interfacing.

Kamau Prince received the B.Sc. degree (first class honours) in electrical engineering from the University of the West Indies, St. Augustine, Trinidad, in 1999; a Graduate Diploma in telecommunications engineering and M.Eng.Sci. degree from the University of Melbourne, Victoria, Australia, in 2003 and 2006, respectively. He is currently pursuing a Ph.D. in optical communications engineering at DTU Fotonik, Technical University of Denmark.

Antonio Caballero received the B.Sc. and M.Sc. degree in Telecommunications Engineering from Centro Politécnico Superior, Zaragoza, Spain, in 2008. He is currently pursuing a Ph.D. in optical communications engineering at DTU Fotonik, Technical University of Denmark.

Paper F

Alexey V. Osadchiy, Kamau Prince, Idelfonso Tafur Monroy, "Converged delivery of WiMAX and wireline services over an extended reach passive optical access network," **Optical Fibre Technology**, 16, no. 3, pp 182-186 (2010)

Optical Fiber Technology 16 (2010) 182–186

Contents lists available at ScienceDirect

Optical Fiber Technology

www.elsevier.com/locate/yofte

Converged delivery of WiMAX and wireline services over an extended reach passive optical access network

Alexey V. Osadchiy *, Kamau Prince, Idelfonso Tafur Monroy

DTU Fotonik, Technical University of Denmark, Oersteds Plads 343, DTU Campus, 2800 Kgs. Lyngby, Denmark

ARTICLE INFO

Article history:
Received 28 September 2009
Revised 9 February 2010
Available online 3 April 2010

Keywords:
Radio-over-fiber
WiMAX
Long-reach
Access
Convergence

ABSTRACT

In this paper we present long-reach fiber access links supporting transmission of Worldwide Interoperability for Microwave Access (WiMAX) compliant signals. We present bi-directional full-duplex transmission of 256-state quadrature amplitude modulation (256-QAM) modulated WiMAX-compliant signals on a 2.4-GHz RF carrier over an 80-km long-reach access link at 100 Mb/s (down) and 64 Mb/s (up). Transmission of 64-QAM and 256-QAM-modulated signals on a 5.8-GHz RF carrier over a 118.8-km access link converged with four baseband differential quadrature phase shift keying (DQPSK) modulated wireline channels, along with ultra-wide band (UWB) and phase shift keying (PSK) radio-over-fiber (RoF) wireless signals over a deployed optical fiber link is also presented.

1. Introduction

Network operators are investigating novel methods of extending the reach of optical access networks to reduce the unit delivery cost of data bandwidth to the end-user. Significant cost reduction is expected to come from eliminating intermediate local exchange nodes within the access network and consolidating access infrastructure across existing last-mile network segments into enhanced-range next-generation systems that interface directly with high-bandwidth metro or core network nodes. In such scenarios, the access network is expected to span up to 100 km, a significant increase over the standard 20 km reach of contemporary networks [1,2]. Additionally, the demand for bandwidth from the individual access network user is being stimulated by novel bandwidth-intensive network services like high-definition (HD) video-on-demand, peer-to-peer file sharing and remote access services. Such trends have also driven increases in the data rates supported by wireless data access networks as well, with emerging wireless access technologies, such as Worldwide Interoperability for Microwave access (WiMAX) [3–5] and 3GPP long-term evolution (LTE) [6], offering higher data access speeds and supporting more users. There are several reasons for this interest: wireless access networks solutions allow client mobility, so that interactions to occur in real-time allowing faster information flow across organizations performed on the move, and the precious time is being utilized more efficiently; at the same time, wireless solutions provide on-demand availability of various entertainment services.

Worldwide Interoperability for Microwave Access (WiMAX) [7] is becoming a widespread wireless access technology with standards for fixed as well as mobile coverage. However, the emergence of high-bitrate wireless access standards creates a new challenge – high-bandwidth signals generated by and destined to the customer premises equipment (CPE), has to be delivered from and to the central office (CO). One way of tackling the problem is transport of WiMAX signals over the already-deployed or newly-installed optical fiber infrastructure. Such an approach, generally known as radio-over-fiber (RoF), allows for low-loss distribution of wireless services and simplifies the structure of the base stations, as all complex signal generation and detection-related equipment is consolidated at the CO, and the base station only performs optical-to-radio and radio-to-optical signal conversion. Another advantage provided by RoF transmission is the prospect of transport of both wireless and wireline signals over the same fiber infrastructure, which reduces installation costs for both services and simplifies coverage of the areas with established fiber infrastructure with the wireless services.

In this article, we report the results obtained during a series of experiments with RoF WiMAX transmission, including bi-directional transmission of WiMAX-compliant signals over an 80-km long-reach PON with air transmission between a CPE and a wireless subscriber unit (WSU). Moreover to show the feasibility of convergence over an extended reach access link, we report on a WDM transmission of WiMAX-compliant signals over 78 km of deployed fiber simultaneously with the transmission of four

* Corresponding author. Address: DTU Fotonik, Technical University of Denmark, Oersteds Plads 343, DTU campus, Office 214, 2800 Kgs. Lyngby, Denmark.
E-mail address: avos@fotonik.dtu.dk (A.V. Osadchiy).

1068-5200/$ - see front matter © 2010 Elsevier Inc. All rights reserved.
doi:10.1016/j.yofte.2010.02.009

10.7 Gbaud DQPSK channels, two 1 Gb/s PSK RoF channels and an ultra-wide band (UWB) over fiber channel.

2. Wireline and wireless converged signal transport scenario

High-bandwidth wireless access technologies are gaining recognition from the end-users as convenient and reliable means of access connection, which causes an increase in the amount of traffic generated by wireless sources. This puts up a challenge – an effective solution for transport and distribution of such traffic is required to interconnect the ever-increasing amount of wireless base stations. Current point-to-multipoint wireless access systems have carrier frequencies ranging from 900 MHz (GSM/UMTS networks) to 5 GHz (WiFi and WiMAX), although there are standards being developed for communications with carrier frequencies above 20 GHz [8]. High carrier frequencies enable high capacities but at the same time put significant limitations on the maximum cell size, which is the coverage area serviced by each wireless access point. For this reason, high-frequency systems' cells are sometimes referred to as picocells. Small cell sizes enable efficient frequency reuse, as the signals from the next cells are greatly attenuated, especially indoors, which removes the need for frequency interleaving [9,10]. At the same time due to small cell size, more base stations are required to ensure adequate coverage. This makes RoF technologies very appealing, since the operation costs of a system counting myriads of picocells can be greatly reduced if the complex and power-hungry part of each base station – the signal generation and detection equipment – can be placed at the CO.

Low attenuation of the optical fiber makes such an equipment placement even more beneficent – if the maximal reach of optical links measures tens to hundreds of kilometers, single CO can potentially host equipment providing coverage for an area measuring thousands of square kilometers. Another argument in favor of long-reach access links is the absence of intermediate nodes between the access-level and the metro-level networks, as the CO can serve as both an access and a metro node, including the bridging between the two segments of network hierarchy.

However, installation of fiber links exclusively to support wireless access networks might be rather costly, so convergence of wireline and wireless access networks within the existing or planned fiber infrastructure is very important: such a convergence reduces both systems' installation costs, since the same infrastructure installation costs are shared between two different access systems. Another interesting prospect of such a convergence is possibility to create access surroundings for the user – wherever the user goes, she will have an ability to use her access network, as long as current location is covered by either the wireless or the wireline component of the access system.

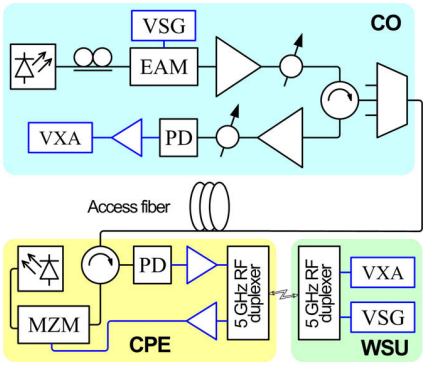

Fig. 1. Long-reach PON link with bi-directional WiMAX transmission. CO – central office; CPE – customer premises equipment; WSU – wireless subscriber unit; VSG – vector signal generator; EAM – electro-absorption modulator; VXA – signal analyzer; MZM – Mach–Zehnder Modulator; and PD – photodiode.

We propose a long-reach access system that implements these design objectives in Fig. 1: a long-reach access link connects the central office (CO) with the customer premises equipment (CPE), which serves as the interface between optical and wireless transmission segments of the communication path between the CO and each wireless subscriber unit (WSU) within each coverage cell. In this work we also demonstrate simultaneous transport of wireless and wireline signals over a common long-reach access link, however, we focus on the performance of signal transport of WiMaX signals. We define the downlink (DL) data path as originating at the CO and terminating at the WSU, and the uplink (UL) data path from the WSU to the CO; and present a series of measurements for WiMaX-compliant signals with a 5.8-GHz RF carrier. The operating frequency was selected for compliance with the European unlicensed 5-GHz communications band.

3. Experimental setup

3.1. Extended reach PON link with bi-directional WiMAX signal transport

The experiment setup is presented in Fig. 1. A 40 GHz electro-absorption modulator (EAM) was used at the CO to modulate the light from a continuous-wave (CW) optical source; the downlink transmit power level was adjusted by an amplifier and a variable optical attenuator (VOA) to limit it to a value that does not introduce non-linear effects. A pre-amplified 10 GHz receiver was used at the CO. The CPE was built with the use of uncooled, commercially-available equipment: 10 GHz photodiode, Mach–Zehnder modulator (MZM) and RF bandpass amplifiers and duplexer. The received signal power at the CPE photodiode was measured to be −5 dBm. Both intensity modulators (EAM and MZM) used in the experiment were biased for operation in the linear regime; input optical power levels into the modulators were +8 dBm and +7 dBm, respectively. The system performance was evaluated for various RF input power levels. The measurements were taken with both transmitters simultaneously active. Results were taken with both transmitters using the same electrical modulation format.

IEEE 802.kd WiMAX-compliant [3,4,11] signals in the unlicensed 2.4 GHz band were obtained from independent Agilent E4438C signal generators operating at unequal carrier frequencies, and signal quality after transmission was assessed using Agilent N9020A-MXA signal analyzers. Signal quality was assessed for bi-directional transmission conditions and evaluated in terms of RMS error-vector magnitude (EVM); uplink (UL) and downlink (DL) signal paths were simultaneously observed.

3.2. Converged transport of WiMAX over a long-reach link

The experiment layout of the converged signal transport is presented in Fig. 2. Field-deployed standard single mode fiber connecting the campus of the Technical University of Denmark (DTU) and facilities located in the suburb of Taastrup was used in this experiment. The total link loss was measured at 25 dB. The eight channels were wavelength-division multiplexed at a 200-GHz channel separation, occupying ITU-compliant wavelengths, denoted λ_1 = 1549.3 nm through λ_8 = 1560.0 nm: four wavelengths (λ_5–λ_8) were used for the 21.4 Gb/s NRZ-DQPSK channels; two (λ_2 and λ_4) for the 250 Mb/s RoF channels with an RF carrier frequency

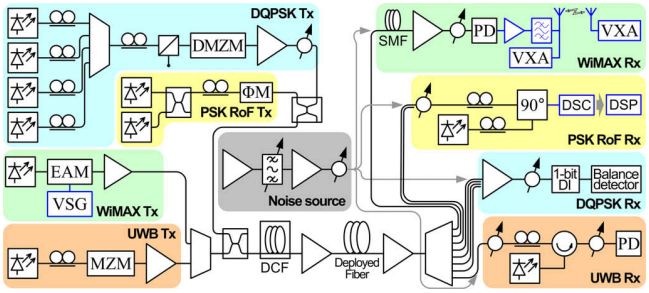

Fig. 2. Converged WiMAX transport experiment setup. (D)MZM – (double) Mach–Zehnder modulator; EAM – electro-absorption modulator; VSG – vector signal generator; VXA – signal analyzer; 1-bit DI – one-bit delay interferometer; DSC – digital sampling scope; and DSP – software-based digital signal processing.

of 5 GHz; a 3.125-Gb/s impulse ultra-wide band (UWB) channel and a 100-Mb/s 256-QAM WiMAX-over-fiber channel with an RF carrier frequency of 2.4 GHz – a single wavelength used for each (λ_3 and λ_1, respectively).

Launch power into the deployed fiber was set to 0 dBm for each of the eight channels. Dispersion compensating fiber (DCF) of length 13-km was used at the transmitter, to match the dispersion of the deployed fiber; the DCF also ensured signal decorrelation at the input of the transmission fiber. An erbium doped fiber amplifier (EDFA) pre-amplifier was used to compensate for the transmission losses before wavelength demultiplexing in an arrayed waveguide grating (AWG). The channel spacing in the system was dictated by the equipment availability, and we expect the system to function properly with a narrower channel spacing [12].

An EAM fed by an optical carrier at λ_2 was modulated with a 256-QAM RF signal, centered at 5.8 GHz, obtained from an Agilent E4438C vector signal generator (VSG); a boost EDFA and VOA controlled the launch power. A pre-amplified receiver was implemented with a 30 dB gain EDFA, optical bandpass filter (BPF) and a 10 GHz PIN photodiode. The electrical signal obtained was amplified by 35 dB, filtered by 25 MHz RF duplexers for 5 GHz unlicensed ISM band operation and radiated by 12 dBi omni-directional 5 GHz antenna. The wireless signal was detected with an identical antenna at 40 cm separation, amplified and assessed with an Agilent 9020 MXA vector signal analyzer (VXA) with the 89600 VSA signal analyzer software. We report error-vector magnitude (EVM) sensitivity to RF source power at both ends of the wireless link for the single active wavelength, and for all WDM transmitters active. We additionally assessed the performance with extra 40 km of uncompensated SMF, after DF and preamp and the post-detection eye diagram.

4. Results

4.1. Extended reach PON link with bi-directional WiMAX signal transport

We assessed the performance with 35-km NZDSF access fiber (Fig. 1): for this case, the OSNR at the CO for the UL was sufficient for reliable measurements to be taken with a received power level of −18 dBm. We report on an un-amplified UL, and bypassed array waveguide (AWG) at the CO. We used DL wavelength (λ_{DL}) of 1549.5 nm and UL at (λ_{UL}) of 1550.6 nm: we assessed full-duplex transmission of 64-QAM at 8 Mb/s (1 Mbaud) for UL and DL and report the results in Fig. 3: the 3.1% IEEE 802.16d EVM threshold for 64-QAM is shown. These results indicate at a bitrate of 6 Mb/s (1 Mbaud), the WiMAX EVM threshold for 4-QAM is satisfied with launch RF power in the range [−18, 4] dBm and [−31, −9] dBm for the DL and UL, respectively. We observed a difference of less than 0.2% between the best-case RMS EVM for UL and DL. We also present results for full-duplex 256-QAM transmission: at 8 Mb/s (1 Mbaud), DL performance closely followed that observed for the 64-QAM transmission at 6 Mb/s. At 64 Mb/s, the 256-QAM UL yielded better than 3.1% EVM for launch RF power values within the range [−19, −11] dBm.

We extended our fiber link in Fig. 1 to 80 km NZDSF: in this case, system losses resulted in insufficient received optical power level at the CO. We thus implemented a pre-amplified CO receiver with −5 dBm into the lightwave converter and inserted AWG to improve OSNR. We assessed full-duplex operation using a single optical wavelength ($\lambda_{DL} = \lambda_{UL}$ = 1549.5 nm), and present the results in Fig. 3. With full-duplex 256-QAM transmission at 64 Mb/s (8 Mbaud), the RMS EVM was below 3.1% for launch power in the range [−11, 1] dBm and [−25, −23] dBm for the DL and UL, respectively. When the DL bitrate was increased to 100 Mb/s, this EVM threshold was satisfied with launch power within the range [−7, 0] dBm.

4.2. Converged transport of WiMAX over a long-reach link

The 256-QAM signals at 12 Mbaud were successfully transmitted over the deployed fiber and an additional 40 km of distribution SMF with no further optical amplification, Fig. 2. The assessment of the error-vector magnitude (EVM) at the remote transmit antenna showed a value below 3% – within the standard specifications – as shown in Fig. 4.

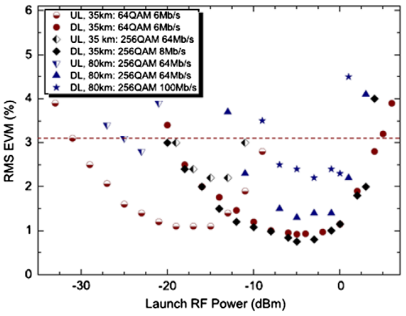

Fig. 3. RMS EVM obtained for 64-QAM and 256-QAM WiMAX-compliant signals.

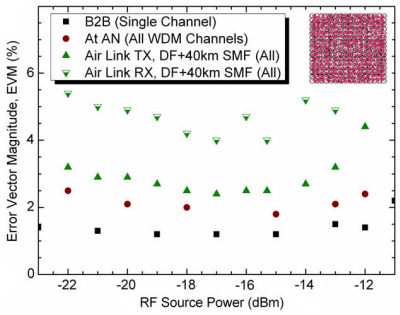

Fig. 4. RMS EVM obtained for the 100 Mb/s 256-QAM channel.

In this article, we focus on the performance of the WiMaX channel and will review briefly the performance of the other channels' propagating simultaneously over the same deployed fiber. The co-existent channels were successfully received at their respective receivers. For the DQPSK channels, a BER of 10^{-9} was observed for OSNRs of between 22 dB (λ_5) and 23.3 dB (λ_8), with transmission penalties not exceeding 0.3 dB. A BER of 10^{-3} was achieved for the coherent-detected RoF PSK channels at OSNRs of approximately 9.6 and 11 dB, and transmission penalties of 0.5 and 2 dB, for channels 2 and 4, respectively. The UWB signal was recorded in form of samples, and then digitally processed offline: a BER of 10^{-3} was obtained for 13 dB OSNR, and transmission penalty comprised only 0.5 dB.

5. Conclusion

We have demonstrated a bi-directional WiMAX-over-fiber signal transmission scheme. The presented scheme supports IEEE 802.16d-compliant signal transmission on a 2.4 GHz carrier: for 256-QAM signals, full-duplex operation at a bit rate of 100 Mb/s in downlink direction and 64 Mb/s in the uplink direction was demonstrated in an 80-km access fiber link. No RF signal processing was performed at CPE, and the use of commercially-available optical transceivers facilitates the implementation of such links.

We also demonstrated successful converged transport of 100 Mb/s WiMAX-compliant signals with a 5.8 GHz RF carrier over a 78.8-km deployed SMF and a 40-km distribution SMF: in total the WiMAX signal stayed within 5% RMS EVM after 118.8-km fiber link transmission and air transmission. Co-existing channels transmitted together with the WiMAX-over-fiber channel over the deployed fiber were also received successfully.

The presented demonstrations of WiMAX signals transport over fiber show prospects for efficient converged transport of high-bandwidth wireless and wireline signals over long-reach links. This enables a new type of access networks to be created or built over the existing fiber-based ones – hybrid wireless-fixed access networks with significantly greater coverage then the currently deployed ones.

Acknowledgments

This work was partly supported by the European Community's Seventh Framework Programme (FP7/2007-2013) within the project ICT ALPHA under Grant agreement 212 352 and ICT GigaWAM under Grant agreement 224 409. We would like to acknowledge Agilent Technologies Denmark for providing access to the WiMAX signal analysis equipment used in the experiment.

References

[1] R.P. Davey, D.B. Grossman, M. Rasztovits-Wiech, D.B. Payne, D. Nesset, A.E. Kelly, A. Rafel, S. Appathurai, Yang Sheng-Hui, Long-reach passive optical networks, J. Lightw. Technol. 27 (3) (2009) 273–291.
[2] C. Lin, Broadband Optical Access Networks and Fiber-to-the-Home, John Wiley & Sons, Inc., 2006.
[3] S.J. Vaughan-Nichols, Achieving wireless broadband with WiMAX, Computer 37 (6) (2004) 10–13.
[4] IEEE Std. 802.16-2004, IEEE LAN/MAN Standards Committee Std., October 2004.
[5] IEEE Std. 802.16e-2005, IEEE LAN/MAN Standards Committee Std., 2006.
[6] D. Mcqueen, The momentum behind LTE adoption [3GPP LTE], IEEE Commun. Mag. 47 (2009) 44–45.
[7] K.H. Teo, Z. Tao, J. Zhang, The mobile broadband WiMAX standard [Standards in a Nutshell], IEEE Signal Proc. Mag. 24 (5) (2007) 144–148.
[8] A.M.J. Koonen, M.G. Larrode, A. Ng'oma, K. Wang, H. Yang, Y. Zheng, E. Tangdiongga, Perspectives of radio over fiber technologies, in: OFC/NFOEC Proceedings, 2008.
[9] C. Park, T.S. Rappaport, Short-range wireless communications for next-generation networks: UWB, 60 GHz millimeter-wave WPAN, and ZigBee, IEEE Wireless Commun. 14 (4) (2007) 70–78.
[10] M. Sauer, A. Kobyakov, J. George, Radio over fiber for picocellular network architectures, J. Lightw. Technol. 25 (11) (2007) 3301–3320.
[11] W. Konhauser, Broadband wireless access solutions – progressive challenges and potential value of next generation mobile networks, Wireless Pers. Commun. 37 (3–4) (2006) 243–259.
[12] D. Zibar, X. Yu, C. Peucheret, P. Jeppesen, I. Tafur Monroy, Digital coherent receiver for phase-modulated radio-over-fiber optical links, IEEE Photon. Technol. Lett. 21 (3) (2009) 155–157.

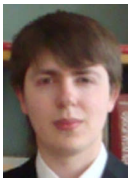

Alexey V. Osadchiy received the M.Sc. degree in fiber optical communications from the Bonch-Bruevich State University of Communications, St. Petersburg, Russia, in 2006. He is currently pursuing a Ph.D. in optical communications engineering at DTU Fotonik, Technical University of Denmark, with main focus on access networks and interaction between access networks and higher level of network hierarchy networks, namely, metro-access interfacing.

Kamau Prince received the B.Sc. degree (first class honours) in electrical engineering from the University of the West Indies, St. Augustine, Trinidad, in 1999; a Graduate Diploma in telecommunications engineering and M.Eng.Sci. degree from the University of Melbourne, Victoria, Australia, in 2003 and 2006, respectively. He is currently pursuing a Ph.D. in optical communications engineering at DTU Fotonik, Technical University of Denmark.

Idelfonso Tafur Monroy received the M.Sc. degree in multichannel telecommunications from the Bonch-Bruevitch Institute of Communications, St. Petersburg, Russia, in 1992, the Technology Licenciate degree in telecommunications theory from the Royal Institute of Technology, Stockholm, Sweden, and the Ph.D. degree from the Electrical Engineering Department, Eindhoven University of Technology, The Netherlands, in 1999. He is currently Head of the metro-access and short range communications group of the Department of Photonics Engineering, Technical University of Denmark. He was an Assistant Professor until 2006 at the Eindhoven University of Technology. Currently, he is an Associate Professor at the Technical University of Denmark. He has participated in several European research projects, including the ACTS, FP6, and FP7 frameworks (APEX, STOLAS, LSAGNE, MUFINS).

At the moment, he is in involved the ICT European projects Gi-GaWaM, ALPHA, BONE, and EURO-FOS. His research interests are in hybrid optical–wireless communication systems, coherent detection technologies and digital signal processing receivers for baseband and radio-over-fiber links, optical switching, nanophotonic technologies, and systems for integrated metro and access networks, short range optical links, and communication theory.

Paper G

Kamau Prince, Jesper Bevensee Jensen, Antonio Caballero, Xianbin Yu, Timothy Braidwood Gibbon, Darko Zibar, Neil Guerrero, Alexey V. Osadchiy, Idelfonso Tafur Monroy, "Converged Wireline and Wireless Access Over a 78-km Deployed Fiber Long-Reach WDM PON," **IEEE Photonics Technology Letters**, 21, no. 17, pp 1274-1276 (2009)

Converged Wireline and Wireless Access Over a 78-km Deployed Fiber Long-Reach WDM PON

Kamau Prince, *Student Member, IEEE*, Jesper Bevensee Jensen, Antonio Caballero, Xianbin Yu, Timothy Braidwood Gibbon, Darko Zibar, Neil Guerrero, Alexey Vladimirovich Osadchiy, and Idelfonso Tafur Monroy

***Abstract*—In this letter, we demonstrate a 78.8-km wavelength-division-multiplexing passive optical network supporting converged transport of 21.4-Gb/s nonreturn-to-zero differential quadrature phase-shift keying, optical phase-modulated 5-GHz radio-over-fiber, fiber and air transmission of 3.125-Gb/s pulse ultrawideband, and 256-quadratic-amplitude modulation wireless interoperability for microwave access.**

***Index Terms*—Coherent optical systems, converged access networks, ultrawideband (UWB) signaling, wireless interoperability for microwave access (WiMAX).**

I. Introduction

HYBRID optical/wireless access network architectures are considered a promising solution for large-scale deployment of broadband access as they combine the advantages of high capacity offered by optical access with the flexibility provided by wireless networks [1], [2]. Simultaneous transport of wireline and wireless types of signals, fulfilling power budget, dispersion, and other quality requirements for both signal types, over a common fiber infrastructure is an important aspect for hybrid optical wireless access networks.

We report on a converged wireless and wireline, wavelength-division multiplexing (WDM) passive optical network (PON) access link over a 78.8-km-long commercially deployed optical fiber in Copenhagen. We successfully implemented an eight-channel, single-fiber, WDM transmission system simultaneously supporting 85.6-Gb/s baseband via four 21.4-Gb/s nonreturn-to-zero (NRZ) differential quadrature phase-shift keying (DQPSK) channels, 500 Mb/s via two coherently detected phase-modulated radio-over-fiber (RoF) channels, 3.125 Gb/s via impulse radio ultrawideband (UWB), and intensity-modulated, direct-detected RoF link with quadratic-amplitude modulation (QAM) at 12 megabaud (MBd). Air transmission was demonstrated after fiber transmission for the UWB and WiMAX signals.

Manuscript received April 21, 2009; revised June 08, 2009. First published July 10, 2009; current version published August 19, 2009. This work was supported in part by the European Union FP7 Information Communication Technology (ICT)-ALPHA and in part by the ICT GigaWaM projects.

The authors are with the Department of Photonics Engineering, Technical University of Denmark, DK-2800 Kgs. Lyngby, Denmark (e-mail: kpri@fotonik.dtu.dk; jebe@fotonik.dtu.dk; acaj@fotonik.dtu.dk; xiyu@fotonik.dtu.dk; tbgi@fotonik.dtu.dk; dazi@fotonik.dtu.dk; nggo@fotonik.dtu.dk; avos@fotonik.dtu.dk; idtm@fotonik.dtu.dk).

Color versions of one or more of the figures in this letter are available online at http://ieeexplore.ieee.org.

Digital Object Identifier 10.1109/LPT.2009.2025699

II. System Layout

Fig. 1 shows a block diagram of the field trial and setup used in the experiment. The field-deployed fiber connects the Kongens Lyngby campus of the Technical University of Denmark (DTU) and facilities located in the suburb of Taastrup. The fiber is a G.652 standard single-mode fiber (SMF) type (16.5 ps/nm·km chromatic dispersion, 0.20 dB/km attenuation, polarization dispersion coefficient < 0.20 ps/$\sqrt{\text{km}}$). The total link loss was measured at 25 dB. The eight WDM channels employed were separated by 200 GHz, at standard International Telecommunication Union (ITU) wavelengths, denoted by $\lambda_1 = 1549.3$ nm through $\lambda_8 = 1560.0$ nm. Four wavelengths ($\lambda_{5\text{–}8}$) were used for NRZ-DQPSK: two ($\lambda_{2,4}$) for coherent RoF, λ_3 for UWB, and λ_1 for WiMAX. Launch power into the deployed fiber was set to 0 dBm for each of the eight channels. A dispersion-compensating fiber (DCF) was used at the transmitter; this also ensured decorrelated signals at the input to the transmission fiber. A preamplifier erbium-doped fiber amplifier (EDFA) overcame transmission losses before wavelength demultiplexing by arrayed waveguide grating (AWG). AWG spacing of 200 GHz was used due to equipment availability; we anticipate good system performance with closer spacing [3].

A. NRZ-DQPSK Baseband

The transmitter setup comprises four DFB lasers at wavelengths $\lambda_5 - \lambda_8$ multiplexed in an AWG and NRZ-DQPSK modulated using an inphase/quadrature (I/Q) modulator driven by two electrical pseudorandom bit sequences (PRBSs) of length $2^7 - 1$ bits and bit rate 10.7 Gb/s, resulting in a per-channel bit rate of 21.4 Gb/s at a symbol rate of 10.7 GBd. The $2^7 - 1$ bit pattern length was selected due to limitations of the bit error rate tester (BERT) functionality. Since we used phase modulation, no pattern dependency was expected from nonlinear effects in the transmission fiber. After transmission and wavelength demultiplexing, the NRZ-DQPSK signals were demodulated using a one-symbol delay Mach–Zehnder interferometer (MZI) and detected by a pair of balanced photodetectors (BPDs). The BER of each DQPSK tributary was measured independently, and we report the average obtained.

B. Coherent RoF

A 5-GHz RF carrier at $+8$ dBm was BPSK modulated at 250 Mb/s, and used to optically phase modulate signals at wavelengths of λ_2 and λ_4. At the receiver, the desired channel was optically mixed with a continuous-wave local oscillator (LO) signal, derived from a tunable laser source at 0 dBm output power, and coherently detected using a 90° optical hybrid with integrated photodetectors. The in-phase (I) and quadrature (Q)

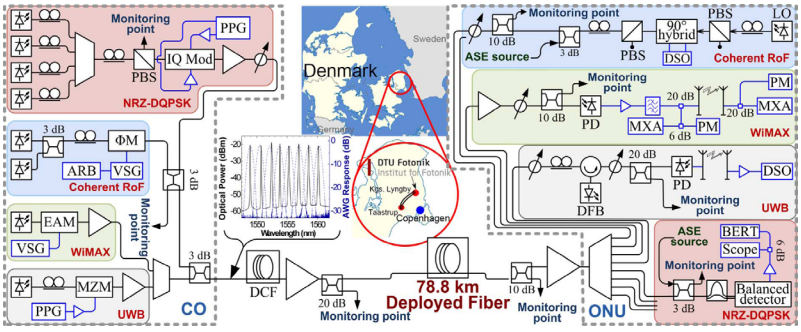

Fig. 1. Detail of the experimental setup. PPG: pulse pattern generator; PBS: polarization beam splitter; PM: optical phase modulator; ARB: arbitrary waveform generator; VOA: variable optical attenuator. ASE added to evaluate system OSNR sensitivity for phase-modulated signals: precompensating DCF-implemented decorrelation of RoF and NRZ-DQPSK signals. (Inset) Spectra of launched WDM optical signal (solid line) and AWG response (dashed line).

electrical signals were sampled at 40 GSa/s by a sampling oscilloscope (SO) with a 13 GHz bandwidth. The stored signals were processed offline using DSP algorithms described in [3] to perform signal demodulation and BER evaluation.

C. Impulse Radio UWB

A lightwave at λ_3 (1552.80 nm wavelength) was modulated by a 12.5-Gb/s pattern "1000" using a Mach–Zehnder modulator (MZM). An uncooled DFB laser was optically injected with the incoming signal from the fiber link. Under optical injection, cross-gain modulation and relaxation oscillations governing the dynamic response of the DFB shape its output signal [4]. The incoherent combination of the injected and DFB wavelengths after photodetection generated a pulse with a postdetection RF spectrum that is compliant with the impulse radio UWB mask. Air transmission of 40 cm was implemented. These UWB signals were sampled by a 40 GSa/s sampling scope with 13 GHz bandwidth, and processed offline using a DSP algorithm.

D. WiMAX

An electroabsorption modulator (EAM) fed by an optical carrier at λ_2 was modulated with a 256-QAM RF signal, centered at 5.8 GHz, obtained from an Agilent E4438C vector signal generator (VSG); a boost EDFA and a variable optical attenuator (VOA) controlled the launch power. A preamplified receiver was implemented with a 30-dB gain EDFA, an optical bandpass filter (BPF), and a 10-GHz PIN photodiode. The electrical signal obtained was amplified by 35 dB, filtered by 25 MHz RF duplexers for 5 GHz unlicensed ISM band operation, and radiated by a 12 dBi omnidirectional 5 GHz antenna. The wireless signal was detected with an identical antenna at 40 cm separation, and amplified and assessed with an Agilent 9020 MXA vector signal analyzer (VSA) with the 89 600 VSA signal analyzer software. We report error vector magnitude (EVM) sensitivity to RF source power at both ends of the wireless link for the single active wavelength and for all WDM transmitters active. We additionally assessed the performance with extra 40 km of uncompensated SMF, after DF and preamp and the postdetection eye diagram.

III. Results

A. NRZ-DQPSK Baseband

The BER of the four NRZ-DQPSK-modulated baseband channels back-to-back (B2B) and after fiber transmission is plotted in Fig. 2(a) with filled symbols/solid lines for the back-to-back case and hollow symbols/dashed lines for the transmitted. OSNR requirement for a BER of 10^{-9} was observed between 22 dB (λ_5) and 23.3 dB for λ_8. At λ_7, a penalty of 0.3 dB was observed after transmission; for all other channels, no penalty was measured. The eye diagrams before and after transmission shown in Fig. 2(b) show no transmission distortion, thus confirming good transmission properties.

B. Coherent RoF

A 250-MBd BPSK data signal modulating a 5-GHz RF carrier for each WDM channel was successfully recovered after transmission through the dark fiber with input power to the coherent receiver set to -15.77 and -16.77 dBm, respectively. In Fig. 2(b), the BER curves for back-to-back and after fiber transmission are computed as a function of OSNR values from 7 to 12 dB. We observed a receiver sensitivity penalty of 0.5 dB at λ_2 for BER at 10^{-3}, whereas a 2 dB penalty was observed in channel 4, which we believe was caused by partial misalignment of the source with the AWG passband.

C. Impulse Radio UWB

We generated 3.125-Gb/s ON–OFF key (OOK) modulation with $2^7 - 1$ PRBS; an example of "1110111" pattern and the resulting RF spectrum are shown in Fig. 3(a). The frequency spectra observed are compatible with the FCC (indoor) UWB mask. We used a sample size of 684 kilosamples, and a DSP algorithm was employed to calculate the BER offline. From the BER measurement curves, we observed less than 0.5 dB penalty between B2B and fiber transmission (for both single-channel and WDM transmissions).

D. WiMAX

We successfully transported 256-QAM signals at 12 MBd over the deployed fiber and an additional 40 km SMF with no

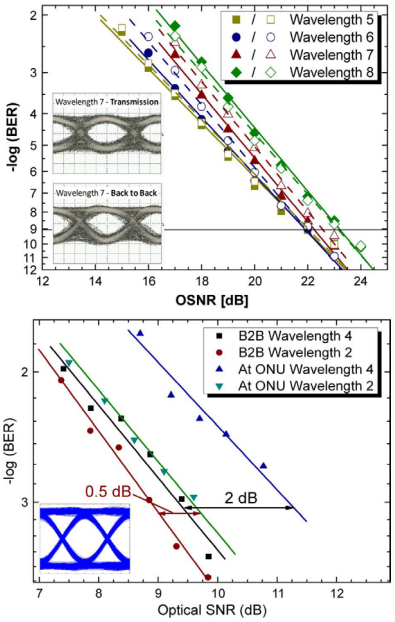

Fig. 2. BER results. (Top) 21.4-Gb/s NRZ-DQPSK. (Bottom) Coherent RoF. Sample eye diagrams are also shown.

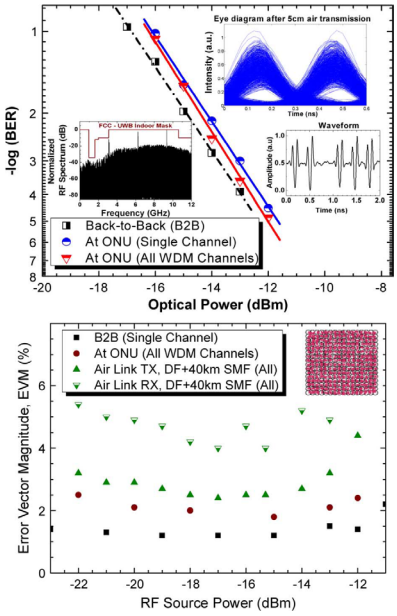

Fig. 3. (Top) BER results, RF spectrum, and eye diagrams obtained for 3.125-Gb/s UWB. (Bottom) WiMAX EVM sensitivity and constellation.

further optical amplification, with below 3% EVM at the remote transmit antenna, as shown in Fig. 3(b). System spur-free dynamic range was 74 dB/Hz$^{2/3}$.

IV. Conclusion

We successfully demonstrated combined transport over a single 78.8-km field-installed fiber of NRZ-DQPSK-modulated baseband access at 21.4 Gb/s per channel, coherent RoF at 250 Mb/s per channel, impulse-radio UWB at a record speed of 3.2 Gb/s, and a 256-QAM WiMAX signal at 12 MBd. For the UWB and WiMAX signals, air transmission was included after the fiber link. This is the first known demonstration of its kind, and it proves that the existing standard SMF based fiber infrastructure can support the seamless coexistence of various wireless and wireline signals for future converged broadband access networks. Prior results [5] also suggest the feasibility of WDM transmission with 100-GHz channel separation.

Acknowledgment

The authors would like to thank M. M. Nedergaard and D. Fryd of the Agilent Technologies Denmark for access to RF signal quality evaluation platforms, and N. Raun of GlobalConnect Denmark for access to the deployed fiber.

References

[1] S. Sarkar, S. Dixit, and B. Mukherjee, "Hybrid wireless-optical broadband-access network (WOBAN): A review of relevant challenges," *J. Lightw. Technol.*, vol. 25, no. 11, pp. 3329–3340, Nov. 2007.

[2] W.-T. Shaw, S.-W. Wong, N. Cheng, K. Balasubramanian, X. Zhu, M. Maier, and L. G. Kazovsky, "Hybrid architecture and integrated routing in a scalable optical-wireless access network," *J. Lightw. Technol.*, vol. 25, no. 11, pp. 3443–3451, 2007.

[3] D. Zibar, X. Yu, C. Peucheret, P. Jeppesen, and I. Tafur Monroy, "Digital coherent receiver for phase-modulated radio-over-fiber optical links," *IEEE Photon. Technol. Lett.*, vol. 21, no. 3, pp. 155–157, Feb. 1, 2009.

[4] X. Yu, T. B. Gibbon, D. Zibar, and I. Tafur Monroy, "A novel incoherent scheme for photonic generation of biphase modulated UWB signals," presented at the Opt. Fiber Commun. Conf. (OFC), San Diego, CA, Mar. 2009, Paper JWA60.

[5] J. Jensen, T. Torkle, C. Peucheret, and P. Jeppesen, "Transmission of WDM multilevel 8 × 30 Gbit/s single polarization RZ-D8PSK with a total capacity of 240 Gbit/s," presented at the 33rd Annu. Eur. Conf. Exhib. Opt. Commun. (ECOC), Berlin, Germany, Sep. 2007, Paper P097.

Paper H

Alexey V. Osadchiy, Idelfonso Tafur Monroy, "Coherent detection for spectral amplitude coded optical label switching systems," **Microwave and Optical Technology Letters** (UNDER REVIEW) (2010)

Coherent detection for spectral amplitude coded optical label switching systems

A. V. Osadchiy[1] and I. Tafur Monroy[1]
[1]DTU Fotonik, Department of Photonics Engineering, Technical University of Denmark, DK-2800 Kgs. Lygnby, Denmark.
Corresponding author details: Tel: +45 45 25 36 57, Fax: +45 45 93 65 81, E-mail: avos@fotonik.dtu.dk

Coherent detection for spectrally encoded optical labels is proposed and experimentally demonstrated for three label tones spectrally spaced at 1 GHz. The proposed method utilizes a frequency swept local oscillator in a coherent receiver supported by digital signal processing for improved flexibility and upgradeability while reducing label detection subsystem complexity as compared to the conventional optical auto-correlation based approaches.

Introduction: Optical labeling is a promising approach to optimize the overall efficiency, both in terms of processing time and power consumption, in routing nodes for burst switched optical communication networks. This comes from the fact that high baud rate payload signals can be switched with the routing information carried in simple accompanying labels that can be processed at lower bit rates. Although several optical labelling schemes have been proposed and experimentally demonstrated [1,2], one simple and robust way of creating optical labels is introducing spectral tones into the payload signal spectrum – spectral amplitude coding (SAC) labelling [3,4]. The conventional approach of detecting SAC labels is to use an array of optical auto-corellators that are tuned to label (spectral tone) wavelengths [5]. In case of the label's presence, a strong correlation product is generated and can be used to

control a switching fabric; otherwise a low-power cross-correlation product is generated. However, this scheme requires a number of label signal copies equal to the amount of the labels used in the system and a corresponding number of auto-correlators. Moreover, each auto-correlator has to be designed to operate for a particular wavelength (tone), which makes the system complex and difficult to upgrade and scale. We introduce a SAC label detection system based on optical coherent detection, which produces an electronic signal that can be shaped into a control signal for an optical switching fabric by applying digital signal processing (DSP) algorithms. Our proposed system is flexible, allowing for upgrading and scaling the system in terms of number of labels and labelling schemes by reconfiguring the DSP algorithms rather than optical components. We present below an experimental demonstration of the principle of operation of such a system for 3 label tones and using off-line DSP post-processing.

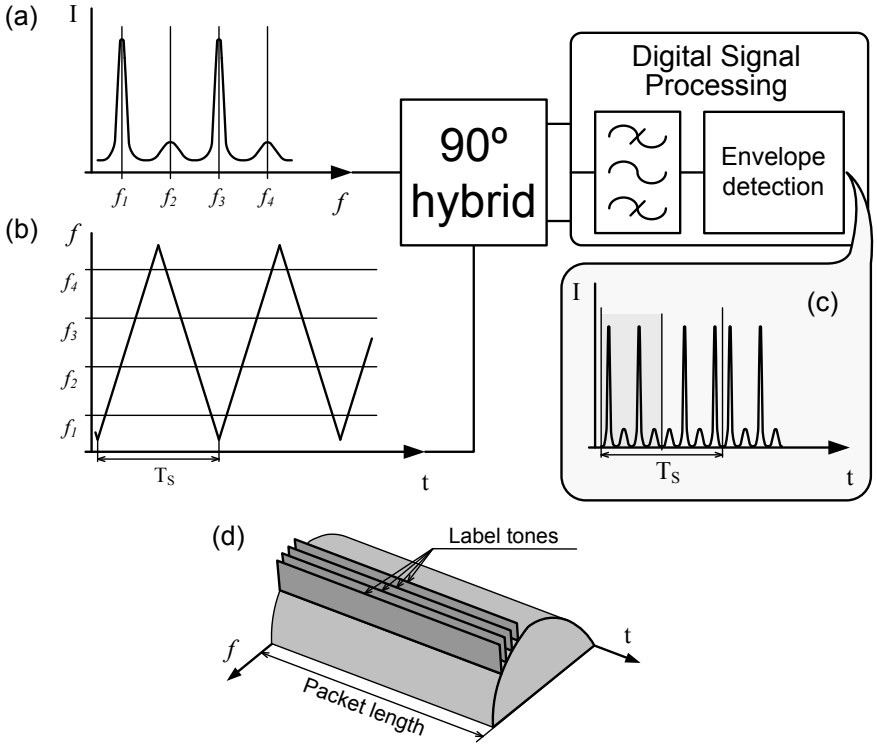

Fig. 1 Operation principle of SAC label recognition by optical coherent detection (a) SAC label in spectral domain (b) LO frequency sweep (c) SAC label in electrical domain after the recognition (d) SAC labelling principle.

Operation principle: The schematic diagram of coherent detection of SAC labels is shown in Fig. 1. The payload and label signals are transmitted during the same packet duration as shown in Fig. 1(d), where the label is encoded in the spectral domain and distinguished by the amplitude of the used wavelength tones (Fig. 1(a)). A frequency swept laser source is used as a local oscillator which covers the label's spectral occupancy (as shown in Fig. 1(b)). After mixing of the label signal and LO in a coupler, the spectral label information is transferred into electrical domain, in the intensity domain, as shown in Fig. 1(c). After balanced photo-detection and corresponding signal post-processing, label detection can be realized; as explained below.

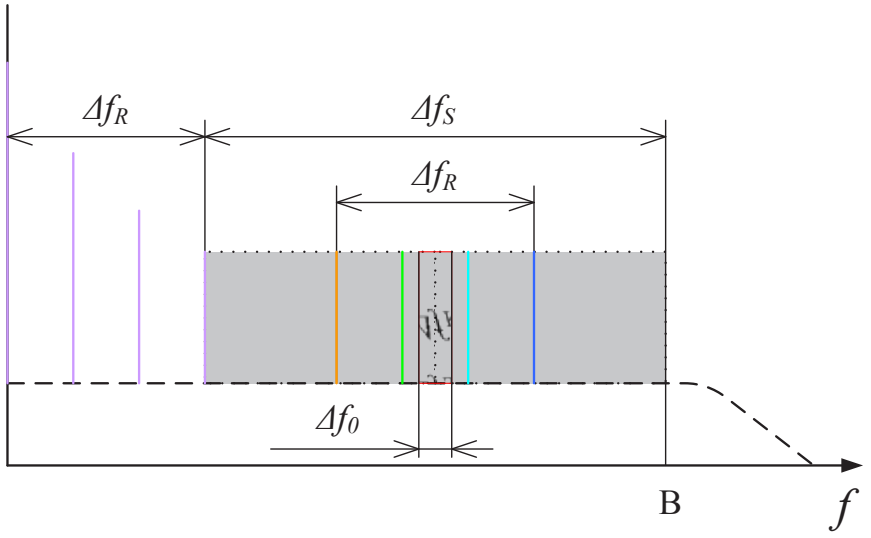

Fig. 2 Spectral composition of the obtained products.

The spectrum of the resultant signal (after coherent detection) is composed of several beating products between local oscillator and label signal, as it is shown on Fig. 2, for illustrative purposes. Δf_R denotes the spectral width occupied by the labels and Δf is the spacing between the labels. We denote by Δf_S the sweep frequency range of the local oscillator that should at lest cover the spectral bandwidth occupied by the labels. As we can see from Fig. 2, the frequency products in the lower part of the spectrum, up to Δf_R, originate from the mutual beating among the label tones. The highest frequency of such beating component is determined by the spectral width of the label group – Δf_R. Another group of beating products, also Δf_R wide, contains the products of beating between the local oscillator (LO) and the labels; which is the useful information for our labelling system. Our system operates by implementing band-pass filtering on this frequency band; see Fug. 2. The central frequency position of this band of interest is determined by the difference in nominal wavelengths between the label wavelength and

the local oscillator. As depicted in Fig. 2, let's consider an observation window of width Δf_0 and a band-pass filter of bandwidth Δf_F. We can observe that having the observation window Δf_0 significantly larger than the filter width Δf_F is beneficent, because it improves system's tolerance to frequency instability of either the LO or the labels. The minimal required bandwidth B_{min} for the system to function can be expressed as; see Fig. 2:

$B_{min} \geq \Delta f_R + (\Delta f_S - \Delta f_R)$, or (1)

$B_{min} \geq \Delta f_S$. (2)

This comes from the fact that it is not necessary to keep the whole range of frequency beating products, since only a narrow band is used by the band-pass filter, limiting in this way the detecting equipment's bandwidth that results in improved the system's cost efficiency.

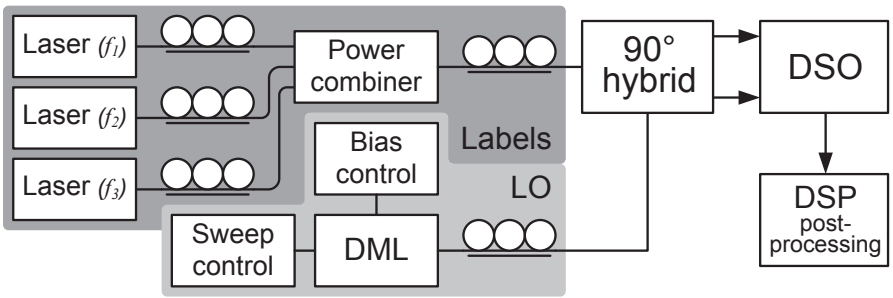

Fig. 3 Setup diagram. DML – direct modulated laser; DSO – digital sampling scope.

Experimental results: A diagram of the experimental setup is shown in Fig. 3. Three SAC labels with 1 GHz spacing were used to simulate all possible combinations of presence and absence of the labels (000 through 111 labels amplitude encoded frequency tones) to demonstrate the principle of operation of our proposed scheme. The light from three software-controlled external cavity tuneable lasers, around 1550.2 nm wavelength with 1 GHz separation, was combined and inserted into one of the inputs of a 90 degree optical hybrid coherent receiver. A direct current modulated laser source connected

to the other input of the coherent receiver was used as a frequency-swept local oscillator. In our experiment, the central emission wavelength of the LO was adjusted in such a manner, that the label beating products would appear in the electrical spectrum of the received signal around 6-12 GHz. The LO was swept with a sine wave with repetition rate of 1 MHz, and the powers of the label sources were adjusted to create beating products with visibly difference in power, so that they could be identified for demonstration of the principle of operation, namely: 3.3 dBm, 6,9 dBm and 9,0 dBm, respectively. Faster and larger frequency sweep for LOs can be achieved than those used in our experiment for operation principle demonstration purposes.

The obtained electrical signal ware recorded by a digital sampling scope (DSO) at a rate of 40 Gs/s, and the obtained samples were offline processed – narrow-band filtered at 9 GHz with a 100 MHz-wide filter, and then the envelope of the filtered signal was obtained through an averaging-based algorithm. Examples of the detected label signals are presented in Fig. 4 up to scale, for two different cases – a 101 and a 111 label (Fig. 4 (1) through (3) and (4) through (6), respectively). The LO frequency swept magnitude was equal to 4.2 GHz, which produced a Δf_S of 2 GHz, centred around 9 GHz.

Fig. 4 presents the results for two different labels – 101 and 111 – for comparison purposes, the plots are of the same scale so one can clearly see separate label tones on the band-pass filtered signal and it corresponding envelope. In the plots for the 111 label, one can also see, that the spacing between the labels in time domain is not equal, although in the frequency domain the spacing does not differ from the declared 1 GHz by more than 50 MHz (this can be seen in the spectrum plot – the frequencies of the

beating products at 1 GHz do not differ much). The small unequal observed spacing is due to the non-linear regions of the sine wave used for frequency sweeping the LO frequency, so the resulting conversion from frequency to time domain is not fully linear. For both presented examples, we achieved successful recovery of the spectral amplitude information in the electrical baseband domain that can be used to control an optical switching fabric.

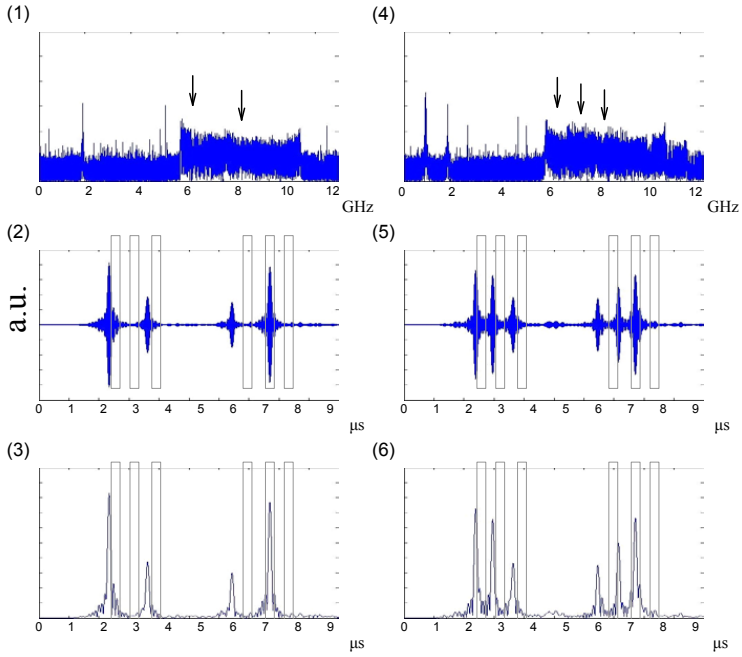

Fig. 4. Measured detected label signals: 1 – original signal spectrum for a 101 label; 2 – Band-pass filtered signal for a 101 label; 3 – recovered envelope for the 111 label; 4 – original signal spectrum for a 111 label; 5 – Band-pass filtered signal for a 101 label; 6 – recovered envelope for the 111 label.

Conclusion: We have proposed and experimentally demonstrated a coherent detection-based SAC label recognition method reliant on DSP post processing. The proposed method can be used in optical routers, and has advantages over the conventional optical auto-correlator-based SAC label detectors. The proposed label detector produces an electrical image of the label spectrum makes software-defined timing and threshold setting possible.

This enables firmware-based upgradability of the networks' label density, number and spectral positioning. At the same time, it avoids the use of numerous auto-correlators with optical amplifiers, by employing a single coherent detection receiver that can reduce the complexity and power consumption of each label detection block which represent significant positive impact on routers and network scalability. Furthermore, the use of digital signal processing (DSP) based receivers also opens the way for straightforward integration with digital control of optical switching fabrics.

References

1 Blumenthal D. J., Olsson B. E., Rossi G., et al.: "All-optical swapping networks and technologies", IEEE Journal of Lightwave Technology, 2000, 18, (12), pp. 2058-2075

2 Meagher M., Chang G. K., Ellinas G., et al.: "Design and implementation of ultra-low latency optical label switching for packet-switched WDM networks", IEEE Journal of Lightwave Technology, 2000, 18, (12), pp. 1978-1987

3 Seddighian P., Ayotee S., Fernandez J. B. R., et al.: "Label stacking in photonic packet switched networks with spectral amplitude code labels", IEEE Journal of Lightwave Technology, 2007, 25, (2), pp. 463-471

4 Fernandez J. B. R., Ayotte S., Rusch L. A., ea al.: "Ultrafast forwarding architecture using a single optical processor for multiple SAC-label recognition based on FWM", IEEE Journal of Selected Topics in Quantum Electronics, 2008, 14, (3), pp. 868-878

5 Cincotti G., Manzacca G., Wang X., et al.: "Reconfigurable multiport optical en/decoder with enhanced auto-correlation", IEEE Photonics Technology Letters, 2008, 20, (2), pp. 268-170

Authors' affiliations:
A.V. Osadchiy (avos@fotonik.dtu.dk) and I. Tafur Monroy (idtm@fotonik.dtu.dk) (DTU Fotonik, Department of Photonics Engineering, Technical University of Denmark, 2800 Kgs. Lyngby, Denmark)

Paper I

Yongsheng Cao, Alexey V. Osadchiy, Xiangjun Xin, Xiaoli Yin, Chongxiu Yu and Idelfonso Tafur Monroy, "Recognition of spectral amplitude codes by frequency swept coherent detection for flexible optical label switching," **Photonic Network Communications** (ACCEPTED FOR PUBLICATION) (2010)

Photon Netw Commun
DOI 10.1007/s11107-010-0253-3

Recognition of spectral amplitude codes by frequency swept coherent detection for flexible optical label switching

Yongsheng Cao · Alexey V. Osadchiy · Xiangjun Xin · Xiaoli Yin · Chongxiu Yu · Idelfonso Tafur Monroy

Received: 23 August 2009 / Accepted: 29 March 2010

Abstract We propose a new method of recognizing spectral amplitude codes by using optical coherent detection with a frequency swept local light source oscillator. Our proposed method offer a substantial simplification in terms of required components to built optical label processing units with enhanced flexibility to accommodate for wavelength tuneability and a large number of labels. We present a performance analysis, comparison with conventional spectral codes recognition methods, based on computer simulation results. We consider a payload bit rate of 40 Gb/s.

Keywords Optical code (OC) label switching · Spectral amplitude code (SAC) · Frequency swept local oscillator coherent detection · Eyeopening factor

1 Introduction

Optical label switching (OLS) enables optical packets routing and forwarding in IP over wavelength division multiplexing (WDM) networks [1]. OLS supports high-bit rate payloads to be switched and routed transparently, while applying low-speed electronic labels processing. So far, several approaches for optical labelling techniques have been studied and demonstrated, such as sub-carrier multiplexing modulated label and orthogonal modulation label schemes [2–7]. Currently, optical code (OC) label switching has attracted much attention, and it is considered as one of the most promising labelling scenarios, due to its high throughput, high speed and potential flexibility [8–10]. Although OC label can be encoded in time, phase, wavelength and polarization domains, spectral amplitude code (SAC) is an attractive implementation, which has been applied in OC division multiple access and OC labelled systems, due to its simple structure and because label generation/recognition can be done with relative low complexity [11–16].

For a SAC labelled system, payload and label signals occupy different wavelengths, and they are transmitted during the same packet (burst) duration. Labels are encoded in the wavelength domain, and distinguished by its amplitude. The schematic diagram of a SAC labelled packet in time and wavelength domains are shown in Fig. 1 [13].

In conventional SAC label processing unit, a $1 \times N$ splitter, N correlators, N photodiodes (PDs) and N filters are utilized to recognize the labels (as shown in Fig. 2) [14]. This configuration results in a complex structure, large optical insert/splitting loss and high cost, in particular as the network scale to accommodate a large number of label entries.

In this article, we proposed a new method of recognizing SAC labels by using optical coherent detection with a frequency swept local oscillator (LO). For our proposal, the $1 \times N$ splitter, N correlators, N PDs and N filters in the conventional configuration are replaced by a 3 dB coupler, a frequency swept LO and a balanced detection receiver. Therefore, this novel method significantly simplifies the label processing unit, reduces the cost and avoids the large optical insertion loss. We demonstrate the principle of operation of this idea by simulating a four-code 156 Mb/s label and 40 Gb/s intensity modulation (IM) payload signal. The performances of the label and payload signals are measured by the eye diagram opening and bit rate error (BER).

Y. Cao · A. V. Osadchiy · X. Yin · I. T. Monroy (✉)
DTU Fotonik, Department of Photonics Engineering,
Technical University of Denmark, 2800 Kongens Lyngby, Denmark
e-mail: idtm@fotonik.dtu.dk

Y. Cao · X. Xin · X. Yin · C. Yu
Key Laboratory of Information Photonics and Optical Communications,
Beijing University of Posts and Telecommunications,
Ministry of Education, Beijing 100876, China

Published online: 14 April 2010

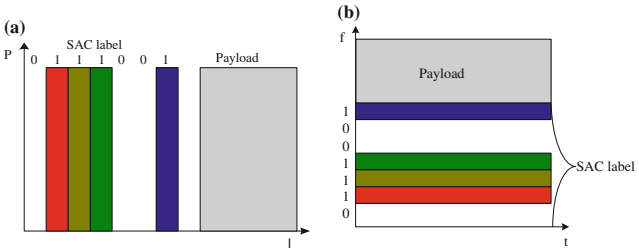

Fig. 1 Schematic diagram of SAC labelled packet: **a** SAC labelled packet in wavelength domain, **b** SAC labelled packet in time domain

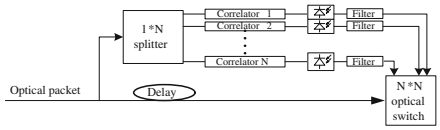

Fig. 2 Conventional configuration of SAC label recognition

2 Frequency swept coherent detection of spectral amplitude codes

The structure of the time-to-frequency swept coherent detection of SAC labels recognition as shown in Fig. 3.

As it can seen from Fig. 3, a four-code SAC label '1010' in frequency (wavelength) domain (as shown in Fig. 3a) signal and a time-to-frequency swept LO signal, whose frequency swept covers all the label's frequencies (as shown in Fig. 3b) are combined in a 3 dB coupler. After photodetection, the frequency label signal is transferred to the time domain, in the baseband frequency region. Therefore, after electrical low-pass filtering, the label signals can be recovered as shown in Fig. 3c. As we can see from Fig. 3, our proposed label detection method provides a configuration that replaces several optical components of the conventional SAC, optical-correlator-based approach.

3 Simulation setup

The simulation setup of our proposed frequency swept coherent detection of SAC labels recognition system is shown in Fig. 4. The simulation software VPI Transmission Maker is used for this purpose. For simulation purposes, a four-code 156 Mb/s label and a 40 Gb/s IM payload are considered to demonstrate and assess its performance.

A four-continuous wave (CW) laser array and a label encoder are used to generate 2^7-1, pseudo-random binary sequence (PRBS) label signals, with 30 dB extinction ration (ER), at label rate of 156 Mb/s. The chosen label frequencies are at 1552.83, 1552.86, 1552.89 and 1552.92 nm, and the average emission power 0 dBm, with linewidth 1 MHz.

For the generation of the payload signal, a CW laser at 1553.33 nm, with 0 dBm average emission power and 1 MHz linewidth, a Mach-Zehnder modulator, and a $2^{15}-1$ PRBS electrical signal generator are used to produce a non return-to-zero (NRZ), 40 Gb/s IM payload signal with 30 dB ER.

A frequency swept laser is simulated by using an optical frequency modulator, driven by a ramp wave generator, a CW laser at 1552.93 nm. The frequency-swept range is from 1552.82 to 1552.93 nm, in order to cover all the label available frequencies. The SAC labels are combined with the frequency-swept LO by a 3 dB coupler, and the combined signal is transferred to electrical domain by a balanced photodetection receiver. The electrical label signal is filtered by a 120 MHz dual-low-pass filter (LPF). An eye diagram analyzer and an oscilloscope are utilized to measure label signal quality. For the payload signal analysis, an optical band-pass filter (OBPF) at 1553.33 nm, with 60- GHz bandwidth, a PD, a LPF with 30- GHz bandwidth, a clock recovery module and a BER tester, are used.

4 Performance analysis

At a label rate of 156 Mb/s, and a payload bit rate of 40 Gb/s, a packet duration of 6.5536 μs is considered, that means 256 labels (1,024 bits) are included. For the simulation, every label occupies a 25.6ns time window, and all time windows are stitched after the photodetection. Therefore, stitched label signals and eye diagrams are utilized to estimate the label quality.

In Fig. 5, we illustrate the results at monitoring points A and B as shown in Fig. 4. The recovered label eye diagram is shown in Fig. 6. As it can be seen from Figs. 5 and 6, a 39 Mb/s (156/4 Mb/s) frequency-swept LO was obtained, and its swept range (1552.82–1552.93 nm) covers all the labels' frequencies. The resultant label waveforms and eye diagrams in the electrical domain reveal that the system provide highsignal contrast for label recognition processing.

We study the relationship between the LO power level and linewidth and the label detection quality. The label quality performance is measured by using eye opening factor (EOF),

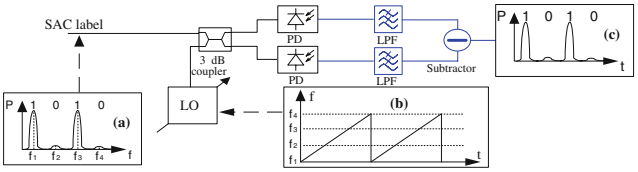

Fig. 3 Operation principle of frequency swept SAC label recognition by optical coherent detection: **a** SAC label in frequency domain, **b** time-to-frequency swept LO, (**c**) SAC label in electrical domain after the recognition

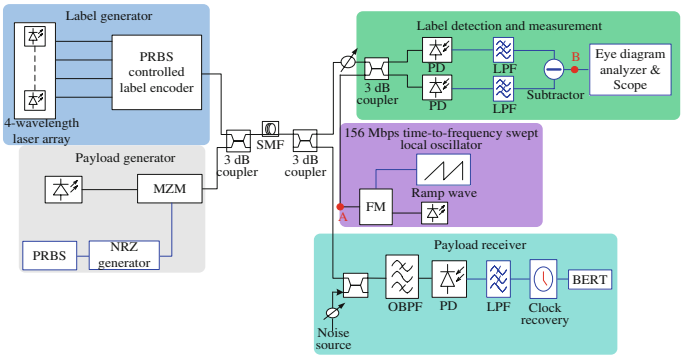

Fig. 4 Simulation setup of the time-to-frequency swept coherent detection of SAC label recognition

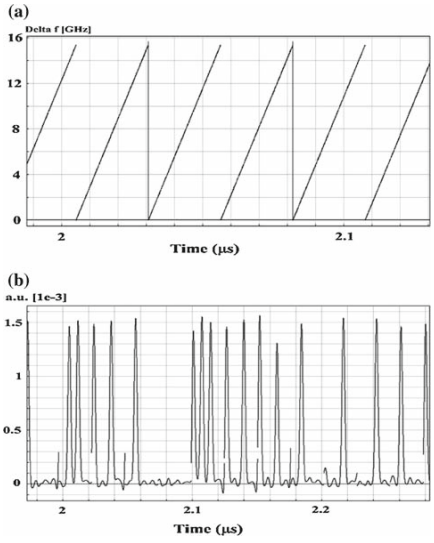

Fig. 5 Waveforms at monitoring points A and B: **a** Spectrum of frequency-swept LO, **b** SAC labels after balanced detection

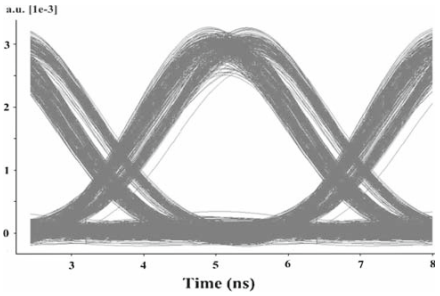

Fig. 6 Label eye diagram

and its expression is EOF $= \frac{EA-(\sigma_1+\sigma_0)}{EA}$, where EA is the eye amplitude, σ_0 and σ_1 are the standard deviations of the sample points of 'zero' bits and 'one' bits within the sample range. The simulation result is shown in Fig. 7.

Assuming the label optical power and linewidth of −30 dBm and 1 MHz, respectively, the results shown in Fig. 7 imply that when LO power is increasing from −28 to −18 dBm, the label EOF changes from 0.45 to 0.88. Therefore, increasing LO power can enhance the label quality. Moreover, different LO linewidth values, up to 10 MHz show little influence on the label quality, this is due to the fact, that

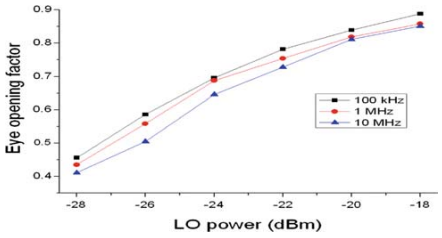

Fig. 7 Label EOF as a function of LO power and linewidth

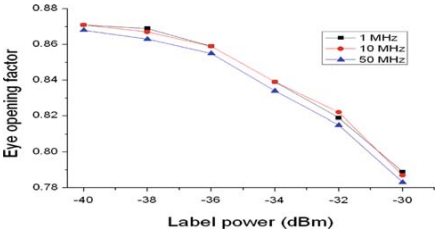

Fig. 9 Label EOF as a function of label power and linewidth

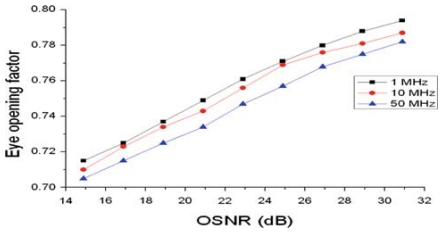

Fig. 8 Label EOF as a function of OSNR

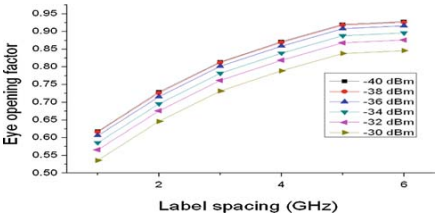

Fig. 10 Label EOF as a function of label power and spacing

each label wavelength is basically a CW signal (no modulation) during the packet duration time. This shows that the system can operate with current conventional distributed feedback lasers with a typical linedwith value in the order of 2–10 MHz.

In Figs. 8, 9, 10, we assess the performance with respect to the power level, linewidth and optical signal-to-noise ratio (OSNR) values of the label signals. Assuming the LO power and linewidth is −20 dBm and 100 kHz, respectively. In Fig. 8, the label EOFs with different OSNRs and linewidths are measured for a label wavelength spacing and power is 4-GHz and −35 dBm; in Fig. 9, the label EOFs with different powers and linewidths are measured for a label wavelength spacing is 4-GHz; in Fig. 10, the label EOFs with different powers and spacing are measured for a label linewidth is 1 MHz.

The results in Figs. 8 and 9 indicate that when the OSNR increases from 15 to 31 dB, the label EOF is between 0.71 and 0.79 (linewidth is 1 MHZ), and the label linewidth has no significant impact on the label EOF. As we show below, those OSNR values are also acceptable for the payload quality and therefore suggest a good achievable performance for the whole labelled signal. Figure 10 shows that label EOF decreases from 0.86 to 0.77, if label power is increased from −40 to −30 dBm (linewidth is 1 MHz); label spacing increases from 1 to 6 GHz, label EOF changes from 0.53 to 0.84 (power is −30 dBm). Above results mean that increasing label power is a negative factor to its EOF; large OSNR and label spacing can enhance the label quality.

We also study the performance of the 40 Gb/s IM payload signal by assessing its BER performances with respect to the values of the OBPF bandwidth, and the wavelength spacing between payload wavelength and label wavelengths.

In order to provide an efficient utilization of the spectrum, the spacing between payload and label should be limited; however, for reducing the interference between payload signal and label signal, this spacing should be above the main frequency components of a given payload bit rate. Therefore, 50-GHz spacing and a 60-GHz bandwidth (1.5 × payload bit rate) OBPF are considered as the typical parameters in the simulation.

The BER is measured with respect to the received optical power and OSNR, and shown in Figs. 11 and 12.

As seen from Figs. 11 and 12, for a 60-GHz bandwidth OBPF and 50-GHz spacing system, the payload signal BER reaches 10^{-9} when the received power and OSNR are about −18.1 dBm and 23 dB, respectively. The power penalty and OSNR penalty between 40- and 60/80-GHz bandwidths are 1.7/1.4 and 2/1 dB, respectively; besides, the power penalty and OSNR penalty between 50- and 60-GHz spacing, with/without labelling, are 0.1/0.8 and 0.5/1.1 dB, respectively.

The above payload signal BER curves reveal that a 60-GHz bandwidth OBPF for a 40 Gb/s, NRZ IM, payload, yields satisfactory results for labels spaced 50 GHz away, showing compatibility with a 100-GHz wavelength grid

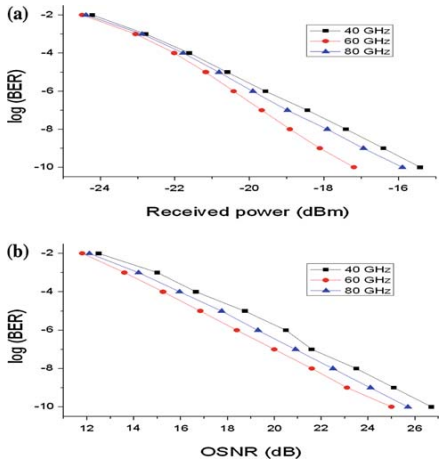

Fig. 11 40 Gb/s IM payload BER performance as a function of OBPF bandwidth, when the spacing between payload and label is 50 GHz: **a** BER versus received power, **b** BER versus OSNR

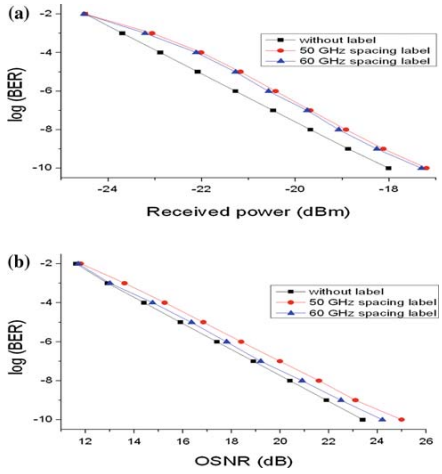

Fig. 12 40 Gb/s IM payload BER performance as a function of spacing between payload and label, when the OBPF bandwidth is 60 GHz: **a** BER versus received power, **b** BER versus OSNR

assignment. Studies on our proposed labelling concept for other modulation types and spectral separations are underway; however, we focus in this article on the proof-of-concept of our coherently detected SAC labelling scheme.

5 Conclusions

In this article, we proposed to our best knowledge, for the first time a novel method for recognizing SAC label by optical coherent detection with a frequency-swept LO. This approach reduces the complexity of the conventional configuration of SAC labelling processing nodes using optical correlators. The operation principle of our approach was demonstrated by computer simulation. A 156 Mb/s continuous SAC labels with a 40 Gb/s NRZ IM payload signal scheme was examined.

The label performance is assessed by EOF. Label EOFs as a function of different values for LO output power, LO linewidth, label OSNR, label optical power, label spacing and label linewidth were investigated. The results reveal that satisfactory EOF values are achieved for OSNR values in the order of 15–25 dB and that linewidth values up to 10 MHz have no significant influence on label quality. These results indicate that conventional semiconductors laser could be used to implement the proposed scheme.

The performance of the payload signal was assessed by its BER as a function of the OSNR, OBPF bandwidth and spacing between the payload central wavelength and labels. The simulation results show that using a 60- GHz bandwidth OBPF and 50- GHz spacing between payload and labels, payload BER values of 10^{-9} are achieved for an OSNR value of 23 dB. The OSNR penalty for a payload with and without labelling was 0.8 dB, which indicates operational compatibility with a 100- GHz WDM channel spacing with low-power performance penalty.

We have demonstrated the proof-of-principle of our proposed approach for coherent detection of SAC labels showing good performance with reduced complexity indicating its potential application in future all OLS networks.

Acknowledgements The financial support from National Basic Research Program of China (2010CB328300), National Natural Science Foundation of China (60677004), National High Technology Research and Development Program of China (2007AA03Z447), (2009AA01Z220) are gratefully acknowledged, and partly supported by the Teaching and Scientific Research Foundation for the Returned Overseas Chinese Scholars (State Education Ministry) and Program for New Century Excellent Talents in University of China (NCET-07-0111). The simulations were performed by using the VPI Transmission Maker software.

References

[1] Vlachos, K.G., Monroy, I.T., Koonen, A.M.J. et al.: STOLAS: switching technologies for optically labeled signals. IEEE Opt. Commun. **41**(11), 9–15 (2003)

[2] Meagher, M., Chang, G.K., Ellinas, G. et al.: Design and implementation of ultra-low latency optical label switching for packet-switched WDM networks. IEEE/OSA J. Lightwave Technol. **18**(12), 1978–1987 (2000)

[3] Blumenthal, D.J., Olsson, B.E., Rossi, G. et al.: All-optical swapping networks and technologies. IEEE/OSA J. Lightwave Technol. **18**(12), 2058–2075 (2000)
[4] Xin, X.J., André, P.S., Teixeira, A.L.J. et al.: Improvement of amplitude-shift-keying signal quality by employing an effective spectrum equalization method in a combined FSK/ASK modulation scheme. Chin. Phys. Lett. **22**(8), 1948–1950 (2005)
[5] Olmos, J.J.V., Zhang, J.F., Nielsen, P.V.H. et al.: Simultaneous optical label erasure and insertion in a single wavelength conversion stage of combined FSK/IM modulated signals. IEEE Photon. Technol. Lett. **16**(9), 2144–2146 (2004)
[6] Kawanishi, T., Higuma, K., Fujita, T. et al.: High-speed optical FSK modulator for optical packet labelling. IEEE/OSA J. Lightwave Technol. **23**(1), 87–94 (2005)
[7] Chi, N., Zhang, J.F., Nielsen, P.V.H. et al.: Demonstration of cascaded transmission and all-optical label swapping of orthogonal IM/FSK labelled signal. Electron. Lett. **39**(8), 676–678 (2003)
[8] Wada, N., Furukawa, H., Miyazaki, T.: Prototype 160-Gbit/s/port optical packet switching based on optical code label processing and related technologies. IEEE J. Sel. Top. Quantum Electron. **13**(5), 1551–1559 (2007)
[9] Wang, X., Wada, N.: Experimental demonstration of OCDMA traffic over optical packet switching network with hybrid PLC and SSFBG en/decoders. IEEE/OSA J. Lightwave Technol. **24**(8), 3012–3020 (2006)
[10] Cincotti, G., Manzacca, G., Wang, X. et al.: Reconfigurable multiport optical en/decoder with enhanced auto-correlation. IEEE Photon. Technol. Lett. **20**(2), 168–170 (2008)
[11] Yoshino, M., Kaneko, S., Taniguchi, T. et al.: Beat noise mitigation of spectral amplitude coding OCDMA using heterodyne detection. IEEE/OSA J. Lightwave Technol. **26**(8), 962–970 (2008)
[12] Fernandez, J.B.R., Ayotte, S., Rusch, L.A. et al.: Ultrafast forwarding architecture using a single optical processor for multiple SAC-label recognition based on FWM. IEEE J. Sel. Top. Quantum Electron. **14**(3), 868–878 (2008)
[13] Habib, C., Baby, V., Chen, L.R. et al.: All-optical swapping of spectral amplitude code labels using nonlinear media and semiconductor fiber ring lasers. IEEE J. Sel. Top. Quantum Electron. **14**(3), 879–888 (2008)
[14] Seddighian, P., Ayotee, S., Fernandez, J.B.R. et al.: Label stacking in photonic packet switched networks with spectral amplitude code labels. IEEE/OSA J. Lightwave Technol. **25**(2), 463–471 (2007)
[15] Fernandez, J.B.R., Huang, G., Aw, E.T., et al.: Ultrafast FWM self routing between 10 ports of spectral amplitude coded 10 Gb/s packets set on 25 GHz grid with unequally spaced bins. In: *Proceeding of the IEEE Optical Fiber Communication/National Fiber Optic Engineers Conference (OFC/NFOEC'2008)*. Paper OTuL6. San Diego, CA, USA, February (2008)
[16] El-Sahn, Z.A., Shastri, B.J., Zeng, M. et al.: Experimental demonstration of a SAC-OCDMA PON with burst-mode reception: local versus centralized source. IEEE/OSA J. Lightwave Technol. **26**(10), 1192–1203 (2008)

Author Biographies

Yongsheng Cao received the Bachelor's degree in Electronics Engineering from Beijing University of Posts and Telecommunications (BUPT), Beijing, China, in 2005. He is currently working towards the PhD degree in Photonics Engineering, working on optical label switching networks, at Institute of Information Photonics and Optical Communications, BUPT. From October 2008 to January 2010, he was a Guest PhD student in Metro-Access & Short Range Systems Group, DTU Fotonik, Department of Photonics Engineering, Technical University of Denmark.

Alexey V. Osadchiy is a PhD student in Metro-Access & Short Range Systems Group, DTU Fotonik, Department of Photonics Engineering, Technical University of Denmark. His PhD project is Optical label-controlled transparent metro-access network interface.

Xiangjun Xin received the PhD degree in Electromagnetic Fields and Electromagnetic Waves from Beijing University of Posts and Telecommunications (BUPT), Beijing, China, in 2003. He was a Postdoctoral Researcher in the Institute of Telecommunications, University of Aveiro, Portugal. Now, he is a professor of BUPT, and research interests are optical networks and all-optical signal processing.

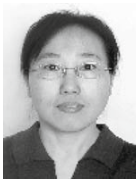

Xiaoli Yin received her Bachelor in Applied Electronics Technology, MSc in Optics and PhD degrees in Physical Electronics from Beijing University of Posts and Telecommunications (BUPT), Beijing, China, in 1993, 1996 and 2008, respectively. Since 2003, she has been an associate professor of School of Electronics Engineering, BUPT. From February 2009 to January 2010, she was a Guest Researcher in Metro-Access & Short Range Systems Group, DTU Fotonik, Department of Photonics Engineering, Technical University of Denmark.

Chongxiu Yu is currently a professor of Institute of Information Photonics and Optical Communications, Beijing University of Posts and Telecommunications. Her research interests are optoelectronic components and optical information processing.

Idelfonso Tafur Monroy received MSc degree in multi-channel telecommunications from Bonch-Bruevitch Institute of Communications, St. Petersburg, Russia, in 1992. In 1996, he received a Technology Licenciate degree in telecommunications theory from Royal Institute of Technology, Stockholm, Sweden. He earned his PhD degree in Technical University of Eindhoven, Netherlands, in 1999. He is currently a Professor of DTU Fotonik, Department of Photonics Engineering, Technical University of Denmark.

Paper J

Alexey V. Osadchiy, Neil Guerrero, Jesper Bevensee Jensen, Idelfonso Tafur Monroy, "Coherent spectral amplitude coded label detection for DQPSK payload signals in packet-switched metropolitan area networks," **Optical Fiber Technology** (ACCEPTED FOR PUBLICATION) (2010)

Coherent spectral amplitude coded label detection for DQPSK payload signals in packet-switched metropolitan area networks

Alexey V. Osadchiy[1,*], Neil Guerrero[1], Jesper Bevensee Jensen[1], Idelfonso Tafur Monroy[1]

[1] *DTU Fotonik, Technical University of Denmark, Oersteds Plads 343, DTU Campus, 2800 Kgs. Lyngby, Denmark*

** Alexey V. Osadchiy*

DTU Fotonik, Technical University of Denmark

Oersteds Plads 343, DTU campus, Office 214

2800 Kgs. Lyngby, Denmark

Tel.: +45 4525 3657

Email: avos@fotonik.dtu.dk

Abstract: We report on an experimental demonstration of a frequency swept local oscillator-based spectral amplitude coding (SAC) label detection for DQPSK signals after 40 km of fiber transmission. Label detection was performed for a 10.7 Gbaud DQPSK signal labeled with a SAC label composed of four-frequency tones with 500 MHz spectral separation. Successful label detection and recognition is achieved with the aid of digital signal processing that allows for substantial reduction of the complexity of the detection optical front-end.

Keywords: optical packet switching; DQPSK; SAC labeling; metropolitan networks; coherent detection.

1. Introduction

Packet switching provides high network resource utilization efficiency and is used in the conventional IP networks. The appearance of bandwidth-demanding services and subsequent growth of bandwidth capacity in the access network segment are expected to cause the data streams going through the metro area network (MAN) nodes to reach tens of Tb/s [1]. Both complexity and power consumption of the conventional routing nodes (factually, conventional IP routers with optical front-ends) are reaching the point where it becomes obvious that a new approach is required in order to help MANs keep up with the data streams from the access networks [2].

Optical packet switching (OPS) is considered a promising approach capable of increasing packet routers capabilities by reducing the amount of optical to electrical conversions and offering optical bypass of high speed signals [3]. However, an efficient solution is required for labeling of high speed optical payload signals.

Spectral Amplitude Coding (SAC) label is one of the realizations of optical labeling: a SAC label is a group of continuous waves at particular wavelengths. Power level of each of those wavelengths – spectral tones – represents a “one” or a “zero” [4]. As none of the label tones are modulated, their spectral width is very low: they are more resistant to dispersion, and their effect on the payload signal is minimal, so the SAC label occupies the same wavelength channel as the payload.

State-of-the-art setups for SAC label detection rely on an array of optical correlators to detect either individual spectral tones or complete label combinations [5]. Such an approach utilizes rather complex components – optical correlators – which feature a number of drawbacks: they require substantial power levels in order to operate, so the label has to be amplified. Another drawback is caused by the fact that such a correlator is a planar waveguide structure designed and built for a particular label tone wavelength, which makes correlator-based SAC label detection systems incapable of label reconfiguration, and makes such systems intolerant to label misalignment.

Quadrature phase-shift keying (QPSK) is one of the signal formats which is believed to become the standard for MAN networks: it is robust and has high spectral efficiency [6], so it can be used for long-range transmission of 100 Gb/s signals within the standard 100 GHz ITU-T grid, and polarization division multiplexing (PDM) technique is capable of doubling the bit rate. But in order to reliably receive QPSK signals at such bandwidths, coherent detection with the aid of digital signal processing (DSP) has to be employed in order to recover the phase information and compensate for the transmission impairments. Burst-mode detection of QPSK signals with DSP-assisted coherent receivers has been demonstrated for high-bit rate packets [7], and implementation of a flexible label detection technique which shares the operation principle with those receivers is a logic next step towards overall system unification and simplification.

In this paper, we propose a novel technique for SAC label detection employing coherent detection with a wavelength-swept local oscillator (LO) assisted by digital processing. The

proposed method provides flexibility of reconfiguration and additional reliability of detected labels through respective DSP algorithms. We also experimentally demonstrate SAC label detection and recognition for a SAC-labeled 10.7 Gbaud differential quadrature phase-shift keying (DQPSK) signal. The following section describes the operation principle of our proposed system. Next section contains the experimental setup description and the experimental results.

2. System description and discussion

The following principle is utilized in our proposed setup to detect the SAC labels: the signal containing both payload and a SAC label (Fig. 1 (a)) is mixed with a continuous wave (CW) from the local oscillator (LO). The LO frequency is periodically linearly swept, as presented in Fig. 1 (b): the LO frequency oscillates around the frequency range covering expected spectral tone frequencies f_1 through f_4, so that the mixing product contains spectral components produced by mixing of the spectral tones with the LO (label products).

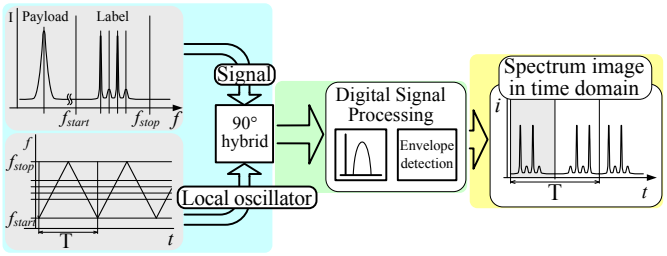

Fig. 1 Swept LO-based label detection principle: a) SAC label spectrum; b) swept LO f(t) diagram; c) recovered electrical representation of the SAC label; d) packet structure – payload and SAC labels.

Since the LO frequency is swept in a linear fashion, the spectral position of the label products in the mixing product varies in a linear fashion as well. After applying a narrow pass-band filter positioned within the frequency range covering expected spectral tone frequencies f_1 through f_4 to the mixing product, an image of the SAC label in time domain is obtained. In our proposed setup, we acquire samples of the mixing product, and perform digital signal processing by applying a narrow digital pass-band filter to the obtained samples and detecting an envelope to create an image of the SAC label (Fig. 1 (c)).

Digital signal processing (DSP) for label recognition has a significant advantage: it provides the flexibility for label structure rearrangement – through the possibility to change the pass-band filter position and width, the setup can be optimized for given label tone spacing, and LO central frequency and sweep range can be adjusted to handle SAC labels with a different spectral position and occupying a different spectral range. Additional processing is then applied to the obtained signal: time (for label tone position) and amplitude thresholding is performed to recognize the label.

SAC-labeled signal structure is presented in Fig. 1 (d): the SAC label is transmitted over the whole packet duration, and multiple scans may be performed for a single label to improve the reliability of label recognition through redundancy. Due to the linear nature of the LO frequency sweep, the resulting image will have inverted images of the SAC label in time domain (Fig. 1 (c)).

3. Experimental description and results

We assessed the quality of the labels after detection. Since label tones are converted from spectral components into electrical amplitudes in time domain, resulting electrical signal SNRs were measured and used to evaluate the detected label tones quality. Measured SNRs were then plotted against the input optical SNRs to present the relation between the input and the output signal quality.

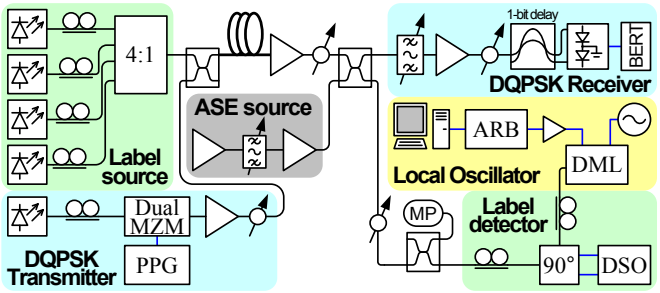

Fig. 2 Experimental setup configuration.

In our experiment, a 10.715 Gbaud DQPSK signal was labeled with a four-tone SAC label. The experimental setup is presented in Fig. 2. The spectral separation between the label tones was 500 MHz, making the overall SAC label spectral width 1.5 GHz. Four tunable DFB lasers with linewidths of less than 10 MHz centered around 1550.380 nm, offset from one another by 500 MHz, were used as a SAC label source. The outputs of the lasers were polarization-aligned with polarization controllers and combined in a 4-by-1 power combiner. A dual Mach-Zehnder IQ modulator was used to modulate the output of a tunable laser with the DQPSK payload. The output of the payload laser with a linewidth of

about 200 kHz at 1550.362 nm was amplified in a low-noise EDFA prior to being modulated in the IQ modulator.

The DQPSK payload was then combined with the four-tone SAC label in a 3-dB power combiner. The output powers were adjusted to simulate two different scenarios: payload with a peak power of -0.48 dB and SAC label with a peak power -4.16 dB representing high-power payload case; and payload at a peak power of -19.35 dB and SAC label at -4.28 dB, respectively, representing the equalized total powers case.

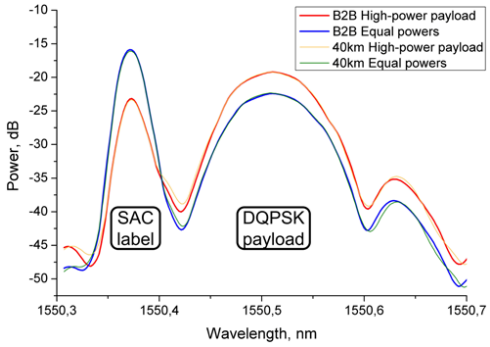

Fig. 3 Signal spectra: a), b) back-to-back; c), d) after fiber transmission, for high-power payload and for equal powers cases, respectively.

Fig. 3 presents the spectra of the labeled DQPSK signal after amplification in an EDFA: due to the resolution of the optical spectrum analyzer lower than the spectral tone separation, the four-tone SAC label appears as a single wide spectral component.

DQPSK signal showed no significant degradation after all four cases: error-free operation was observed at the receiving end. The results for DQPSK payload were omitted

in favor of label detection analysis. Fig. 4 presents the SNR of the detected labels versus the OSNR of the labels prior to detection.

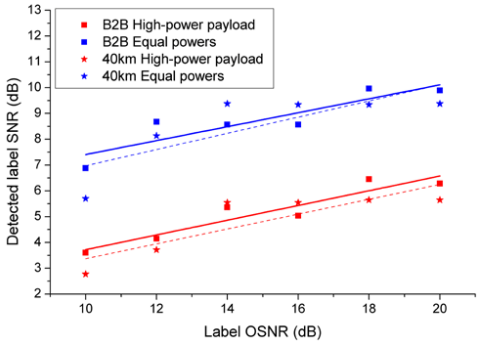

Fig. 4 Detected label SNR vs. input OSNR.

As expected, the high-power payload case demonstrates lower performance due to unequal amplification in an EDFA, resulting in about 3.5 dB lower detected label SNR compared to equalized total powers case. At the same time, transmission over 40 km of SMF introduced only about 0.5 dB SNR degradation for both cases.

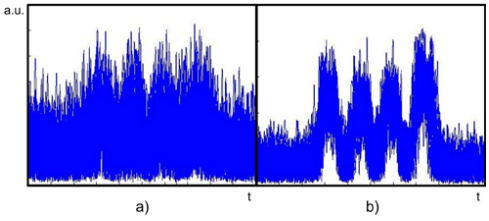

Fig. 5 Examples of detected labels: a) 10 dB OSNR; b) 20 dB OSNR.

Fig. 5 features the labels recovered with the use of simple DSP algorithms. From the figure it is evident that employing a simple label recognition algorithm, such as integration

over a time interval, can provide significantly higher label detection reliability than simple threshold setting.

5. Conclusion

We have proposed a coherent detection-based DSP-assisted technique for SAC label detection. Our experimental validation demonstrates that the label can be detected and recognized after transmission in a 40-km SMF span, and we observe minimal degradation of the SAC label after the transmission.

At the same time, the use of DSP for label recognition ensures high degree of re-configurability and flexibility for label tones position, their number and power levels, which means that no equipment replacement is required in order to accommodate to the new operation conditions, reducing system operation cost and extending its lifespan.

We believe that our proposed technique can be implemented in the metro networks in the foreseeable future, as the SAC labeling technique is compatible with the 10.7 Gbaud DQPSK payload, and there is no indication of it not being compatible with the 100 Gb/s DQPSK payloads. And since both signal detection and label detection for 100-Gb/s systems and our proposed label detection system rely on coherent detection and DSP, their cost may be reduced due to the use of a common receiver technology approach and partial component unification for payload and label detection.

References

[1]R.P. Davey, D.B. Payne, The future of optical transmission in access and metro networks - an operator's view, in 31st European Conference on Optical Communication Proceedings (2005), vol. 5, 53-56

[2]J. Baliga, R. Ayre, K. Hinton, W.V. Sorin, R.S. Tucker, Energy Consumption in Optical IP Networks, in Journ. Lightw. Technol., 27 (2009), no. 13, 2391-2403

[3]S. Yao, S. Yoo, B. Mukherjee, and S. Dixit, All-optical packet switching for metropolitan area networks: opportunities and challenges, in IEEE Commun. Mag., 39 (2001), no. 3, 142–148

[4]C. Habib, V. Baby, L.R. Chen, All-optical swapping of spectral amplitude code labels using nonlinear media and semiconductor fiber ring lasers. IEEE J. Sel. Top. Quantum Electron., 14(2008), no. 3, 879–888

[5]G. Cincotti, G. Manzacca, X. Wang, Reconfigurable multiport optical encoder/decoder with enhanced auto-correlation. IEEE Photon. Technol. Lett., 20 (2008), no. 2, 168–170

[6]R. A. Griffin, A. C. Carter, Optical differential quadrature phase-shift key (DQPSK) for high capacity optical transmission, in OSA OFC procs. (2002), 367-368

[7]Jesse E. Simsarian, Jurgen Gripp, Alan H. Gnauck, Gregory Raybon, Peter J. Winzer 'Fast-Tuning 224 Gb/s Intradyne Receiver for Optical Packet Networks,' in 2010 OFC/NFOEC Post-deadline Proceedings

Biography

Alexey V. Osadchiy received the M.Sc. degree in fiber optical communications from the Bonch-Bruevich State University of Communications, Saint-Petersburg, Russia, in 2006. He is currently pursuing a Ph.D. in optical communications engineering at DTU Fotonik, Technical University of Denmark, with main focus on access networks and interaction between access networks and higher level of network hierarchy networks, namely, metro-access interfacing.

Neil Guerrero received the B.Sc. degree in electronics engineering from the Universidad Nacional de Colombia, Manizales, in 2005; a Graduate Diploma in M.Eng.Sci. degree from the Universidad Nacional de Colombia, Manizales, in 2007. He is currently pursuing a Ph.D. in Photonics at the Technical University of Denmark, with the metro-access and short range systems research group of the department of Photonics Engineering.

Jesper Bevensee Jensen received his PhD in 2008 from the Technical University of Denmark, DTU Fotonik. Since 2008 he has been employed as a postdoc at DTU Fotonik, involved in the European project ICT-Alpha. His research interests include advanced modulation formats, access and in-home network technologies, ultrawideband-over-fiber, polymer optical fibers, carrier remodulation, and photonic crystal fibers.

Idelfonso Tafur Monroy received the M.Sc. degree in multichannel telecommunications from the Bonch-Bruevich Institute of Communications, St. Petersburg, Russia, in 1992, the Technology Licenciate degree in telecommunications theory from the Royal Institute of Technology, Stockholm, Sweden, and the Ph.D. degree from the Electrical Engineering Department, Eindhoven University of Technology, The Netherlands, in 1999.

He is currently Head of the metro-access and short range communications group of the Department of Photonics Engineering, Technical University of Denmark. He was an Assistant Professor until 2006 at the Eindhoven University of Technology. Currently, he is a Professor at the Technical University of Denmark. He has participated in several European research projects, including the ACTS, FP6, and FP7 frameworks (APEX, STOLAS, LSAGNE, MUFINS). At the moment, he is in involved the ICT European projects Gi-GaWaM, ALPHA, BONE, and EURO-FOS. His research interests are in hybrid optical-wireless communication systems, coherent detection technologies and digital signal processing receivers for baseband and radio-over-fiber links, optical switching, nanophotonic technologies, and systems for integrated metro and access networks, short range optical links, and communication theory.

Paper K

Alexey V. Osadchiy, Xianbin Yu, Xiaoli Yin, Idelfonso Tafur Monroy, "Spectral Encoded Optical Label Detection for Dynamic Routing of Impulse Radio Ultra-Wideband Signals in Metro-Access Networks," **Microwave and Wireless Components Letters** (UNDER REVIEW) (2010)

Spectral Encoded Optical Label Detection for Dynamic Routing of Impulse Radio Ultra-Wideband Signals in Metro-Access Networks

Alexey V. Osadchiy, Xianbin Yu, Xiaoli Yin, Idelfonso Tafur Monroy

***Abstract*— In this paper we propose and experimentally demonstrate the principle of coherent label detection for dynamic routing of wavelength division multiplexed impulse radio ultra-wideband signals by using four-tone spectral amplitude coded labels with 250 and 500 MHz spectral tone separation after a 40-km transmission in a single-mode fiber.**

***Index Terms*— wireless ultra-wideband, optical transmission, digital signal processing, dynamic routing, label detection.**

I. INTRODUCTION

Optical access networks architectures are adopting wavelength division multiplexing (WDM) to connect metro nodes directly to the local routing cabinets (LRC) via long-reach optical links [1]. By concentrating complex data processing at the metropolitan area routing nodes, and only assigning data distribution and aggregation tasks to the LRC, we expect to reduce overall network costs. Furthermore, current trends in access networks show a clear demand for support of various wireless services. This brings the importance to consider metro-access networks architectures capable of supporting delivery of both wireline and wireless signals with dynamic routing for efficient use of resources and enhanced flexibility.

Indeed, wireless signals have taken a niche in the access systems: they became popular because they do not require cables to provide connectivity to the user and offer certain degree of mobility. However, an issue has arisen from this popularity: the available frequency range is becoming more and more congested with various wireless formats, with the unlicensed frequency range moving to tens of GHz. An impulse radio ultra-wideband (IR-UWB) signal format has been introduced to coexist with the existing cellular and data transmission systems in the frequency range between 3.1 and 10.6 GHz [2]. Transport of IR-UWB signal over fibre extends the reach of these wireless links while using a common optical fibre access infrastructure [3].

In this paper we propose to use spectral amplitude carrier (SAC) labelling on the downstream direction in order to enable dynamic signal routing to the end user terminals. Our proposed optical labelling scheme requires low label detection equipment complexity and has insignificant detrimental effect on the payload signal performance. In particular, we experimentally demonstrate our proposed labelling technique for dynamic routing of optically-generated impulse radio ultra-wideband (UWB) wireless signals over optical fibre access networks [4].

All authors are with the DTU Fotonik-Department of Photonics Engineering, Technical University of Denmark, DK-2800 Kgs. Lygnby, Denmark. (E-mail: avos@fotonik.dtu.dk). Xiaoli Yin is also with the School of Electronic Engineering, Beijing University of Posts and Telecommunications, 100876, China.

II. DYNAMIC ROUTING SCENARIO WITH SAC LABELING

In our considered network architecture, end user terminals (EUT) are connected to LRC in either point-to-point (in case of high subscriber density) or point-to-multipoint (via WDM) fashion (Fig. 1). On the downstream, the LRC is performing optical routing based upon SAC labels. On the upstream, locally generated packets are simply aggregated into a common stream and are detected by the metropolitan area network node.

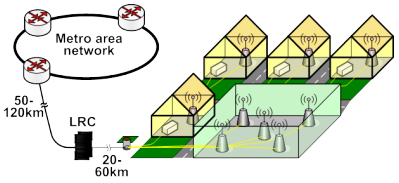

Fig. 1. Network scenario for dynamically routed impulse radio ultra-wideband services in metro-access networks.

For the labelling system, we propose a flexible, robust and relatively simple technology. Fig. 2 shows the principle used for SAC label detection. The operation is based on coherent detection – or rather, heterodyne-like scanning of the frequency range occupied by the SAC label with a periodically-swept local oscillator (LO). We employ subsequent digital signal processing (DSP), consisting of digital narrow pass-band filtering and envelope detection. This allows us to recover an image of the label spectrum in time domain. The obtained signal is then used to determine the label combination. DSP makes this system easily adjustable for different label settings (i.e., different label size, spectral position or spacing between the label tones) through simple modification of the digital filter properties and LO sweep range.

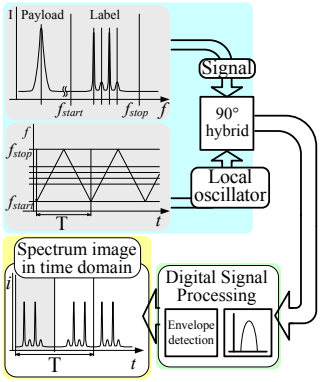

Fig. 2. SAC label detection principle: an image of the spectrum is obtained after DSP.

III. Experimental Setup

The schematic diagram of our experimental setup is presented in Fig. 3. An FCC mask-compliant optically-generated UWB [5] signal at 2 Gb/s was used as payload [6]. Four DFB lasers were used to create a SAC label with four label tones. The experiment was performed for 250 and 500 MHz separation between the label tones. The payload and SAC label signals were spaced at 1.6 nm, which was dictated by the available equipment. The payload was combined with the labels, and the powers equalized after the booster EDFA at 0 dBm for back-to-back and 5 dBm for the 40-km transmission. A 6-km spool of DCF fiber was used to compensate the dispersion of the 40-km transmission link.

At the receiver side, the UWB payload was direct detected and sampled for off-line digital signal processing. For label detection, the received signal was mixed in a 90-degree optical hybrid receiver with light from a frequency-swept local oscillator LO: the output signal was stored in form of samples for subsequent off-line label processing. A direct-modulated laser (DML) was used as a swept LO for label recognition. It was centered around a 1550.3 nm wavelength by biasing it with a 65 mA DC current. A saw tooth-shaped electric signal with 1 MHz repetition rate generated with the aid of an arbitrary waveform generator was used to produce a 6-GHz LO frequency sweep. The input power into the 90-degree optical hybrid receiver was kept at −18.5 dBm – well above the receiver sensitivity threshold, but below the saturation level.

A narrow (300 MHz) digital pass-band filter was applied to the samples at 2.5 GHz: as a result, an integral over the 300-MHz range was obtained for each sample. Since the spacing between the SAC labels was greater than 300 MHz, an image of the label spectrum was obtained with resolution sufficient to recognize individual SAC tones in time domain.

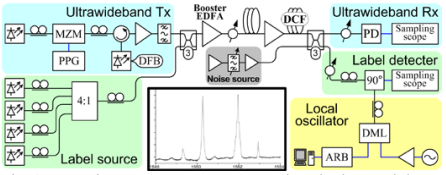

Fig. 3. Experiment setup: MZM – Mach-Zehnder modulator; MP – monitoring point; PPG – pulse pattern generator; DFB – seeded DFB laser; PD – photodetector; DML – direct-modulated laser; ARB – arbitrary waveform generator. **Inset**: signal spectrum before fiber transmission.

IV. Experimental Results

System performance was assessed for both the UWB payload and the four-tone SAC label. Fig. 3, Inset features the measured signal spectrum after the booster EDFA. The spectra for the 250 and 500 MHz spectral tone spacing appeared identical as the available spectrum analyzer resolution was insufficient to distinguish between individual spectral tones. Fig. 4(a) shows the UWB payload BER curve as a function of the optical signal to noise ratio (OSNR) measured over 0.4 nm bandwidth for both back-to-back case and for a 40-km transmission over SMF. We did not observe substantial degradation of the payload in presence of the label and vice versa.

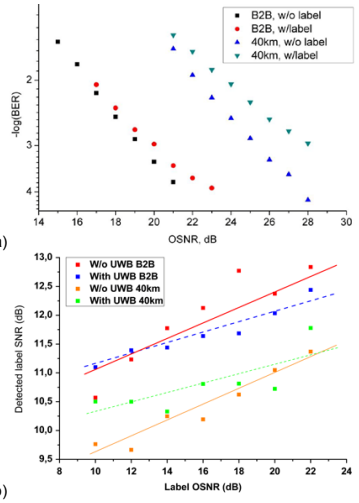

Fig. 4. (a) BER curves as a function of OSNR for UWB payload signal. (b) Detected label SNR as a function of OSNR (500 MHz tone spacing case).

The power penalty observed for the UWB payload comes from fiber chromatic dispersion. Fig. 4(b) features the relation

between the signal-to-noise-ratio (SNR) of the digitally recovered label and the OSNR of the received optical signal for the label with spectral tones spaced at 500 MHz: 40-km fiber transmission resulted in a 1 to 1.5 dB penalty on the label SNR. Fig. 5 shows an identical relation for the 250 MHz spectral tone separation. For this case, 40-km fiber transmission resulted in 1.5 to 2 dB label SNR penalty.

In this paper, SNRs are used to evaluate the label recovery reliability; however, different approaches to thresholding can be used for more reliable label detection. Integration over a pre-defined interval of time can provide higher reliability then thresholding at a single point of time. At the same time, the overall label detection reliability can be further improved by increasing LO scan rate: the redundant results due to larger number of recognitions during a set timeframe provide higher reliability and robustness. Label recognition for shorter packets for dynamic routing systems with high packet granularity is also possible with the increased LO scan rate. DSP algorithms can also be altered to accommodate for a larger number of label tones

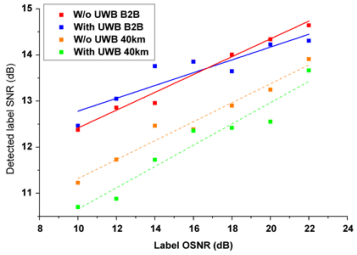

Fig. 5. Detected label SNR as a function of OSNR (250 MHz tone spacing case).

V. Conclusion

We experimentally demonstrate the use of SAC labelling of a 2 Gb/s UWB signals for dynamic routed metro-access optical networks. Reliable label detection is shown for four-tone 250 and 500-MHz spectral tone separation SAC labels after a 40-km SMF transmission. The use of SAC labels has insignificant effect on the transmitted UWB payload.

Coherent detection and DSP algorithms are used for label post-processing. The use of DSP algorithms makes this approach attractive for implementation due to the flexibility and high degree of reconfigurability provided by the use of DSP algorithms: algorithm parameters may be adjusted in order to accommodate for different SAC label parameters – spectral position, size and spectral tone separation.

References

[1] R.P. Davey ET AL., "Long-Reach Passive Optical Networks," J. Lightwave Technol., 27, no. 3, 273-291 (2009)

[2] Federal Communications Commission, "Revision of part 15 of the commission's rules regarding ultra-wideband transmission systems" (2002)

[3] T. Braidwood Gibbon, Xianbin Yu, R. Gamatham, N. Guerrero Gonzalez, R. Rodes, J.B. Jensen, A. Caballero, I. Tafur Monroy, 3.125 Gb/s Impulse Radio Ultra-Wideband Generation and Distribution over a 50 km Fiber and 2.9 m Wireless Link, IEEE Microwave and Wireless Components Letters, 20 (2010), no.2, 127-129

[4] T.B. Gibbon, X. Yu, D. Zibar, and I. Tafur Monroy, "Novel ultra-wideband photonic signal generation and transmission featuring digital signal processing bit error rate measurements", OFC/NFOEC2009, March 2009, California, USA, Paper: OTuB8

[5] H. Sheng, P. Orlik, A.M. Haimovich, L.J. Cimini, and J. Zhang, "On the spectral and power requirements for ultra-wideband transmission", ICC2003, Alaska, USA, vol. 1, 738- 742 (2003)

[6] Xianbin Yu et al., "Experimental demonstration of all-optical 781.25-Mb/s binary phase-coded UWB Signal Generation and Transmission," IEEE Phot. Technol. Lett., 21, no. 17, 1235-1237 (2009)

References

[1] World Bank development report, http://data.worldbank.org/indicator/IT.CMP.PCMP.P2 (2006-2008)

[2] Berkman Center for Internet & Society, "Next generation connectivity: A review of broadband Internet transitions and policy from around the world," http://cyber.law.harvard.edu/sites/cyber.law.harvard.edu/files/Berkman_Center_Broadband_Final_Report_15Feb2010.pdf Harvard University (2010)

[3] S. Cherry, "Edholm's law of bandwidth, IEEE Spectrum," 41, no. 7, pp 58-60 (2004)

[4] S. Fox, I.F.A.G. Bedford, "Submarine optical fibre cable system applications," Journal of the Institution of Elec. and Radio Engineers, 58, no. 5, pp 123-130 (1988)

[5] S. Abbott, "Review of 20 years of undersea optical fiber transmission system development and deployment since TAT-8," 34th European Conference on Optical Communication (2008)

[6] J. Read, IP-Switching optimiert Datenverkehr, NTZ – Nachrichten-technische Zeitschrift, 49, no.9, p 48 (1996)

[7] J. McQuillan, “The arrival of IP switching,” Business Communications Review, 26, no. 6, p 10 (1996)

[8] W.-T. Shaw, G. Kalogerakis, S.-W. Wong, Y.-L. Hsueh, N. Cheng, S.-H. Yen, M.E. Marhic, L.G. Kazovsky, “MARIN: Metro-Access Ring Integrated Network,” IEEE Global Telecommunications Conference, Globecom 2006

[9] IEEE Standard 802.3av-2009,

http://www.ieee802.org/3/av/ (2009)

[10] ITU-T. Recommendation G.984.1: Gigabit-capable passive optical networks (GPON): General characteristics,

http://www.itu.int/rec/T-REC-G.984.1/en (2009)

[11] Rasmus Kjaer, Leif Katsuo Oxenlowe, Bera Palsdottir, Palle Jeppesen, "All-optical equalization of power transients on four 40 Gbit/s WDM channels using a fiber-based device," 34th European Conference on Optical Communication (2008)

[12] IEEE Std. 802-2001, IEEE Standard for Local and Metropolitan Area Networks: Overview and Architecture,

http://standards.ieee.org/getieee802/download/802-2001.pdf (2005)

[13] R.P. Davey, D.B. Payne, "The future of optical transmission in access and metro networks - an operator's view," 31st European Conference on Optical Communication, 5, pp 53-56 (2005)

[14] D. Payne and J. Stern, “Transparent single-mode fiber optical networks,” Journal of Lightwave Technology, 4, no. 7, pp 864-869 (1986)

[15] Kevin D. Stalley, Donald E. A. Clarke, Paul A. Rosher, “Optical fibre communications system,” U.S. Patent No. 5,479,286 (1995)

[16] Paul W. Shumate, "Fiber-to-the-home: 1977–2007," Journal of Lightwave Technology, 26, no. 9, pp 1093-1103 (2008)

[17] Chang-Hee Lee, Sang-Mook Lee, Ki-Man Choi, Jung-Hyung Moon, Sil-Gu Mun, Ki-Tae Jeong, Jin Hee Kim, and Byoungwhi Kim, "WDM-PON experiences in Korea (invited)," Journal of Optical Networking, 6, no. 5, pp 451–464 (2007)

[18] J.R. Stern, J.W. Ballance, D.W. Faulkner, S. Hornung, D.B. Payne, K. Oakley, "Passive optical local networks for telephony applications and beyond," Electronics Letters, 23, no. 24, pp 1255–1256 (1987)

[19] ITU-T recommendation G.983.1: Broadband optical access systems based on Passive Optical Networks (PON), http://www.itu.int/rec/T-REC-G.983.1/en (2005)

[20] ITU-T recommendation G.983.4: A broadband optical access system with increased service capability using dynamic bandwidth assignment (DBA), http://www.itu.int/rec/T-REC-G.983.4/en (2005)

[21] ITU-T Recommendation G.984.1: Gigabit-capable passive optical networks (G-PON): General characteristics, http://www.itu.int/rec/T-REC-G.984.1/en (2009)

[22] ITU-T Recommendation G.984.2: Gigabit-capable passive optical networks (G-PON): Physical media dependent (pmd) layer specification,

http://www.itu.int/rec/T-REC-G.984.2/en (2008)

[23] ITU-T Recommendation G.984.3: Gigabit-capable passive optical networks (G-PON): Transmission convergence layer specification,

http://www.itu.int/rec/T-REC-G.984.3/en (2008)

[24] ITU-T Recommendation G.984.4: Gigabit-capable passive optical networks (G-PON): Ont management and control interface specification,

http://www.itu.int/rec/T-REC-G.984.4/en (2008)

[25] ITU-T Recommendation G.984.5: Gigabit-capable passive optical networks (G-PON): Enhancement band, http://www.itu.int/rec/T-REC-G.984.5/en (2009)

[26] IEEE Standard 802.3ah-2004,

http://ieeexplore.ieee.org.globalproxy.cvt.dk/stamp/stamp.jsp?tp=&arnumber=1337489&isnumber=29503 (2004)

[27] IEEE Standard 802.3av-2009,

http://www.ieee802.org/3/av/ (2009)

[28] “IEEE Approves 10G-EPON Standard”,

http://standards.ieee.org/announcements/stdbd_approves_ieee802.3av.html (2009)

[29] M. Chacinski, U. Westergren, L. Thylen, B. Stoltz, J. Rosenzweig, R. Driad, R. E. Makon, J. Li, A. Steffan, "ETDM transmitter module for 100-Gb/s Ethernet," IEEE Photonics Technology Letters, 22, no.2, pp 70–72 (2010)

[30] S.S. Wagner, H. Kobrinski, T.J. Robe, H.L. Lemberg, L.S. Smoot, "Experimental demonstration of a passive optical subscriber loop architecture," Electronics Letters, 24, no. 6, pp 344-346 (1988)

[31] J.R. Stern, J.W. Ballance, D.W. Faulkner, S. Hornung, D.B. Payne, K. Oakley, "Passive optical local networks for telephony applications and beyond," Electronics Letters, 23, no. 24, pp 1255-1256 (1987)

[32] J.A. Salehi "Code division multiple-access techniques in optical fiber networks. I. Fundamental principles," IEEE Transactions on Communications, 37, no. 8, pp 824-833 (1989)

[33] J.A. Salehi, C.A. Brackett, "Code division multiple-access techniques in optical fiber networks. II. Systems performance analysis," IEEE Transactions on Communications, 37, no. 8, pp 834-842 (1989)

[34] M. Maier, "WDM Passive Optical Networks and Beyond: the Road Ahead [Invited]," IEEE/OSA Journal of Optical Communications and Networking, 1, no. 4, pp C1-C16 (2009)

[35] M. Achouche, V. Magnin, J. Harari, D. Carpentier, E. Derouin, C. Jany, D. Decoster, "Design and fabrication of a p-i-n photodiode with high responsivity and large alignment tolerances for 40-gb/s applications," IEEE Photonics Technology Letters, 18, no. 4, pp 556-558 (2006)

[36] A. Beling, H.-G. Bach, G.G. Mekonnen, R. Kunkel, D. Schmidt, "Miniaturized waveguide-integrated p-i-n photodetector with 120-GHz bandwidth and high responsivity," IEEE Photonics Technology Letters, 17, no. 10, pp 2152-2154 (2005)

[37] Hans-Christian Hansen Mulvad, Michael Galili, Leif K. Oxenlowe, Hao Hu, Anders T. Clausen, Jesper B. Jensen, Christophe Peucheret, Palle Jeppesen, "Demonstration of 5.1 Tbit/s data capacity on a single-wavelength channel," Optics Express, 18, no. 2, pp 1438-1443 (2010)

[38] Reneacute-Jean Essiambre, Gerhard Kramer, Peter J. Winzer, Gerard J. Foschini, Bernhard Goebel, "Capacity limits of optical fiber networks," Journal of Lightwave Technology, 28, no. 4, pp 662-701 (2010)

[39] Qingrong Han, Shuqiang Zhang, Kang Xie, Jie Luo, R. Matai, "Study on low water peak fiber fabricated by PCVD based process," Passive Components and Fiber-based Devices II, 6019 I (2005)

[40] E. Desurvire, J. R. Simpson, P. C. Becker, "High-gain erbium-doped traveling-wave fiber amplifier," Optics Letters, 12, no. 11, pp 888–890 (1987)

[41] R.J. Mears, L. Reekie, I.M. Jauncey, D.N. Payne, "Low-noise erbium-doped fibre amplifier operating at 1.54μm," Electronics Letters, 23, no.19, pp 1026–1028 (1987)

[42] M. Öberg, B. Broberg, S. Lindgren, "InGaAsP-InP laser amplifier with integrated passive waveguides," IEEE Journal of Quantum Electronics, 23, no. 6, pp 1021-1026 (1987)

[43] T. Okoshi, K. Kikuchi, 'Coherent Optical Fiber Communications,' Springer (1988)

[44] H. Takahashi, S. Suzuki, K. Kato, I. Nishi, "Arrayed-waveguide grating for wavelength division multi/demultiplexer with nanometre resolution," Electronics Letters, 26, no. 2, pp 87-88 (1990)

[45] Sungwook Moon, Youngchul Chung, "Design of a low loss N×N waveguide grating router composed of multimode interference couplers and arrayed waveguide grating," Journal of the Korea Institute of Telematics and Electronics D, 34-D, no. 7, pp 79-87 (1997)

[46] ITU-T Recommendation H.323: Packet-based multimedia communications systems,

http://www.itu.int/rec/T-REC-H.323/en/ (2009)

[47] The BitTorrent Protocol Specification,

http://bittorrent.org/beps/bep_0003.html (2008)

[48] ATIS IPTV Exploratory Group Report and Recommendation to the TOPS Council,

http://www.atis.org/tops/IEG/ATIS_IPTV_EG_RPT_final.pdf (2005)

[49] IEEE Std. 802-2001, IEEE Standard for Local and Metropolitan Area Networks: Overview and Architecture,

http://standards.ieee.org/getieee802/download/802-2001.pdf

[50] J.-P. Elbers, K. Grobe, "Optical metro networks 2.0," Proceedings of the SPIE - Optical Metro Networks and Short-Haul Systems II (2010)

[51] Jesse E. Simsarian, Jurgen Gripp, Alan H. Gnauck, Gregory Raybon, Peter J. Winzer "Fast-Tuning 224 Gb/s Intradyne Receiver for Optical Packet Networks," OFC/NFOEC Post-deadline Proceedings (2010)

[52] D. van den Borne, T. Duthel, C. Fludger, E. Schmidt, T. Wuth, C. Schulien, E. Gottwald, G. Khoe, H. de Waardt, "Coherent equalization versus direct detection for 111-Gb/s ethernet transport", 2007 Digest of the IEEE/LEOS Summer Topical Meetings, pp 11-12 (2007)

[53] D. van den Borne, S. Jansen, E. Gottwald, E. Schmidt, G. Khoe, H. de Waardt, "DQPSK modulation for robust optical transmission", 2008 Conference on Optical Fiber

Communication/National Fiber Optic Engineers Conference (2008)

[54] M.J. Holmes, D.L. Williams, R.J. Manning, "Highly nonlinear optical fiber for all optical processing applications," IEEE Photonics Technology Letters, 7, no. 9, pp 1045-1047 (1995)

[55] S. Yao, S. Yoo, B. Mukherjee, S. Dixit, “All-optical packet switching for metropolitan area networks: opportunities and challenges,” IEEE Communications Magazine, 39, no. 3, pp 142–148 (2001)

[56] P. Gambini et al., "Transparent optical packet switching: network architecture and demonstrators in the KEOPS project," Journal on Selected Areas in Communications, 16, no. 7, pp 1245-1259 (1998)

[57] Pan-Lung Tsai, Chin-Laung Lei, “Analysis and evaluation of a multiple gateway traffic-distribution scheme for gateway clusters,” Computer Communications, 29, no. 16, 3170-3181 (2006)

[58] J.B. Jensen, I. Tafur Monroy, R. Kjaer, Palle Jeppesen, "Reflective SOA re-modulated 20 Gbit/s RZ-DQPSK over distributed Raman amplified 80 km long reach PON link," Optics Express, 15, no. 9, pp 5376-5381 (2007)

[59] Derek Nesset, Paul Wright, "Raman extended GPON using 1240 nm semiconductor quantum-dot lasers," 2010 Conference on Optical Fiber Communication (2010)

[60] Ken-Ichi Suzuki, Youichi Fukada, Derek Nesset, Russell Davey, "Amplified gigabit PON systems (invited)," Journal of Optical Networking, 6, no. 5, pp 422–433 (2007)

[61] S. Appathurai, D. Nesset, R. Davey, "Measurement of tolerance to non-uniform burst powers in SOA amplified GPON systems," Optical Fiber Communication Conference (2007)

[62] C.-J. Chen, W.S. Wong, "Transient effects in saturated Raman amplifiers," Electronics Letters, 37, no. 6, pp 371–372 (2001)

[63] R. Nagarajan, M. Kato, S. Hurtt, A. Dentai, J. Pleumeekers, P. Evans, M. Missey, R. Muthiah, A. Chen, D. Lambert, P. Chavarkar, A. Mathur, J. Bäck, S. Murthy, R. Salvatore, C. Joyner, J. Rossi, R. Schneider, M. Ziari, F. Kish, D. Welch, "Monolithic 10 and 40 channel InP receiver photonic integrated circuits with on-chip amplification," Optical Fiber Communication Conference (2007)

[64] M. Karasek, M. Menif, L.A. Rusch, "Output power excursions in a cascade of EDFAs fed by multichannel burst-mode packet traffic: Experimentation and modeling," Journal of Lightwave Technology, 19, no. 7, pp 933–940 (2001)

[65] C. Tian, S. Kinoshita, Analysis and control of transient dynamics of EDFA pumped by 1480- and 980-nm lasers," Journal of Lightwave Technology, 21, no. 8, pp 1728–1733 (2003)

[66] T. Shiozaki, M. Fuse, S. Morikura, "A study of gain dynamics of erbium-doped fiber amplifiers for burst optical signals," European Conference on Optical Communication (2002)

[67] F. Bruyere, A. Bisson, L. Noirie, J.-Y. Emery, A. Jourdan, "Gain stabilization of EDFA cascade using clamped-gain SOA," Optical Fiber Communication Conference (1998)

[68] T.B. Gibbon, A.V. Osadchiy, R. Kjær, J.B. Jensen, I. Tafur Monroy, "Gain transient suppression for WDM PON networks using semiconductor optical amplifier," Electronics Letters, 44, no. 12, pp 756–758 (2008)

[69] S.J. Vaughan-Nichols, "Achieving wireless broadband with WiMAX," Computer, 37, no. 6, pp 10-13 (2004)

[70] IEEE Stdandard 802.16-2004,

http://standards.ieee.org/getieee802/download/802.16-2004.pdf (2004)

[71] IEEE Std. 802.16e-2005,

http://standards.ieee.org/getieee802/download/802.16e-2005.pdf (2005)

[72] K.H. Teo, Z. Tao, J. Zhang, "The mobile broadband WiMAX standard [Standards in a Nutshell]," IEEE Signal Processing Magazine, 24, no. 5, pp 144–148 (2007)

[73] D. Mcqueen, "The momentum behind LTE adoption [3GPP LTE]", IEEE Communications Magazine, 47, pp 44-45 (2009)

[74] H. Sheng, P. Orlik, A.M. Haimovich, L.J. Cimini, and J. Zhang, “On the spectral and power requirements for ultra-wideband transmission”, ICC2003 Proceedings, pp 738- 742 (2003)

[75] Chia-Kai Weng, Yu-Min Lin, Winston I. Way, "Radio-Over-Fiber 16-QAM, 100-km Transmission at 5 Gb/s Using DSB-SC Transmitter and Remote Heterodyne Detection," IEEE Journal of Lightwave Technology, 26, no. 6, pp 643-653 (2008)

[76] S.H. Xu, Z.M. Yang, T. Liu, W.N. Zhang, Z.M. Feng, Q.Y. Zhang, Z.H. Jiang, "An efficient compact 300 mW narrow-linewidth single frequency fiber laser at 1.5 mum," Optics Express, 18, no. 2, pp 1249-1254 (2010)

[77] Seb J. Savory, "Electronic signal processing in optical communications," Proceedings of SPIE, 7136, pp 71362C1-71362C9 (2008)

[78] N. Guerrero Gonzalez, D. Zibar, A. Caballero, I. Tafur Monroy, "Experimental 2.5-Gb/s QPSK WDM Phase-Modulated Radio-Over-Fiber Link With Digital Demodulation by a K-Means Algorithm," Photonics Technology Letters, 22, no. 5, pp 335-337 (2010)

[79] S. J. Savory, G. Gavioli, R. I. Killey, P. Bayvel, “Transmission of 42.8 Gbit/s polarization multiplexed NRZ-QPSK over 6400 km of standard fiber with no optical dispersion compensation,” IEEE Conference on Optical Fiber Communications (2007)

[80] E. Ip, A. P. Tao Lau, D. J. F. Barros, J. M. Kahn, "Coherent detection in optical fiber systems," Optics Express, 16, no. 2, pp 753-791 (2008)

[81] Yuichi Nakazaki, Shinji Yamashita, "Fast and wide tuning range wavelength-swept fiber laser based on dispersion tuning and its application to dynamic FBG sensing," Optics Express, 17, no. 10, pp 8310-8318 (2009)

[82] André Bösel, Klaus-Dieter Salewski, "Fast mode-hop-free acousto-optically tuned laser: theoretical and experimental investigations," Applied Optics, 48, no. 5, pp 818-826 (2009)

[83] D.J. Blumenthal, B.E. Olsson, G. Rossi, T.E. Dimmick, L. Rau, M. Masanovic, O. Lavrova, R. Doshi, O. Jerphagnon, J.E. Bowers, V. Kaman, L.A. Coldren, J. Barton, "All-optical label swapping networks and technologies", IEEE Journal of Lightwave Technology, 18, no. 12, pp 2058-2075 (2000)

[84] B. Meagher, G.K. Chang, G. Ellinas, Y.M. Lin, W. Xin, T.F. Chen, X. Yang, A. Chowdhury, J. Young, S.J. Yoo, C. Lee, M.Z. Iqbal, T. Robe, H. Dai, Y.J. Chen, W.I. Way, "Design and implementation of ultra-low latency optical label switching for packet-switched WDM networks", IEEE Journal of Lightwave Technology, 18, no. 12, pp 1978-1987 (2000)

[85] P. Seddighian, S. Ayotee, J.B. Rosas-Fernandez, J. Penon, L. A. Rusch, S. LaRochelle, "Label stacking in photonic packet switched networks with spectral amplitude code labels", IEEE Journal of Lightwave Technology, 25, no. 2, pp 463-471 (2007)

[86] C. Habib, V. Baby, L.R. Chen, A. Delisle-Simard, S. LaRochelle, "All-optical swapping of spectral amplitude code labels using nonlinear media and semiconductor fiber ring lasers," IEEE Journal of Selected Topics in Quantum Electronics, 14, no. 3, pp 879–888 (2008)

[87] J.B. Rosas-Fernandez, S. Ayotee, L. A. Rusch, S. LaRochelle, "Ultrafast forwarding architecture using a single optical processor for multiple SAC-label recognition based on FWM", IEEE Journal of Selected Topics in Quantum Electronics, 14, no. 3, pp 868-878 (2008)

[88] G. Cincotti, G. Manzacca, X. Wang X., T. Miyazaki, Naoya Wada, Ken-ichi Kitayama, "Reconfigurable multiport optical en/decoder with enhanced auto-correlation", IEEE Photonics Technology Letters, 20, no. 2, pp 268-170 (2008)

[89] R. A. Griffin, A. C. Carter, "Optical differential quadrature phase-shift key (DQPSK) for high capacity optical transmission," in OSA OFC Proceedings, pp 367-368 (2002)

[90] T. Braidwood Gibbon, Xianbin Yu, R. Gamatham, N. Guerrero Gonzalez, R. Rodes, J.B. Jensen, A. Caballero, I. Tafur Monroy, “3.125 Gb/s Impulse Radio Ultra-Wideband Generation and Distribution over a 50 km Fiber and 2.9 m Wireless Link,” IEEE Microwave and Wireless Components Letters, 20, no.2, pp 127-129 (2010)

[91] T.B. Gibbon, X. Yu, D. Zibar, and I. Tafur Monroy, “Novel ultra-wideband photonic signal generation and transmission

featuring digital signal processing bit error rate measurements", OFC/NFOEC2009, March 2009, California, USA, Paper: OTuB8

[92] Xianbin Yu et al., "Experimental demonstration of all-optical 781.25-Mb/s binary phase-coded UWB Signal Generation and Transmission," IEEE Photonics Technology Letters, 21, no. 17, pp 1235-1237 (2009)